National Library of Canada
Acquisitions and Bibliographic Services Branch
395 Wellington Street
Ottawa, Ontario
K1A 0N4

Bibliothèque nationale du Canada
Direction des acquisitions et des services bibliographiques
395, rue Wellington
Ottawa (Ontario)
K1A 0N4

Your file Votre référence

Our file Notre référence

NOTICE

The quality of this microform is heavily dependent upon the quality of the original thesis submitted for microfilming. Every effort has been made to ensure the highest quality of reproduction possible.

If pages are missing, contact the university which granted the degree.

Some pages may have indistinct print especially if the original pages were typed with a poor typewriter ribbon or if the university sent us an inferior photocopy.

Reproduction in full or in part of this microform is governed by the Canadian Copyright Act, R.S.C. 1970, c. C-30, and subsequent amendments.

AVIS

La qualité de cette microforme dépend grandement de la qualité de la thèse soumise au microfilmage. Nous avons tout fait pour assurer une qualité supérieure de reproduction.

S'il manque des pages, veuillez communiquer avec l'université qui a conféré le grade.

La qualité d'impression de certaines pages peut laisser à désirer, surtout si les pages originales ont été dactylographiées à l'aide d'un ruban usé ou si l'université nous a fait parvenir une photocopie de qualité inférieure.

La reproduction, même partielle, de cette microforme est soumise à la Loi canadienne sur le droit d'auteur, SRC 1970, c. C-30, et ses amendements subséquents.

Canada

UNIVERSITY OF ALBERTA

OPTICAL BIDIRECTIONAL TRANSMISSION IN CASCADED ERBIUM-DOPED FIBRE AMPLIFIERS

BY

Caroline Delisle

©

A thesis submitted to the Faculty of Graduate Studies and Research in partial fulfillment of the requirements for the degree of Master of Science.

DEPARTMENT OF ELECTRICAL ENGINEERING

Edmonton, Alberta
Spring 1995

National Library
of Canada

Acquisitions and
Bibliographic Services Branch

395 Wellington Street
Ottawa, Ontario
K1A 0N4

Bibliothèque nationale
du Canada

Direction des acquisitions et
des services bibliographiques

395, rue Wellington
Ottawa (Ontario)
K1A 0N4

Your file Votre référence

Our file Notre référence

THE AUTHOR HAS GRANTED AN IRREVOCABLE NON-EXCLUSIVE LICENCE ALLOWING THE NATIONAL LIBRARY OF CANADA TO REPRODUCE, LOAN, DISTRIBUTE OR SELL COPIES OF HIS/HER THESIS BY ANY MEANS AND IN ANY FORM OR FORMAT, MAKING THIS THESIS AVAILABLE TO INTERESTED PERSONS.

L'AUTEUR A ACCORDE UNE LICENCE IRREVOCABLE ET NON EXCLUSIVE PERMETTANT A LA BIBLIOTHEQUE NATIONALE DU CANADA DE REPRODUIRE, PRETER, DISTRIBUER OU VENDRE DES COPIES DE SA THESE DE QUELQUE MANIERE ET SOUS QUELQUE FORME QUE CE SOIT POUR METTRE DES EXEMPLAIRES DE CETTE THESE A LA DISPOSITION DES PERSONNE INTERESSEES.

THE AUTHOR RETAINS OWNERSHIP OF THE COPYRIGHT IN HIS/HER THESIS. NEITHER THE THESIS NOR SUBSTANTIAL EXTRACTS FROM IT MAY BE PRINTED OR OTHERWISE REPRODUCED WITHOUT HIS/HER PERMISSION.

L'AUTEUR CONSERVE LA PROPRIETE DU DROIT D'AUTEUR QUI PROTEGE SA THESE. NI LA THESE NI DES EXTRAITS SUBSTANTIELS DE CELLE-CI NE DOIVENT ETRE IMPRIMES OU AUTREMENT REPRODUITS SANS SON AUTORISATION.

ISBN 0-612-01595-5

Canada

UNIVERSITY OF ALBERTA

RELEASE FORM

NAME OF AUTHOR: Caroline Delisle

TITLE OF THESIS: **OPTICAL BIDIRECTIONAL TRANSMISSION IN CASCADED ERBIUM-DOPED FIBRE AMPLIFIERS**

DEGREE: Master of Science

YEAR THIS DEGREE GRANTED: Spring 1995

Permission hereby granted to the University of Alberta Library to reproduce single copies of this thesis and to lend or sell such copies for private, scholarly or scientific research purposes only.

The author reserves all other publication and other rights in association with the copyright in the thesis, and except as hereinbefore provided neither the thesis nor any substantial portion thereof may be printed or otherwise reproduced in any material form whatever without the author's prior written permission.

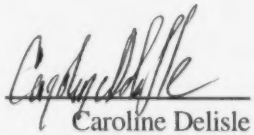

Caroline Delisle
952 Senneterre
Sainte-Foy, Quebec
G1X 3Y3

Date: December 7, 1994

UNIVERSITY OF ALBERTA

FACULTY OF GRADUATE STUDIES AND RESEARCH

The undersigned certify that they have read, and recommend to the Faculty of Graduate Studies and Research for acceptance, a thesis entitled **OPTICAL BIDIRECTIONAL TRANSMISSION IN CASCADED ERBIUM-DOPED FIBRE AMPLIFIERS** submitted by Caroline Delisle in partial fulfillment of the requirements for the degree of Master of Science.

Dr. J. Conradi, Supervisor

Dr. I. MacDonald, Internal examiner

Dr. M. Freeman, External examiner

Date: December 6, 1994

Je dédie cette thèse à mes parents
Gilles et Denise Delisle

ainsi qu'à mes grands-parents
Lucien et Joséphine Delisle

et

à la mémoire de Jean-Baptiste et Jeanne Martel

Abstract

This thesis studies characteristics of signal and noise propagation in an optical bidirectional transmission system with cascaded erbium-doped fibre amplifiers (EDFAs).

Properties of a single amplifier under small signal regime, saturated regime and bidirectional transmission of multi-wavelength signals are studied and presented.

A model for signal and noise propagation in a bidirectional cascade of amplifiers is developed. A computer simulation is coded based on the model equations to simulate multi-wavelength bidirectional transmission in a cascade of optical amplifiers. The simulation yields reasonable agreement with experimental results. We noted that accuracy of parameters such as the emission and absorption cross sections of the erbium-doped fibre (EDF) is important to achieve good agreement between experimental and simulated results.

A series of laboratory experiments were done to study performance of bidirectional systems with EDFAs and explore the behaviour of the amplifiers under such operating conditions. From the experimental results obtained, we learned that accumulation of amplified spontaneous emission (ASE) and Rayleigh backscattering in the fibre have an important effect in compressing the amplifier gain in an open cascade of amplifiers.

Acknowledgment

I first want to thank my supervisor, Dr. Jan Conradi, for the opportunity to come study in Alberta in an impressive research environment and the occasion to broaden my horizons and learn a great deal.

I would also like to thank the members of my committee, Dr. Ian MacDonald and Dr. Mark Freeman, for reviewing this thesis.

I would like to acknowledge some of my fellow students for their help and useful discussions, particularly Ping Wan and Yimin Hua. Thanks to Dave Clegg and Jason Lamont for technical help in the lab.

I would like to acknowledge generous financial support from TR*Labs*, the University of Alberta, and the National Science and Engineering Research Council.

Je voudrais souligner la contribution financière appreciée du Fonds pour la formation de chercheurs et l'aide à la recherche (FCAR) pour encourager les francophones du Québec et les anglophones des autres provinces à poursuivre des études graduées dans une autre province pour ainsi parfaire une langue seconde.

Most of all, I would like to thank my boyfriend Tom Seniuk: his love, patience and support gave me the strength to go on with this project at the most difficult times of the past two years and calmed my ever-worrying mind.

TABLE OF CONTENTS

1. INTRODUCTION 1

1.1 TRANSMISSION SYSTEMS WITH ELECTRONIC REPEATERS 1

1.2 UNIDIRECTIONAL TRANSMISSION SYSTEMS WITH OPTICAL AMPLIFIERS 2

1.3 BIDIRECTIONAL TRANSMISSION SYSTEMS WITH ERBIUM-DOPED FIBRE AMPLIFIERS 4

1.4 ORGANIZATION OF THE THESIS 6

2. ERBIUM-DOPED FIBRE AMPLIFIER THEORY AND CHARACTERIZATION 7

2.1 THEORY 7

2.2 EXPERIMENTAL CHARACTERIZATION 12

2.2.1 AMPLIFIER GAIN 12

2.2.1.1 Output power variation with input power 16

2.2.1.2 Gain variation with signal input power 17

2.2.1.3 Gain compression variation with signal wavelength 18

2.2.2 AMPLIFIED SPONTANEOUS EMISSION 21

2.2.2.1 ASE power spectrum 23

2.2.2.2 ASE compression 24

2.2.3 NOISE FIGURE 27

2.2.4 BIDIRECTIONAL GAIN COMPRESSION 28

3. BIDIRECTIONAL TRANSMISSION SYSTEM MODELLING AND SIMULATION 33

3.1 SYSTEM DESCRIPTION 33

3.2 TRANSMISSION MODEL 34

3.2.1 SYSTEM EQUATIONS FOR A CASCADE OF THREE AMPLIFIERS 34
3.2.2 PROPAGATION MODEL FOR A CASCADE OF N AMPLIFIERS 38
3.3 OPTICAL SIGNAL TO NOISE RATIO AT THE RECEIVER END 41
3.4 NUMERICAL APPLICATIONS 44
3.4.1 SIMPLE SYSTEM SIMULATION 44
3.4.2 ERBIUM-DOPED FIBRE AMPLIFIER CASCADE MODEL 45
3.5 SIMULATION OF BIDIRECTIONAL TRANSMISSION SYSTEMS 49
3.5.1 SIGNAL WAVELENGTH 51
3.5.2 SIGNAL POWER 51
3.5.3 INTER-AMPLIFIER LINK LENGTH 52
3.5.4 AMPLIFIER POSITION 53
3.5.5 RAYLEIGH BACKSCATTERING 53
3.5.6 PUMPING SCHEME 54
3.6 SUMMARY 55

4. BIDIRECTIONAL TRANSMISSION EXPERIMENTS 69

4.1 OPTICAL SOURCES 69
4.2 ERBIUM-DOPED FIBRE AMPLIFIERS 70
4.3 BIDIRECTIONAL TRANSMISSION EXPERIMENTAL SETUP 71
4.4 BIDIRECTIONAL TRANSMISSION EXPERIMENTAL RESULTS 74
4.4.1 SIGNAL WAVELENGTH 74
4.4.2 SIGNAL POWER 103
4.4.3 INTER-AMPLIFIER LINK LENGTH 104
4.4.4 AMPLIFIER POSITION 106
4.4.5 RAYLEIGH BACKSCATTERING 107
4.5 COMPARISON BETWEEN SIMULATED AND EXPERIMENTAL RESULTS 108
4.6 DISCUSSION 116
4.7 BIT ERROR RATE MEASUREMENTS 119

5. CONCLUSION 128

REFERENCES 131

APPENDIX A : RAYLEIGH SCATTERING 135

APPENDIX B : BIDIRECTIONAL CASCADED EDFAS SIMULATION CODE 137

List of Tables

Table 3.1 - Basic bidirectional transmission system simulation parameters 50

Table 4.1 - Optical sources characteristics 69
Table 4.2 - Erbium-doped fibre properties 70
Table 4.3 - Erbium-doped fibre amplifiers' characteristics 70
Table 4.4 - Experimental parameters for each cases 73

Table A.1 - Rayleigh backscattering coefficient of different transmission fibres used 136

List of figures

Figure 1.1 - Schematic of an electronic repeater 1
Figure 1.2 - Erbium-doped fibre amplifier 2
Figure 1.3 - Applications of optical amplifiers in a transmission system.
(a) Pre-amplifier, (b) Post-amplifier, (c) In-line amplifier. 3
Figure 1.4 - Bidirectional transmission system with erbium-doped fibre amplifiers 5

Figure 2.1 - Three level laser energy diagram 7
Figure 2.2 - Propagation and amplification of light in optical amplifier 9
Figure 2.3 - Gain compression experimental setup 13
Figure 2.4 - Bandpass filter spectrum 15
Figure 2.5 - Signal and ASE power saturation in erbium-doped fibre amplifier 16
Figure 2.6 - Gain saturation of erbium-doped fibre amplifier 17
Figure 2.7 - EDFA gain variation with wavelength 18
Figure 2.8 - Small signal gain variation with signal wavelength 19
Figure 2.9 - Output saturated power variation with signal wavelength 20
Figure 2.10 - Gain compression variation with wavelength and input power for an erbium-doped fibre amplifier 21
Figure 2.11 - ASE compression experimental setup 22
Figure 2.12 - Erbium-doped fibre amplifier amplified spontaneous emission spectrum 23
Figure 2.13 - Compression of amplified spontaneous emission in optical amplifier 25
Figure 2.14 - Influence of pump power distribution on ASE generation 26
Figure 2.15 - Spontaneous emission factor and optical noise figure of amplifier 27
Figure 2.16 - Bidirectional gain experimental setup 29
Figure 2.17 - Bidirectional gain compression in erbium-doped fibre amplifier 30

Figure 3.1 - System under study 34
Figure 3.2 - Propagation of signal and noise in a three amplifier cascade 35
Figure 3.3 - Propagation of light from one amplifier to the next 45
Figure 3.4 - Flow chart of EDFA computer simulation 46
Figure 3.5 - Flow chart of bidirectional transmission system simulation 48
Figure 3.6 - Bidirectional transmission cascade of three amplifiers 49
Figure 3.7 - Forward output spectra for simulation case 1. (a) Amplifier 1,
(b) amplifier 2, (c) amplifier 3. 56

Figure 3.8 - Backward output spectra for simulation case 1. (a) Amplifier 1, (b) amplifier 2, (c) amplifier 3. 57
Figure 3.9 - Forward output spectra for simulation case 1. (a) Amplifier 1, (b) amplifier 2, (c) amplifier 3. 58
Figure 3.10 - Backward output spectra for simulation case 1. (a) Amplifier 1, (b) amplifier 2, (c) amplifier 3. 59
Figure 3.11 - Output signal power at each amplifier in simulation case 1 60
Figure 3.12 - Signal gain for each amplifier in simulation case 1 60
Figure 3.13 - Signal to ASE ratio at each amplifier in simulation case 1 60
Figure 3.14 - Output signal power at each amplifier in simulation case 2 61
Figure 3.15 - Signal gain for each amplifier in simulation case 2 61
Figure 3.16 - Signal to ASE ratio at each amplifier in simulation case 2 61
Figure 3.17 - Output signal power at each amplifier in simulation case 3 62
Figure 3.18 - Signal gain for each amplifier in simulation case 3 62
Figure 3.19 - Signal to ASE ratio at each amplifier in simulation case 3 62
Figure 3.20 - Output signal power at each amplifier in simulation case 4 63
Figure 3.21 - Signal gain for each amplifier in simulation case 4 63
Figure 3.22 - Signal to ASE ratio at each amplifier in simulation case 4 63
Figure 3.23 - Output signal power at each amplifier in simulation case 5 64
Figure 3.24 - Signal gain for each amplifier in simulation case 5 64
Figure 3.25 - Signal to ASE ratio at each amplifier in simulation case 5 64
Figure 3.26 - Output signal power at each amplifier in simulation case 6 65
Figure 3.27 - Signal gain for each amplifier in simulation case 6 65
Figure 3.28 - Signal to ASE ratio at each amplifier in simulation case 6 65
Figure 3.29 - Output signal power at each amplifier in simulation case 7 66
Figure 3.30 - Signal gain for each amplifier in simulation case 7 66
Figure 3.31 - Signal to ASE ratio at each amplifier in simulation case 7 66
Figure 3.32 - Output signal power at each amplifier in simulation case 8 67
Figure 3.33 - Signal gain for each amplifier in simulation case 8 67
Figure 3.34 - Signal to ASE ratio at each amplifier in simulation case 8 67
Figure 3.35 - Output signal power at each amplifier in simulation case 9 68
Figure 3.36 - Signal gain for each amplifier in simulation case 9 68
Figure 3.37 - Signal to ASE ratio at each amplifier in simulation case 9 68

Figure 4.1 - Emission and absorption cross sections of erbium-doped fibre 71
Figure 4.2 - Bidirectional transmission experimental setup 72

Figure 4.3 - Forward input and output spectra for experimental case 1.
(a) Amplifier 1, (b) amplifier 2, (c) amplifier 3 75
Figure 4.4 - Backward input and output spectra for experimental case 1.
(a) Amplifier 1, (b) amplifier 2, (c) amplifier 3 76
Figure 4.5 - Output signal power at each amplifier in simulation case 1 77
Figure 4.6 - Signal gain for each amplifier in simulation case 1 77
Figure 4.7 - Signal to ASE ratio at each amplifier in simulation case 1 77
Figure 4.8 - Forward input and output spectra for experimental case 2.
(a) Amplifier 1, (b) amplifier 2, (c) amplifier 3 78
Figure 4.9 - Backward input and output spectra for experimental case 2.
(a) Amplifier 1, (b) amplifier 2, (c) amplifier 3 79
Figure 4.10 - Output signal power at each amplifier in simulation case 2 80
Figure 4.11 - Signal gain for each amplifier in simulation case 2 80
Figure 4.12 - Signal to ASE ratio at each amplifier in simulation case 2 80
Figure 4.13 - Forward input and output spectra for experimental case 3.
(a) Amplifier 1, (b) amplifier 2, (c) amplifier 3 81
Figure 4.14 - Backward input and output spectra for experimental case 3.
(a) Amplifier 1, (b) amplifier 2, (c) amplifier 3 82
Figure 4.15 - Output signal power at each amplifier in simulation case 3 83
Figure 4.16 - Signal gain for each amplifier in simulation case 3 83
Figure 4.17 - Signal to ASE ratio at each amplifier in simulation case 3 83
Figure 4.18 - Forward input and output spectra for experimental case 4.
(a) Amplifier 1, (b) amplifier 2, (c) amplifier 3 84
Figure 4.19 - Backward input and output spectra for experimental case 4.
(a) Amplifier 1, (b) amplifier 2, (c) amplifier 3 85
Figure 4.20 - Output signal power at each amplifier in simulation case 4 86
Figure 4.21 - Signal gain for each amplifier in simulation case 4 86
Figure 4.22 - Signal to ASE ratio at each amplifier in simulation case 4 86
Figure 4.23 - Forward input and output spectra for experimental case 5.
(a) Amplifier 1, (b) amplifier 2, (c) amplifier 3 87
Figure 4.24 - Backward input and output spectra for experimental case 5.
(a) Amplifier 1, (b) amplifier 2, (c) amplifier 3 88
Figure 4.25 - Output signal power at each amplifier in simulation case 5 89
Figure 4.26 - Signal gain for each amplifier in simulation case 5 89
Figure 4.27 - Signal to ASE ratio at each amplifier in simulation case 5 89

Figure 4.28 - Forward input and output spectra for experimental case 6.
(a) Amplifier 1, (b) amplifier 2, (c) amplifier 3 90
Figure 4.29 - Backward input and output spectra for experimental case 6.
(a) Amplifier 1, (b) amplifier 2, (c) amplifier 3 91
Figure 4.30 - Output signal power at each amplifier in simulation case 6 92
Figure 4.31 - Signal gain for each amplifier in simulation case 6 92
Figure 4.32 - Signal to ASE ratio at each amplifier in simulation case 6 92
Figure 4.33 - Forward input and output spectra for experimental case 7.
(a) Amplifier 1, (b) amplifier 2, (c) amplifier 3 93
Figure 4.34 - Backward input and output spectra for experimental case 7.
(a) Amplifier 1, (b) amplifier 2, (c) amplifier 3 94
Figure 4.35 - Output signal power at each amplifier in simulation case 7 95
Figure 4.36 - Signal gain for each amplifier in simulation case 7 95
Figure 4.37 - Signal to ASE ratio at each amplifier in simulation case 7 95
Figure 4.38 - Forward input and output spectra for experimental case 8.
(a) Amplifier 1, (b) amplifier 2, (c) amplifier 3 96
Figure 4.39 - Backward input and output spectra for experimental case 8.
(a) Amplifier 1, (b) amplifier 2, (c) amplifier 3 97
Figure 4.40 - Output signal power at each amplifier in simulation case 9 98
Figure 4.41 - Signal gain for each amplifier in simulation case 8 98
Figure 4.42 - Signal to ASE ratio at each amplifier in simulation case 8 98
Figure 4.43 - Forward input and output spectra for experimental case 9.
(a) Amplifier 1, (b) amplifier 2, (c) amplifier 3 99
Figure 4.44 - Backward input and output spectra for experimental case 9.
(a) Amplifier 1, (b) amplifier 2, (c) amplifier 3 100
Figure 4.45 - Output signal power at each amplifier in simulation case 9 101
Figure 4.46 - Signal gain for each amplifier in simulation case 9 101
Figure 4.47 - Signal to ASE ratio at each amplifier in simulation case 9 101
Figure 4.48 - Comparison of simulation and experiment for small signal regime 109
Figure 4.49 - Comparison of simulation and experiment for saturated regime 110
Figure 4.50 - Comparison of simulation and experiment for forward spectra of case 8.
(a) Amplifier 1, (b) amplifier 2, (c) amplifier 3. 111
Figure 4.51 - Comparison of simulation and experiment for backward spectra of case 8.
(a) Amplifier 1, (b) amplifier 2, (c) amplifier 3. 112
Figure 4.52 - Comparison of simulation and experiment for forward spectra of case 7.
(a) Amplifier 1, (b) amplifier 2, (c) amplifier 3. 114

Figure 4.53 - Comparison of simulation and experiment for backward spectra of case 8. (a) Amplifier 1, (b) amplifier 2, (c) amplifier 3. 115
Figure 4.54 - Bidirectional fibre amplifier 118
Figure 4.55 - Bidirectional isolator 119
Figure 4.56 - Bit error rate measurements experimental setup 121
Figure 4.57 - Bit error rate measurements in the pre/post configuration 122
Figure 4.58 - Setup for back-to-back bit error rate measurements 123
Figure 4.59 - Bit error rate vs. received power 123
Figure 4.60 - Comparison between measured and calculated receiver sensitivities at 1538 nm 127
Figure 4.61 - Comparison between measured and calculated receiver sensitivities at 1540 nm 128

Figure A.1 - Rayleigh backscattering in an optical fibre 135

List of abbreviations

APC	Angled facet physical connector
ASE	Amplified spontaneous emission
BER	Bit error rate
BPF	Bandpass filter
CW	Continuous wave
dB	Decibel
dBm	Decibel with respect to 1mW
DFB	Distributed feedback
EDF	Erbium-doped fibre
EDFA	Erbium-doped fibre amplifier
EDFL	Erbium-doped fibre laser
FCAR	Fonds pour la formation de chercheurs et l'aide à la recherche
Hz	Hertz
K	Kelvin
km	Kilometre
LED	Light emitting diode
m	Metre
Mb	Megabits
MHz	Megahertz
µm	Micrometre
mW	Milliwatts
N.A.	Numerical aperture
NF	Noise figure
nm	Nanometre
NOI	National optics institute
OPM	Optical power meter
ppm	Parts per million
RIN	Relative intensity noise
s	Second
S.N.	Serial number
SAR	Signal to ASE ratio
SNR	Signal to noise ratio
TR*Labs*	Telecommunications Research Laboratories

VOA	Variable optical attenuator
WDM	Wavelength division multiplexer

List of symbols

Roman symbols

A_{21}^{NR}	Non-radiative decay rate from level 2 to level 1
A_{21}^{R}	Radiative decay rate from level 2 to level 1
A_{31}^{R}	Radiative decay rate from level 3 to level 1
A_{32}^{NR}	Non-radiative decay rate from level 3 to level 2
A_{32}^{R}	Radiative decay rate from level 3 to level 2
Al	Aluminium
ASE_b	Backward output ASE power
ASE_f	Forward output ASE power
B_e	Detector electronic bandwidth
B_o	Signal optical bandwidth
D	Relative population inversion
e	Electronic charge
Er	Erbium
F_o	Optical noise figure
G	Amplifier gain
g	Gain coefficient
G_b	Backward amplifier gain
Ge	Germanium
G_f	Forward amplifier gain
G_o	Small signal gain
G_{sat}	Saturated gain
I_N	Received ASE intensity
I_s	Signal intensity
k_B	Boltzmann's constant = $1.38*10^{-23}$ J/K
L	Fibre link loss coefficient
$\mathcal{L}$	Loss of power caused by Rayleigh scattering
l	Incremental length
m_t	Number of transmission modes
N	ASE photon number
N_1, N_2, N_3	Atomic population in energy states 1, 2, 3
n_{sp}	Spontaneous emission factor

$n_{sp,b}$	Backward spontaneous emission coefficient
$n_{sp,f}$	Forward spontaneous emission coefficient
P	Phosphorus
P_{ASE}	ASE power at the output of the fibre
P_b	Backward power
P_{bASE}	Backward propagating ASE contribution to input power
P_{bin}	Backward input power
P_{bsig}	Backward propagating signal contribution to input power
P_f	Forward power
P_{fASE}	Forward propagating ASE contribution to input power
P_{fin}	Forward input power
P_{fsig}	Forward propagating signal contribution to input power
P_{in}	Input power
P_o	Power per amplified spontaneous emission photon
P_{RB}	Rayleigh backscattered power
P_s	Signal power
P_{sat}	Output saturation power
P_{SE}	Spontaneous emission power
R	Load resistor
r	radius
R_{13}	Pumping rate from level 1 to level 3
R_{31}	Pump emission rate from level 3 to level 1
RB_{bASE}	Rayleigh backscattered backward propagating ASE contribution to input power
RB_{bsig}	Rayleigh backscattered backward propagating signal contribution to input power
RB_{fASE}	Rayleigh backscattered forward propagating ASE contribution to input power
RB_{fsig}	Rayleigh backscattered forward propagating signal contribution to input power
R_{bs}	Rayleigh backscattering coefficient
REC	Received power
REC_{ASE}	Received ASE power
REC_{signal}	Received signal power
Rx	Receiver
T	Absolute temperature

Tx	Transmitter
W_{12}	Absorption rate from level 1 to level 2
W_{21}	Stimulated emission rate from level 2 t o level 1

Greek symbols

<n>	Mean photon number
α	Transmission loss
α_c	Coupling loss
α_R	Rayleigh backscattering coefficient
γ_R	Rayleigh scattering coefficient
η	Photodetector quantum efficiency
$\eta(\lambda)$	Ratio of emission to absorption cross-sections
λ_{probe}	Probe signal wavelength
λ_s	Signal wavelength
ν	Frequency
ρ	Total laser ion density
σ^2	Amplifier noise power
σ_a, σ_e	Absorption, emission cross-sections
σ_{shot}^2	Shot noise variance
$\sigma_{sp\_sp}^2$	ASE-ASE beat noise variance
$\sigma_{s\_sp}^2$	Signal-ASE beat noise variance
σ_{th}^2	Thermal noise variance
τ	Fluorescence lifetime
Ψ	Mode envelope

1. Introduction

Optical telecommunications have obvious advantages over conventional methods of transmission of information. The technology for manufacturing optical transmission glass fibre is now well in hand and has brought attractive features. The optical carrier frequency, being around 10^{14} Hz, brings a greater potential transmission bandwidth than is possible in metallic cable systems which operate at frequencies up to 500 MHz. Most of this large available bandwidth has yet to be utilized. The low transmission loss of optical fibre (0.2 dB/km to 0.25 dB/km) is one of the main advantages of optical communications. Long distance transmission links with wide repeater spacing can be achieved. Despite the low loss of optical fibre, periodic signal amplification is still necessary to compensate for transmission losses in long-haul transmission systems or splitting losses in subscriber loop networks. In this introductory chapter, we will present the evolution of signal amplification in optical transmission system from the use of electronic repeaters to bidirectional systems using erbium-doped fibre amplifiers.

1.1 Transmission systems with electronic repeaters

In long-haul telecommunication systems, repeaters have to be installed periodically in the link to compensate for transmission loss. Figure 1.1 illustrates the way an electronic repeater works.

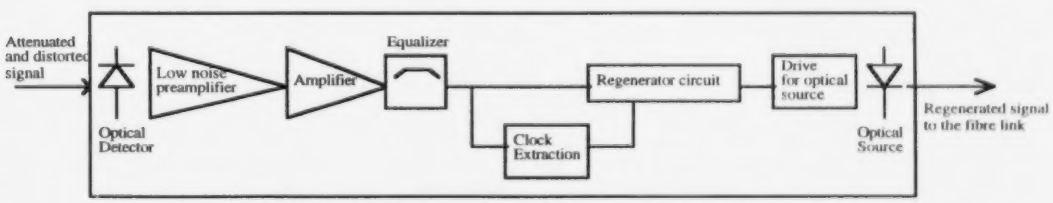

Figure 1.1 - Schematic of an electronic repeater

The digital signal, after travelling through a fibre link, is attenuated and degraded by noise upon entering the repeater. The optical signal is first detected and converted to an electrical signal, which is then amplified and reshaped using an equalizer. Clock information is extracted from the amplified and equalized waveform for precise operation of the

regenerator circuit. The originally transmitted pulse train is reconstituted and retransmitted by an optical source to the fibre link.

The use of repeaters increases the cost and complexity of a communication system. Electronic repeaters used to boost and reshape signals after many kilometres of transmission are expensive, sensitive to bit rate and require optical-to-electrical conversion prior to electronic amplification and electrical-to-optical conversion. As an alternative, we will in the next section look at optical amplifiers to be used as repeaters.

1.2 Unidirectional transmission systems with optical amplifiers

The advent of optical amplifiers has eliminated some of the system impairments related to electronic repeaters. Being all-optical devices, optical amplifiers do not perform optical/electrical conversion, and are transparent to bit rate allowing the system to be upgraded to higher data transmission speed by replacing only the transmitter and receiver and not the amplifiers in the link. Semiconductor laser amplifiers and erbium-doped fibre amplifiers are two types of optical amplifiers in use today. We will study here exclusively erbium-doped fibre amplifiers. Figure 1.2 presents a diagram of an erbium-doped fibre amplifier.

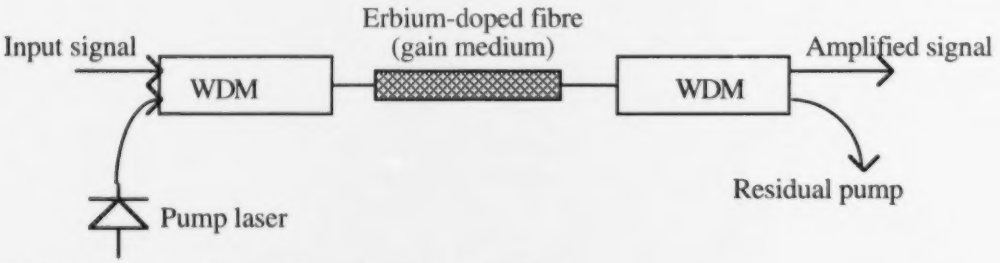

Figure 1.2 - Erbium-doped fibre amplifier

The input signal is combined with light from a pump laser through a wavelength division multiplexer (WDM). The erbium-doped fibre exhibits gain under pumping and the signal is amplified along the doped fibre. At the output, noise internally generated by the amplifier is added to the amplified signal.

Erbium-doped fibre amplifiers have been studied for several years [1]-[4] and have proven effective in amplifying optical signals over a wide range of wavelengths (1530 nm to 1560 nm) and bit rates [5] . The use of wavelength division multiplexing in conjunction with erbium-doped fibre amplifiers [3] has also helped in increasing transmission capacity. Transmission over very long distances [6] has been achieved using erbium-doped fibre amplifiers. These devices, and other types of optical amplifiers, have received much attention in recent years and have been studied extensively so that we have come to understand their properties and main applications [4]-[10]. In unidirectional optical transmission systems, optical amplifiers can be either used as pre-amplifiers, post-amplifiers, or in-line amplifiers, as shown in Figure 1.3.

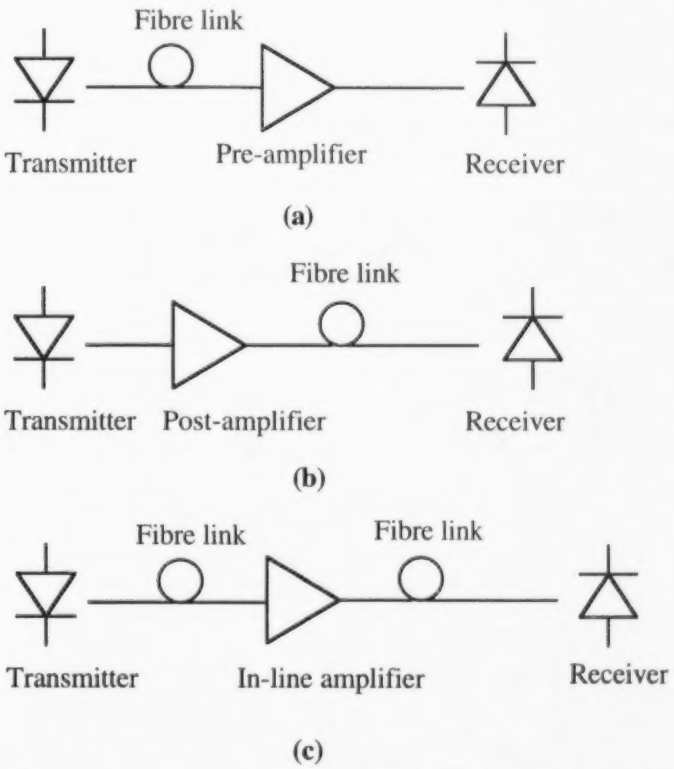

Figure 1.3 - Applications of optical amplifiers in a transmission system. (a) Pre-amplifier, (b) Post-amplifier, (c) In-line amplifier.

Pre-amplifiers are positioned before the receiver to improve receiver sensitivity. Post-amplifiers, or power amplifiers, are used after the transmitter to increase the power of the transmitted signal to be launched in the system. In-line amplifiers are used to compensate for transmission losses and to boost the signal for transmission further along the link. In

unidirectional systems, optical isolators are used to prevent backreflections from splices and connectors and backward propagating amplified spontaneous emission (ASE) which would degrade system performance. Narrow optical bandpass filters centered at the signal wavelength are also used to limit the amount of ASE propagating down the link.

Erbium-doped fibre amplifiers also have drawbacks in comparing to electronic repeaters. As opposed to electronic repeaters, where the signal is regenerated, amplified, and retransmitted noise-free, and hopefully error-free, in systems where optical amplifiers are used, both noise and signal distortions are continuously amplified along the link.

1.3 Bidirectional transmission systems with erbium-doped fibre amplifiers

More recently, interest has grown in using erbium-doped fibre amplifiers in bidirectional transmission. Bidirectional transmission allows propagation of signals in two directions over a single fibre. Different schemes for bidirectional transmission have been presented in the literature to date. One group used intensity modulation of the amplifier pump laser to transmit bidirectionally [11]. Another group used bidirectional amplifiers [12], a variation of the conventional amplifiers permitting separate amplification of the two signals and bandpass limitation of the propagating noise and backreflections along the fibre link. Some others used fused fibre wavelength division multiplexers [13] or 3 dB couplers [14] to transmit and/or receive bidirectional signals over a single fibre in an optical transmission system.

In this thesis, we will study bidirectional transmission systems like the one shown in Figure 1.4 where optical circulators are used to transmit and receive signals at each end of the link.

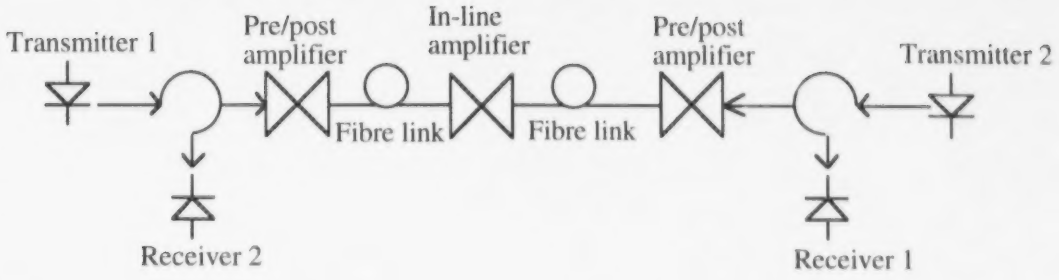

Figure 1.4 - Bidirectional transmission system with erbium-doped fibre amplifiers

In bidirectional systems, contrary to unidirectional systems, isolators cannot be used without affecting the transmission of one of the two contra-propagating signals. The use of narrow bandpass filters around the signal wavelength within the link is generally not possible either since the filter bandwidth would have to allow propagation of signals at different wavelengths. We will not use any bandpass filters in the link to reject amplifier noise even if it could be done [15]. This will impose more limitations on the system since more noise and spurious reflections are now free to propagate.

The erbium-doped fibre amplifiers can, in bidirectional systems as well as in unidirectional systems, be used as pre-amplifiers, post-amplifiers, or in-line amplifiers. In this thesis, we will study erbium-doped fibre amplifiers and their applications in bidirectional transmission systems.

1.4 Organization of the thesis

The research objective of this thesis is to study optical bidirectional transmission systems with cascaded erbium-doped fibre amplifiers. The properties of erbium-doped fibre amplifiers under bidirectional transmission and the propagation of signal and noise and the quality of received signals in bidirectional transmission systems will be assessed. Chapter 2 will present important properties and characteristics of erbium-doped fibre amplifiers to help understand the behaviour of a single amplifier on its own before assessing its performance in a transmission system. Chapter 3 will look at a model of signal and noise propagation in optical bidirectional transmission systems with erbium-doped fibre amplifiers. A similar study has been done for unidirectional systems [16]: here we tackle bidirectional transmission. We will present experimental results of bidirectional transmission in chapter 4, and follow with conclusions in chapter 5.

2. Erbium-doped fibre amplifier theory and characterization

Before studying bidirectional transmission in cascaded erbium-doped fibre amplifiers, the first step is to study and characterize the amplifiers on an individual basis. In this chapter, we will present an overview of erbium-doped fibre amplifier theory and results of an extensive amplifier characterization. Amplifier gain and amplifier spontaneous emission characteristics are studied. Similar theory derivation and more detailed information can be found in references [17]-[23].

2.1 Theory

Lasing in the erbium-doped fibre of optical amplifiers is what gives gain to the medium. A three-level laser system, as illustrated in Figure 2.1, adequately models the Er^{3+}:glass laser system of the amplifiers. Level 1 is the ground level, level 2 is a metastable level , or long lifetime, and level 3 is the level to which the erbium electrons are excited by energy transfer from the pump light. The laser transition occurring between level 2 and level 1 produces light whose wavelength is around 1550 nm, which is the spectral region of interest in optical communications with erbium-doped fibre amplifiers.

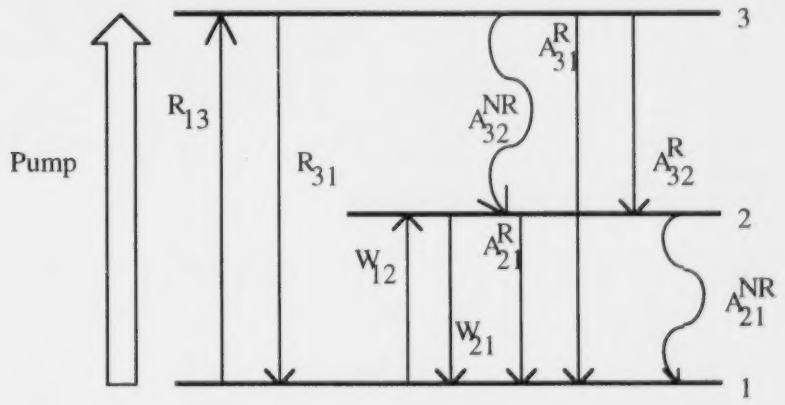

Figure 2.1 - Three level laser energy diagram

The different symbols in Figure 2.1 represent:

R_{13} : pumping rate of erbium electrons from level 1 to level 3

R_{31} : pump emission rate between level 3 and level 1

A_{32}^{R} , A_{31}^{R} : radiative decay from level 3

W_{12} , W_{21} : stimulated absorption, emission rates between levels 1 and 2

A_{21}^{R} : radiative decay rate from level 2 ; $A_{21}^{R}=1/\tau$

τ : fluorescence lifetime

A_{21}^{NR} : non-radiative decay rate from level 2

Energy from the pump light beam photons is absorbed and promotes the erbium electrons from level 1 to the higher energy level 3. Electrons in level 3 then quickly relax to the metastable level 2. Stimulated by photons of the input signal beam, electrons in level 2 are de-excited to level 1, producing a photon of the same wavelength as the input signal: this is the stimulated emission process that gives rise to gain in optical amplifiers. Noise in the form of spontaneous emission is generated as electrons are spontaneously de-excited from level 2 to level 1 resulting in the emission of incoherent light. Stimulated and spontaneous emission are the two types of radiative decay that will produce light emission from the doped fibre. Non-radiative decay is also present in the laser system.

The atom population in energy states 1, 2, 3 are here denoted as N_1, N_2, N_3. The total laser ion density being

$$\rho = N_1 + N_2 + N_3 \qquad \textbf{(2.1)}$$

Assuming that the spontaneous decay from level 3 is mainly non-radiative ($A_{32}^{NR} >> A_{32}^{R}, A_{31}^{R}$) and that the decay from level 2 is mainly radiative ($A_{21}^{R} >> A_{21}^{NR}$), we can write the atomic rate equations corresponding to the level populations:

$$\begin{aligned}
\frac{dN_1}{dt} &= -R_{13}N_1 + R_{31}N_3 - W_{12}N_1 + W_{21}N_2 + A_{21}N_2 \\
\frac{dN_2}{dt} &= W_{12}N_1 - W_{21}N_2 - A_{21}N_2 + A_{32}N_3 \qquad \textbf{(2.2)} \\
\frac{dN_3}{dt} &= R_{13}N_1 - R_{31}N_3 - A_{32}N_3
\end{aligned}$$

where $A_{21}=A_{21}^{R}$ and $A_{32}=A_{32}^{NR}$.

Considering steady-state regime, where the populations are time invariant, and assuming that the non-radiative decay A_{32} dominates over the non-radiative decay rate R_{31} and the pumping rate R_{13}, we can write an expression for the levels population.

$$N_1 = \rho \frac{1+W_{21}\tau}{1+R\tau+W_{12}\tau+W_{21}\tau}$$
$$N_2 = \rho \frac{R\tau+W_{12}\tau}{1+R\tau+W_{12}\tau+W_{21}\tau} \qquad (2.3)$$
$$N_3 = \rho - N_1 - N_2 = 0$$

with $R=R_{13}$.

If, for the moment, we ignore spontaneous emission, then when a light beam of intensity I_s at wavelength λ_s passes through a medium, such as erbium ions in a fibre of thickness dz and atomic population densities N_1 and N_2, the intensity change is given by:

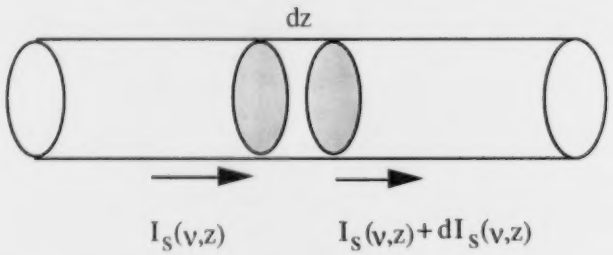

Figure 2.2 - Propagation and amplification of light in optical amplifier

$$dI_s = \{\sigma_e(\lambda_s)N_2 - \sigma_a(\lambda_s)N_1\}I_s(\nu,z)dz \qquad (2.4)$$

where σ_e : emission cross section

σ_a : absorption cross section

The gain coefficient is given by:

$$g = \sigma_e(\lambda_s)N_2 - \sigma_a(\lambda_s)N_1 \qquad (2.5)$$

so that we can now express the intensity change as:

$$\frac{dI_s}{dz} = gI_s \qquad (2.6)$$

We can write an equation for the rate of change of optical power as light propagates along the fibre in the guided mode. The signal propagation equation is given as:

$$\frac{dP_s}{dz} = \int_A \{\sigma_e(\lambda_s)N_2(r,\theta) - \sigma_a(\lambda_s)N_1(r,\theta)\}I_s(r,\theta)rdrd\theta \qquad (2.7)$$

The generation of optical noise comes from the spontaneous de-excitation of the erbium atoms, emitting photons with no coherence characteristics with respect to the incoming signal light. A fraction of the spontaneously emitted photons are collected and amplified by the fibre amplifier and form a background noise added to the input signal. This background noise is referred to as amplified spontaneous emission (ASE). There is a need to derive a propagation equation which includes the effect of amplified spontaneous emission. The rate of creation of spontaneous emission power in bandwidth $\delta\nu$ is given by [23]:

$$\frac{dP_{SE}}{dz} = m_t \frac{P_o}{P_s}\sigma_e(\nu)\int_A N_2(r,\theta)I_s(r,\theta)rdrd\theta \qquad (2.8)$$

where $P_o=h\nu\delta\nu$ is the power per ASE photon emitted in bandwidth $\delta\nu$, and m_t is the number of transmission modes. In erbium-doped fibre amplifiers, the light propagates in two different polarization modes and thus $m_t=2$.

Combining (2.7) and (2.8), we can write a rate equation that describes the propagation of the total power at wavelength λ_s as [23]:

$$\frac{dP_s(\lambda_s)}{dz} = 2\pi\int \{\sigma_e(\lambda_s)N_2(r)[1+\frac{2P_o}{P_s}] - \sigma_a(\lambda_s)N_1(r)\}I_s rdr \qquad (2.9)$$

The amplified spontaneous emission at the output of the erbium-doped fibre amplifier can be expressed as:

$$P_{ASE}(\nu) = 2n_{sp}h\nu\delta\nu(G(\nu)-1) \qquad (2.10)$$

where n_{sp} is the spontaneous emission factor and can be expressed as [23]:

$$n_{sp} = \frac{\eta N_2}{\eta N_2 - N_1} \qquad (2.11)$$

where $\eta=\sigma_e/\sigma_a$.

Full population inversion in the amplifying medium is achieved when all the atoms are in the excited state, or when $N_1=0$. The minimum spontaneous emission factor, and thus ASE output, is obtained for full population inversion of the amplifying medium, see equation (2.11). Complete medium inversion is only possible for three-level systems. An erbium-doped fibre amplifier pumped at 980 nm corresponds to a three-level system and thus in this case, $n_{sp,min}=1$. The spontaneous emission factor cannot have a value lower than one.

The spontaneous emission factor can also be expressed in a more convenient manner:

$$n_{sp} = \frac{P_{ASE}^{out}}{[G-1]2h\nu\Delta\nu} \qquad (2.12)$$

The optical noise figure, F_o, is defined as the ratio of the input optical signal to noise ratio to the output signal to noise ratio.

$$F_o = \frac{SNR_o(0)}{SNR_o(z)} \qquad (2.13)$$

Since the amplifier introduces noise in the system, the output signal to noise ratio is expected to be smaller than the input signal to noise ratio, $SNR_o(z) < SNR_o(0)$, so the amplifier optical noise figure will always be greater than one.

The input optical signal to noise ratio is equal to the mean signal photon number to the amplifier [23]:

$$SNR_o(0)=\langle n(0)\rangle \qquad (2.14)$$

The output optical signal to noise ratio is defined as:

$$SNR_o(z)=\frac{G^2(z)\langle n(0)\rangle^2}{\sigma^2(z)} \qquad (2.15)$$

where G(z) is the amplifier gain and σ^2 the amplifier noise variance.

By replacing the appropriate definitions for signal and noise powers [23] in equations (2.14) and (2.15) and assuming that we have input signals with Poisson statistics and that the input signal power is large enough so that $G\langle n(0)\rangle >> N$, where N is the ASE photon number, we get the following expression for the amplifier optical noise figure.

$$F_o(z)=\frac{1+2n_{sp}(z)[G(z)-1]}{G(z)} \quad \textbf{(2.16)}$$

In the limit of large gain, G>>1, $F_o=2n_{sp}$. The minimum value of optical noise figure for an erbium-doped fibre amplifier is thus $F_{o,min}=2$, or 3 dB.

The next section presents experimental results of the characterization of an erbium-doped fibre amplifier.

2.2 Experimental characterization

We are interested in studying the gain, signal, ASE, and noise figure characteristics that will help to give us a better understanding of the behaviour of EDFAs. In this section, we present some experimental results obtained while extensively characterizing an erbium-doped fibre amplifier, denoted as amplifier #302. Two other amplifiers were used in chapter 4 and characterized the same way.

2.2.1 Amplifier gain

We want to study the gain characteristics of an erbium-doped fibre amplifier. The gain coefficient in the fibre is given by equation (2.5). The gain is obviously wavelength dependent, but it also varies with signal power and pump power.

To study the gain characteristics of the amplifier, we designed an experimental set-up that enables us to measure gain, output signal power and inband ASE as a function of input signal power and wavelength. Gain compression was computed from the data collected using the set-up in Figure 2.3.

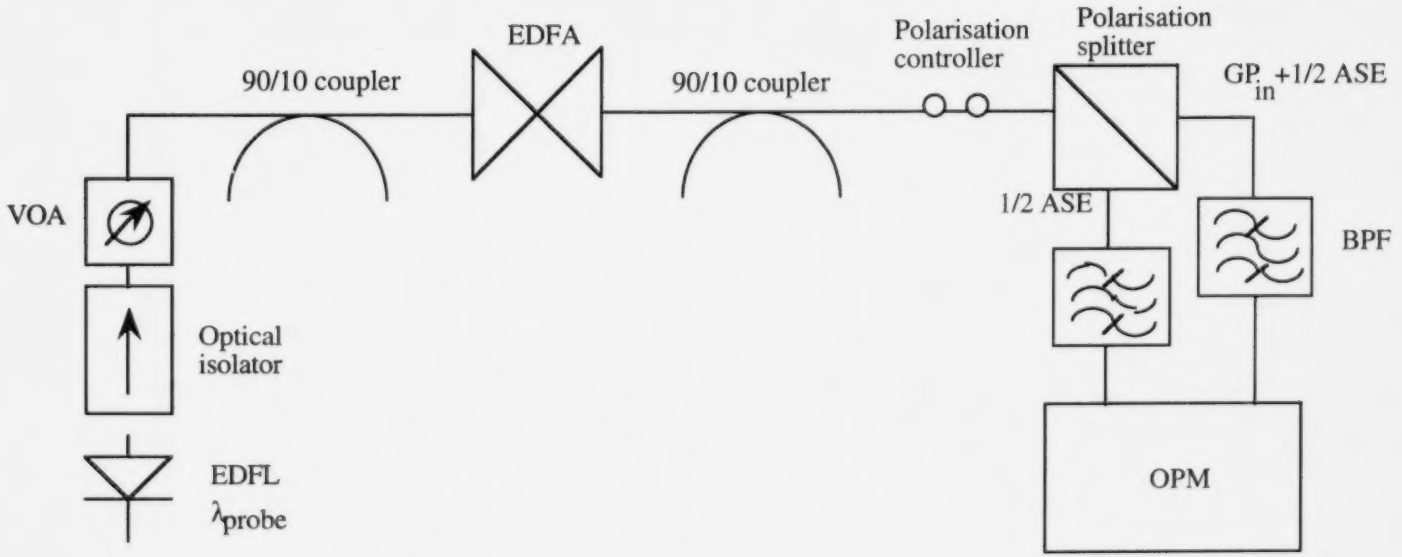

Figure 2.3 - Gain compression experimental setup - EDFL: Erbium-Doped Fibre Laser; VOA: Variable Optical Attenuator; BPF: Bandpass Filter; OPM: Optical Power Meter.

The set-up in Figure 2.3 is based on the fact that light from the erbium-doped fibre laser source is linearly polarized and that the ASE coming out of the amplifier is not polarized. This enables us to separate the signal and ASE components at the output of the amplifier by using a polarization splitter. The outputs of the branches of the polarization splitter are:

$$\text{Output}_1 = GP_{in} + ASE_{\parallel} \qquad (2.17)$$

$$\text{Output}_2 = ASE_{\perp} \qquad (2.18)$$

where $ASE_{\parallel} = ASE_{\perp} = \frac{1}{2} ASE_{total}$

Subtracting (2.18) from (2.17), we can know the gain of the EDFA, the signal output power, and the inband ASE output power.

The two 90/10 couplers in the set-up provide output ports to monitor the input and output power to the amplifier. The tunable bandpass filters limit the ASE to a bandwidth of 1.4 nm around the signal wavelength; both filters are of the same brand and type and were measured to have the same equivalent bandwidth of 1.4 nm. Figure 2.4 shows the optical bandwidth of the bandpass filters used in the measurements. The data in Figure 2.4 were obtained by filtering the light from a broadband source, in this case an LED, which has a constant output power over the spectral range covered by the filter. The equivalent noise bandwidth represents the bandwidth of an ideal filter with the same output power as the actual filter used.

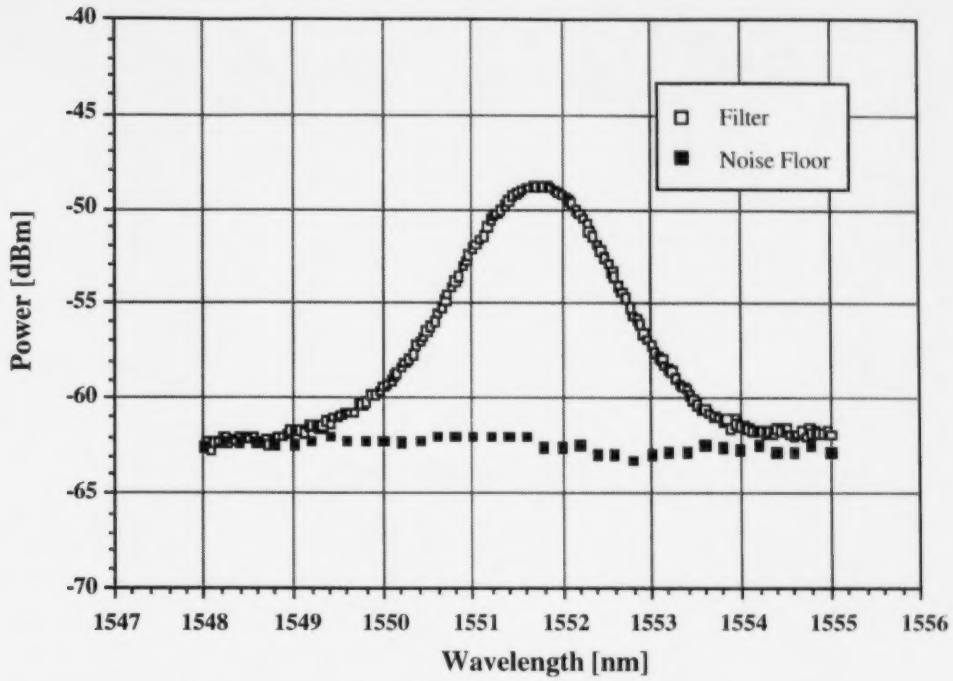

Figure 2.4 - Bandpass filter spectrum

In the setup shown in Figure 2.3, and in every other setup in this thesis, we used angled facet physical connectors (APC) with a reflection coefficient better than 60 dB.

In the following sections, we will present results obtained from experimental measurement taken with the set-up in Figure 2.3. Measurements of output signal power variation with input power, inband ASE output power, gain variation with input signal power, and gain compression variations with signal wavelength characterize the amplifier.

2.2.1.1 Output power variation with input power

The probe signal input power was varied from -40 dBm to -10 dBm, and the output signal power and inband ASE were monitored. An example of the results obtained by testing amplifier #302 with signal at 1536 nm, co-propagating (propagating in the same direction) with the pump, and pump power of 26 mW is shown in Figure 2.5.

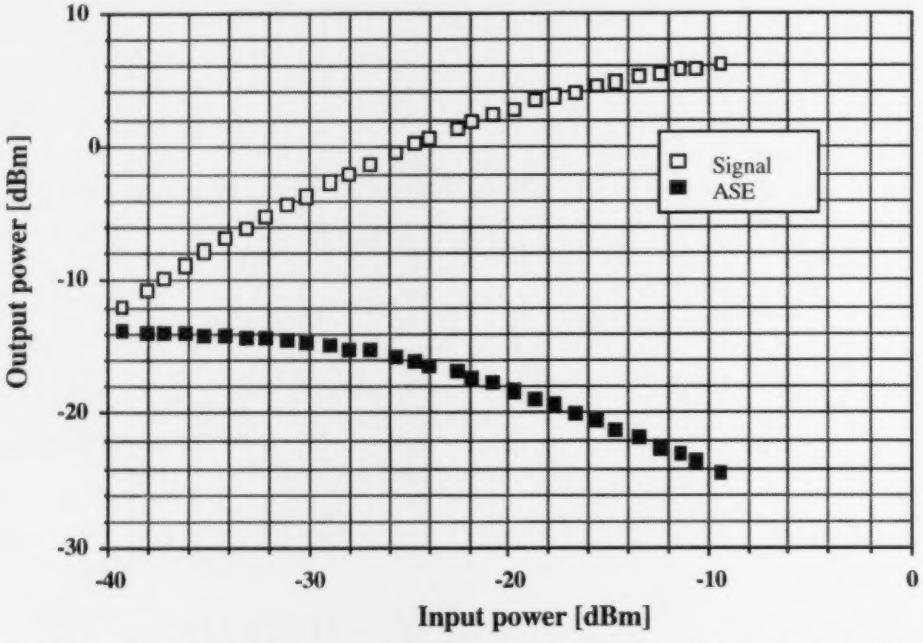

Figure 2.5 - Signal and ASE power saturation in erbium-doped fibre amplifier

For small input signal powers, the signal output power increases linearly with input power until the amplifier reaches saturation while the inband ASE power remains fairly constant. At high input powers, the output signal power saturates while the inband ASE power decreases steadily. Both output signal power and inband ASE power depend directly on the amplifier gain. We will study the gain variations with input signal power in the next section.

2.2.1.2 Gain variation with signal input power

The gain of the erbium-doped fibre amplifier is one of its most important characteristics, along with output saturation power and noise figure. Figure 2.6 shows a graph illustrating gain variation with signal input power for amplifier #302 with signal at 1536 nm, co-propagating with the pump at a power of 26 mW.

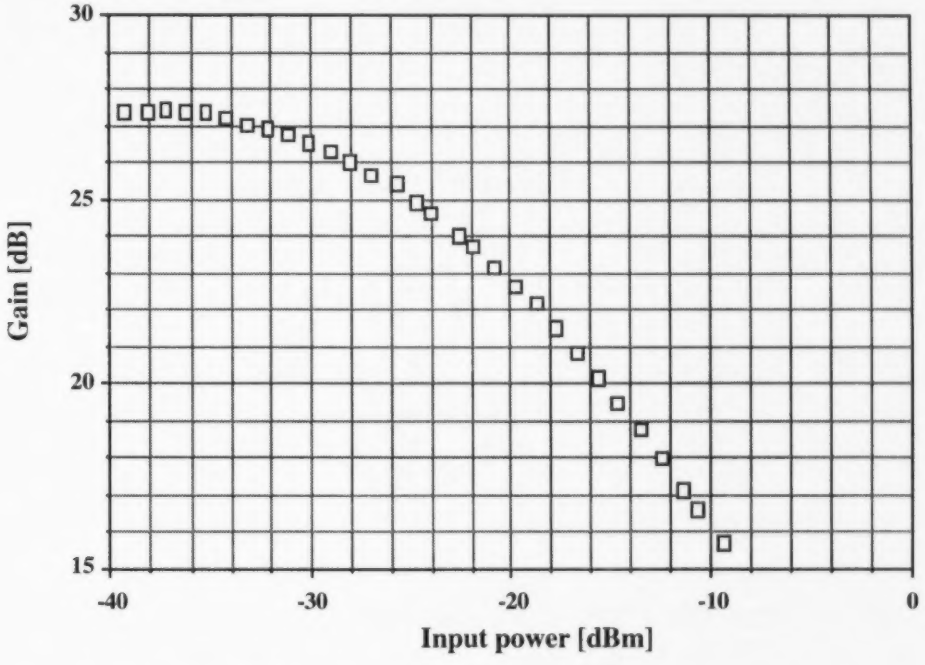

Figure 2.6 - Gain saturation of erbium-doped fibre amplifier

At very small input powers, the gain is independent of signal input power; for higher input powers, the gain characteristic saturates with increasing signal input powers. The output saturation power (P_{sat}) is defined as the output power at which the gain has decreased by 1/e or 4.3 dB from its small signal value (G_o).

$$P_{sat} = P_{in}G_{sat} \qquad \text{where} \qquad G_{sat} = \frac{G_o}{e} \qquad (2.19)$$

In Figure 2.6, a saturation power of 2.5 dBm for a small signal gain of 27.4 dB is measured. The output saturation power is an important characteristic of an erbium-doped fibre amplifier, since it tells how much output power one can expect out of the optical

amplifier for 4.3 dB gain compression. We will see in the next section that the output saturation power is wavelength dependent.

2.2.1.3 Gain compression variation with signal wavelength

We have seen that the gain of an erbium-doped fibre amplifier varies with total input power to the amplifier. We define gain compression by the difference in gain between the signal gain for a given input power P_{in} and the small signal gain, which is the signal gain for an input power of -35 dBm or less. The amount of gain compression at P_{in} is thus

$$\Delta G = G(P_{in}) - G_o \qquad (2.20)$$

The gain saturation characteristic of amplifier #302 with pump power of 26 mW and signal co-propagating with the pump, for several signal wavelengths is shown in Figure 2.7.

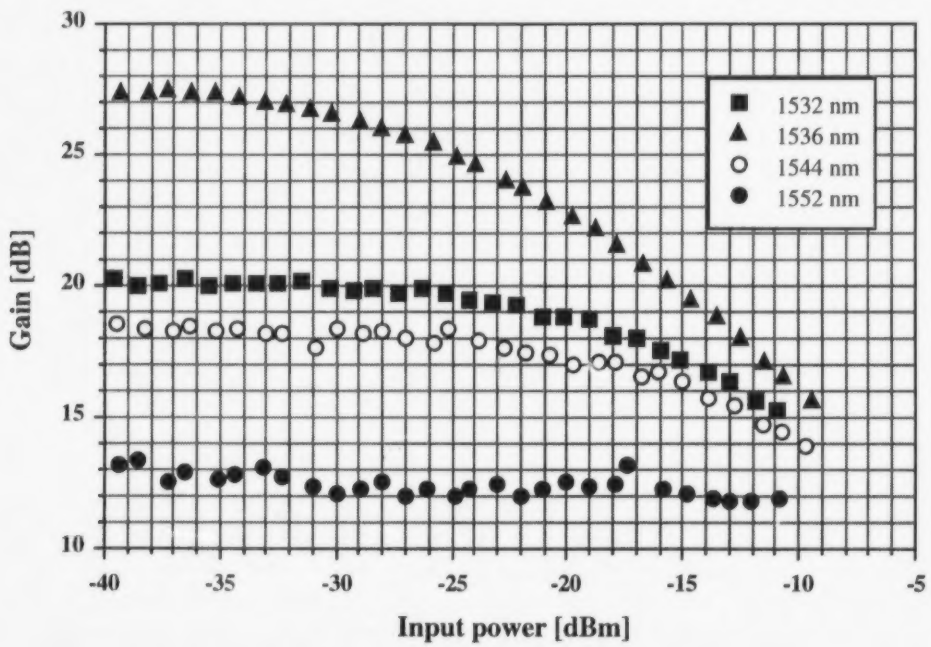

Figure 2.7 - EDFA gain variation with wavelength

We can see in Figure 2.7 that the amplifier gain varies with signal wavelength and power. The output saturation power and small signal gain will also be different for each signal wavelength. Signals at different wavelengths will thus experience different gain compression for different input powers. Variation of small signal gain and output saturated power with signal wavelength are shown in Figure 2.8 and Figure 2.9 for amplifier #302 with pump power of 26 mW and signal co-propagating with the pump.

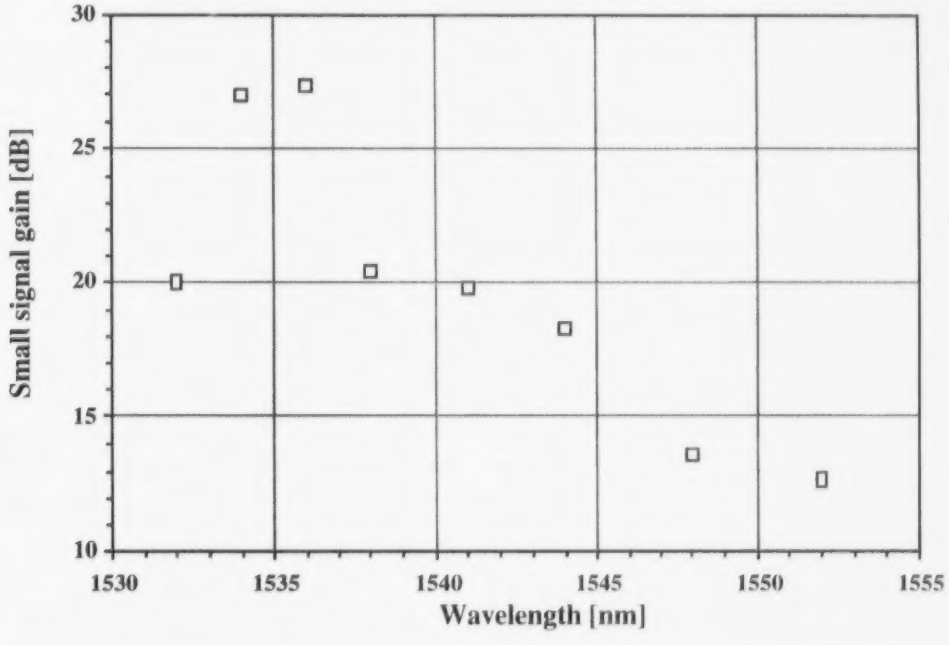

Figure 2.8 - Small signal gain variation with signal wavelength

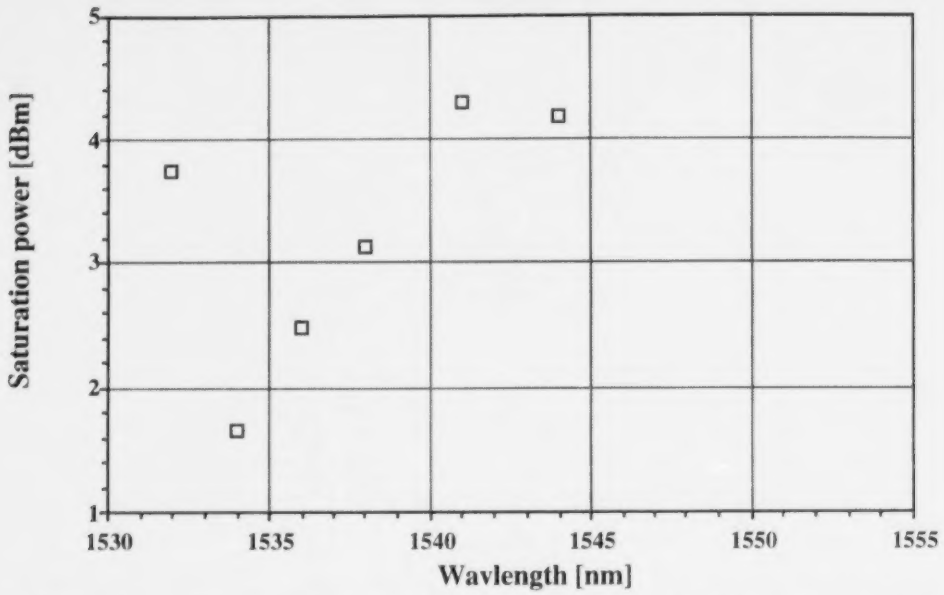

Figure 2.9 - Output saturation power variation with signal wavelength

All the data collected about the gain characteristics of the amplifier for different signal wavelengths now enable us to examine the gain compression behaviour with wavelength. The gain compression is computed as in (2.20) for cases of input powers P_{in}=-10 dBm and P_{in}=-20 dBm. Figure 2.10 illustrates the variation of gain compression with signal wavelength and input power in amplifier #302 with pump power of 26 mW and co-propagating signal and pump.

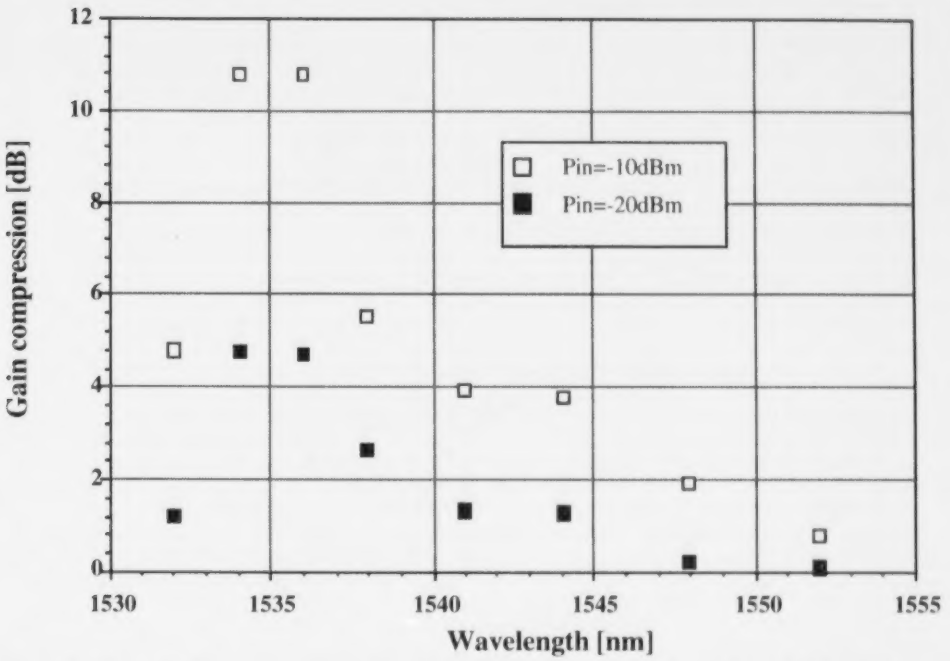

Figure 2.10 - Gain compression variation with wavelength and input power for an erbium-doped fibre amplifier

The gain compression characteristic of an erbium-doped amplifier is an important issue for multi-channel transmission with optical amplifiers. Multiplexed signals of different wavelengths transmitted together on the same fibre will experience different amounts of gain and gain compression if an EDFA is present in the transmission link. Moreover, the gain discrepancies will accumulate in cascaded amplifiers.

2.2.2 Amplified spontaneous emission

As shown in equation (2.10), ASE is gain dependent and thus varies with signal wavelength and power, and pump power. To study ASE power spectrum and compression, we used the experimental set-up shown in Figure 2.11.

The ASE compression experimental set-up is the same as the set-up used for the gain compression measurements except that the bandpass filter is replaced by a monochromator. We again use a polarization controller and splitter to separate signal and ASE components. This time, we are interested in the ASE part of the received light. We measure half of the forward ASE power at the output of the polarization splitter. The backward ASE power is

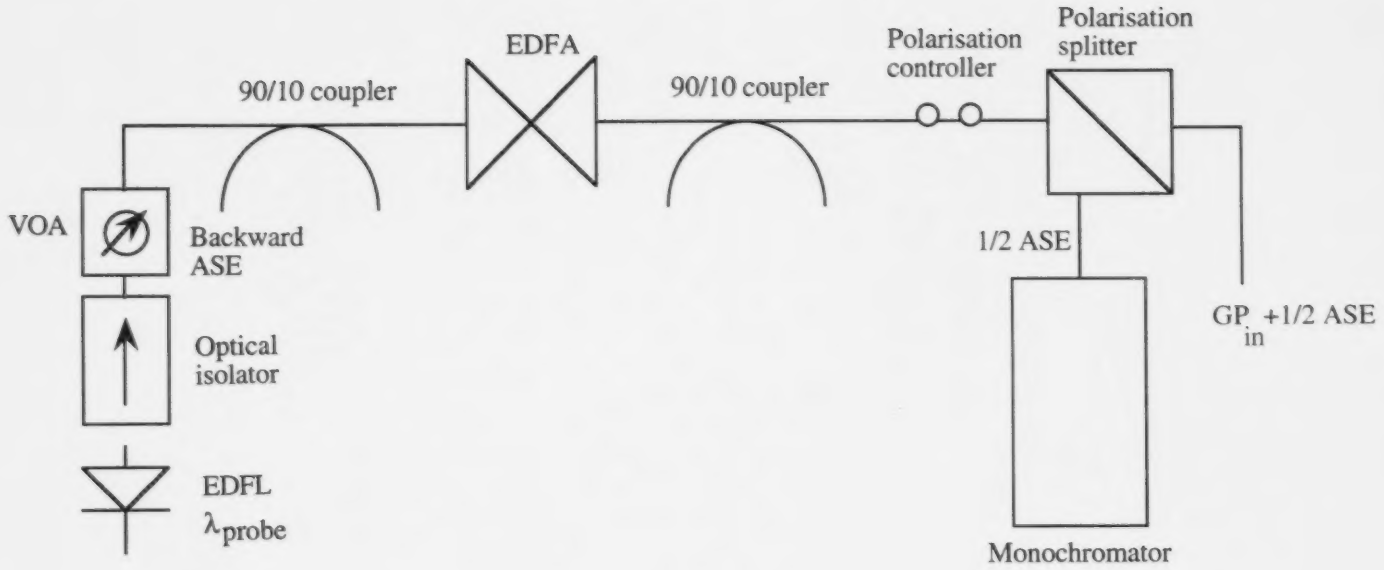

Figure 2.11 - ASE compression experimental setup - EDFL: Erbium-Doped Fibre Laser; VOA: Variable Optical Attenuator.

measured at the output of the 90/10 coupler before the amplifier. The erbium-doped fibre laser is used to launch a saturating signal in the system: -10 dBm for saturated regime, and -35 dBm for the small signal regime. We use the monochromator to scan wavelengths from 1530 nm to 1555 nm to measure the whole ASE spectrum.

2.2.2.1 ASE power spectrum

We used the experimental set-up depicted in Figure 2.11 to study the amplifier ASE characteristics. Figure 2.12 shows an example of the forward and backward ASE output spectrum of the optical amplifier #302 in small signal regime (input power of saturating signal at -35 dBm and wavelength at 1536 nm) with pump power of 26 mW and co-propagating pump and signal.

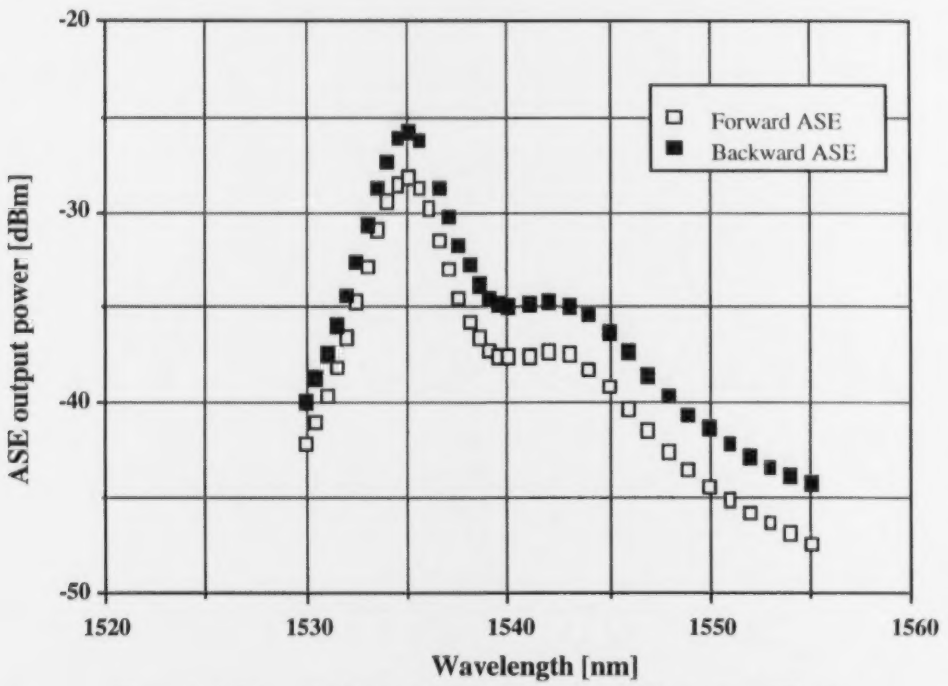

Figure 2.12 - Erbium-doped fibre amplifier amplified spontaneous emission spectrum

ASE is emitted in both directions from the amplifier. We define forward ASE as propagating with the signal and backward ASE as propagating contra-directionally with the signal, i.e. in the opposite direction. We noticed that backward ASE power is higher than

the forward ASE power whether the signal is co-propagating or contra-propagating with the pump: this is related to the population inversion in the fibre. The amount of ASE power at the output of the fibre, in both forward and backward directions, increases with pump power. For high pump power, where the population inversion is high, the difference between backward and forward ASE power decreases, the backward ASE power being larger than the forward ASE power [24]. In the case of complete population inversion, ASE output power in both direction would be almost equal. In the case of Figure 2.12, there is a significant difference between forward and backward ASE power because the fibre is pumped with relatively low power.

2.2.2.2 ASE compression

Since ASE arise from non-lasing fluorescence, it is gain dependent and compressed when the amplifier is in saturation. Over the ASE spectrum, ASE at different wavelengths will experience different levels of compression. The amount of ASE compression also varies with the saturating signal wavelength and power. ASE compression is computed as the difference between the small signal ASE (small or no saturating signal) and the saturated ASE power (large saturating signal). Figure 2.13 shows ASE compression variation with wavelength for different saturating wavelengths for amplifier #302 with pump power of 26 mW and co-propagating pump and signal. ASE compression has, in this case, been computed as the difference between the ASE powers for saturating signals at -35 dBm and -10 dBm.

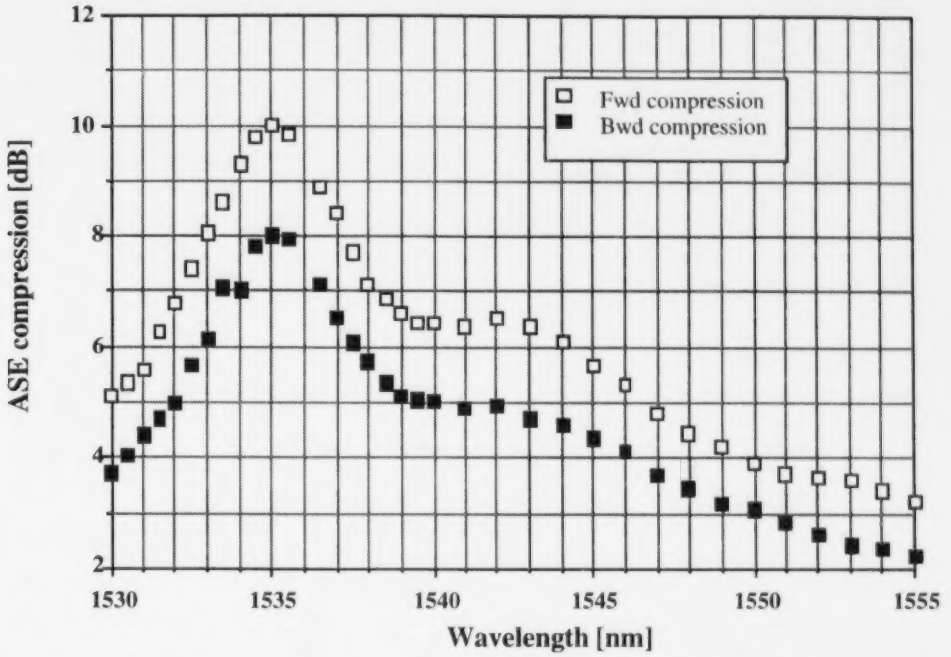

Figure 2.13 - Compression of amplified spontaneous emission in optical amplifier

From our series of measurements, we noticed that backward ASE compression is smaller than the forward ASE compression in all cases. The difference between forward and backward ASE compression is smaller for the contra-propagating pump and signal case than for the co-propagating pump and signal case. Forward ASE is more compressed in the co-propagating pump and signal case, but backward ASE is more compressed in the contra-propagating pump and signal case. A tentative explanation for this phenomenon is given in Figure 2.14.

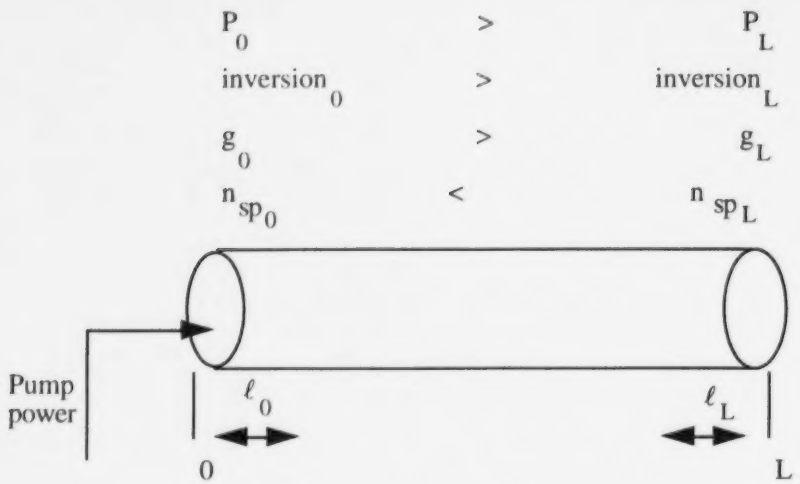

Figure 2.14 - Influence of pump power distribution on ASE generation

The amount of ASE generated in an incremental distance ℓ_L is larger than the amount of ASE generated in the same length of fibre ℓ_0 at the other end of the fibre because $n_{spL}>n_{sp0}$ since $g_L>g_0$ (refer to equation 2.12). Furthermore, the ASE contra-propagating with the pump travels in a direction where the gain is always increasing making the amount of output ASE contra-propagating with the pump power at end 0 of the fibre is larger than the amount of co-propagating output ASE at the end L of the fibre. The next diagram illustrates the direction of propagation of forward and backward ASE relative to the pump power.

Co-propagating pump and signal case

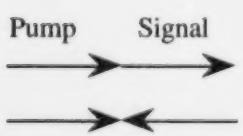

Forward ASE Backward ASE

- Forward ASE co-propagating with signal and co-propagating with pump
- Backward ASE contra-propagating with signal and contra-propagating with pump

Contra-propagating pump and signal case

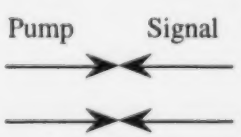

Backward ASE Forward ASE

- Forward ASE co-propagating with signal and contra-propagating with pump
- Backward ASE contra-propagating with signal and co-propagating with pump

As deduced from Figure 2.14, ASE contra-propagating with the pump is higher than ASE co-propagating with the pump. Forward ASE is contra-propagating with the pump in the contra-propagating pump and signal case and backward ASE is contra-propagating with the pump in the co-propagating pump and signal case. In each of these cases, the output forward and backward ASE respectively is larger and we effectively notice less compression.

2.2.3 Noise Figure

During the experimental study of the gain characteristic of the amplifier, we measured the ASE output power and the gain. The spontaneous emission factor can then be computed from the ASE output power, the gain of the amplifier, frequency of the signal, and equation (2.12). Figure 2.15 shows results of n_{sp} measurements for amplifier #302 with a signal at 1536 nm, co-propagating signal and pump, and pump power of 26 mW.

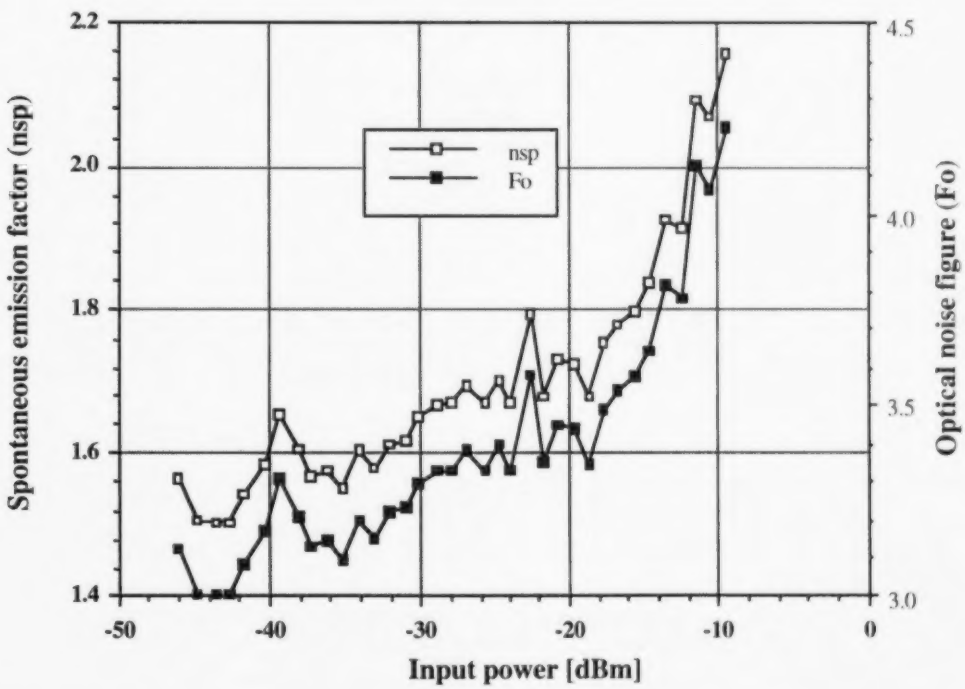

Figure 2.15 - Spontaneous emission factor and optical noise figure of amplifier

The optical noise figure, in decibel, is given by:

$$NF = 10\log(F_o) \qquad (2.21)$$

where F_O is calculated from equation 2.16.

The optical noise figure, which is gain dependent, also varies with wavelength and input power.

2.2.4 Bidirectional gain compression

In the previous sections, we looked at self-saturation in an EDFA: a single signal is launched and acts as a probe and a saturating signal at the same time. In this section, we will explore another possibility with EDFAs: bidirectional transmission. Optical amplifiers operating under bidirectional transmission will also exhibit gain and ASE saturation and compression, but now, two signals are saturating the amplifiers. To study the gain characteristics of bidirectional amplifiers, we designed the set-up shown in Figure 2.16.

A probe and a saturating signal propagate in opposite directions and both undergo gain in the amplifier. The probe is a small signal (-35 dBm) while the saturating signal power is varied. A combination of a polarization controller and a polarization splitter is used to separate the ASE and signal components of the output power.

The gain characteristics of the saturating signal are basically the same as in the self-saturating case discussed previously since the addition of a small probe signal does not have a significant effect on the large saturating signal. Thus, here we will concentrate on examining the influence of the saturating signal on a small probe signal. An EDFL is used as the saturating source: its operating wavelength is varied from 1530 nm to 1555 nm and its output power is varied from -40 dBm to -10 dBm. Two DFB lasers at 1551 nm and 1539 nm are used alternatively as the probe source with an output power of only -35 dBm. With the experimental set-up illustrated in Figure 2.16, we measured output probe signal power, forward ASE, probe signal gain, and forward noise figure variations with saturating signal input power.

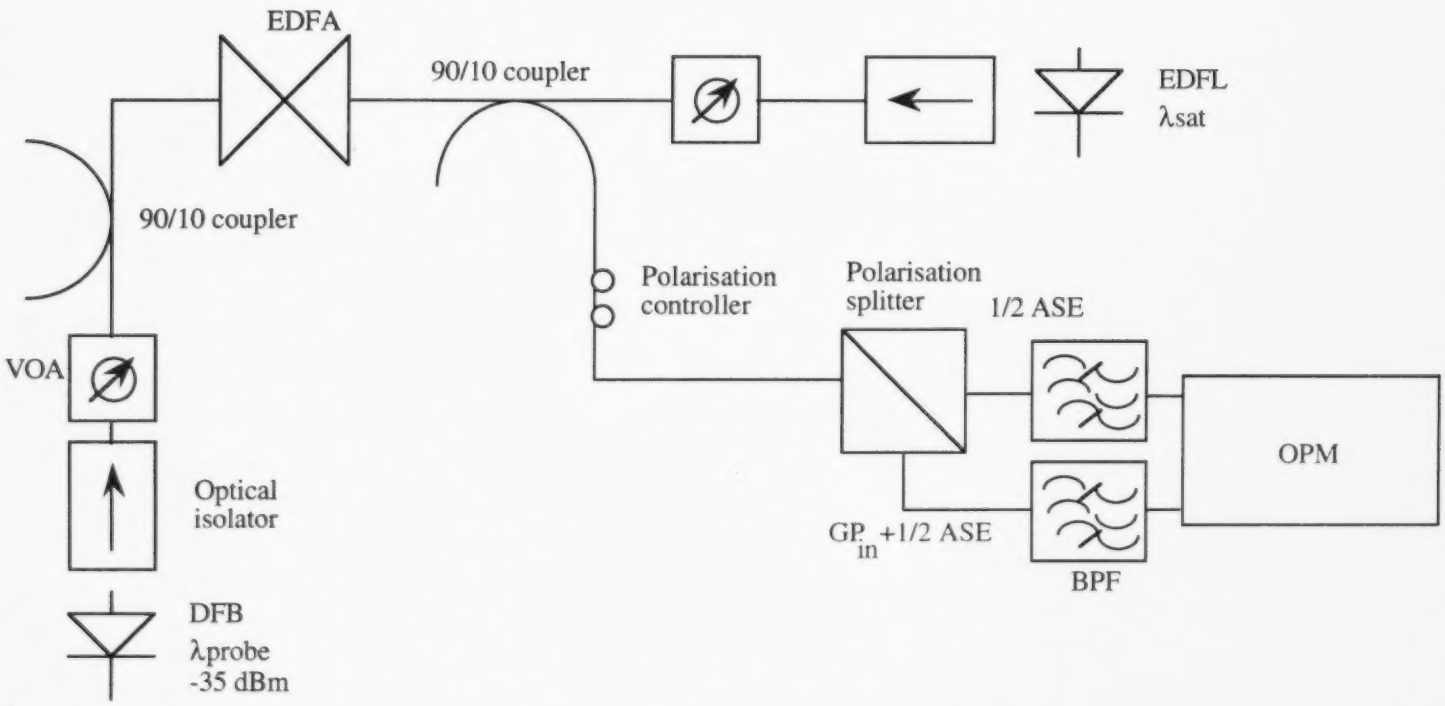

Figure 2.16 - Bidirectional gain experimental setup - EDFL: Erbium-Doped Fibre Laser; VOA: Variable Optical Attenuator; EDFA: Erbium-Doped Fibre Amplifier; BPF: Bandpass Filter; DFB: Distributed Feedback laser; OPM: Optical Power Meter.

Figure 2.17 shows the signal gain compression in amplifier #302, for two different probe wavelengths, varying with saturating signal wavelength. The probe signal is launched at a power of -35 dBm, the saturating signal at -10 dBm; the probe signal is co-propagating with the pump.

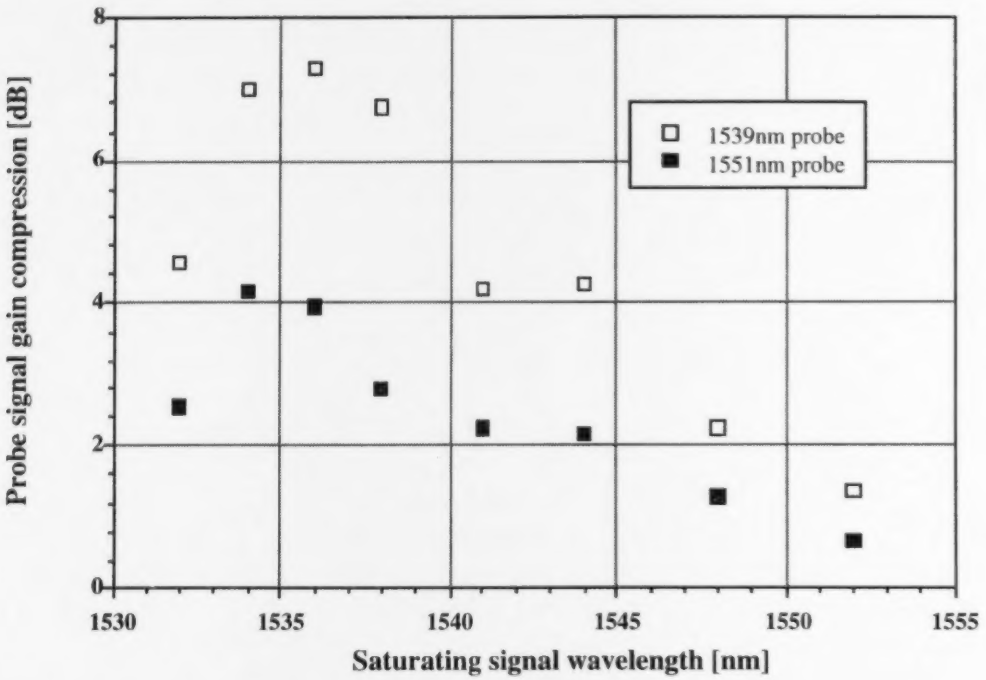

Figure 2.17 - Bidirectional gain compression in erbium-doped fibre amplifier

As was the case in section 2.2.1.3 for a self-saturating amplifier, the gain compression in a bidirectional amplifier varies with wavelength. The amount of gain compression does not only vary with the saturating signal wavelength but it also varies with the probe signal wavelength.

As we recall from equation (2.5), the gain coefficient of the erbium-doped fibre varies with the absorption and emission cross-sections and the level population densities. If we define the relative inversion as

$$D = \frac{N_2 - N_1}{\rho} \qquad (2.22)$$

where N_1 : population density of level 1

N_2 : population density of level 2

ρ: total population density

we can rewrite the gain coefficient as

$$g(\lambda) = \frac{\rho}{2}[\sigma_e(\lambda_s)(1+D) - \sigma_a(\lambda_s)(1-D)] \qquad (2.23)$$

The gain compression the amplifier undergoes is the difference between the gain at $P_{in,1}$ and the gain at $P_{in,2}$.

$$\Delta g(\lambda) = g(\lambda)\big|_{Pin2} - g(\lambda)\big|_{Pin1} = \frac{\rho}{2}[\sigma_e(\lambda_s) + \sigma_a(\lambda_s)]\Delta D \qquad (2.24)$$

where $\Delta D = D|_{Pin2} - D|_{Pin1}$

From equation (2.24), we see that the gain compression is wavelength dependent and will be different for signals at different wavelengths. This is consistent with our experimental results. Moreover, our results show that the gain compression for a given probe signal wavelength also varies with the saturating signal wavelength. Comparison of our results and equation (2.24) leads us to conclude that the relative inversion is wavelength dependent, thus giving

$$\Delta g(\lambda_s) = \frac{\rho}{2}[\sigma(\lambda_s) + \sigma(\lambda_s)]\Delta D(\lambda_s, \lambda_{sat}) \qquad (2.25)$$

The relative inversion can be expressed as:

$$D = \frac{N_2 - N_1}{\rho} = \frac{\rho\left[\frac{R\tau + W_{12}\tau}{1 + R\tau + W_{12}\tau + W_{21}\tau}\right] - \rho\left[\frac{1 + W_{21}\tau}{1 + R\tau + W_{12}\tau + W_{21}\tau}\right]}{\rho} \qquad (2.26)$$

$$= \frac{R\tau + W_{12}\tau - W_{21}\tau - 1}{1 + R\tau + W_{12}\tau + W_{21}\tau}$$

In the case of multi-wavelength input power, the emission and absorption rates can be expressed as [23]:

$$W_{12}(r,z,\nu)=\frac{1}{\tau}\sum_{k}\frac{P_s(z,\nu_k)}{(1+\eta_k)P_{sat}(\nu_k)}\psi_{sk}(r) \qquad (\mathbf{2.27})$$
$$W_{21}(r,z,\nu)=\eta_k W_{12}(r,z,\nu)$$

Where $\psi_{sk}(r)$ is the mode envelope and $P_{sat}(\nu_k)$ is the signal saturation power at wavelength λ_k. The variation in relative inversion, ΔD, is thus dependent on each and every signal wavelength entering the amplifier. This not only applies to multi-signal situations but to the ASE continuum in wavelength.

The results on bidirectional transmission presented in this section show that in bidirectional EDFAs, the gain depends on the wavelength and power of both transmitted signals, and that the signals affect each other's gain. This will be an important fact to consider in chapter 4 when we experiment in laboratory with a bidirectional cascade of three amplifiers.

3. Bidirectional transmission system modelling and simulation

Giles and Desurvire published a paper in February 1991 presenting a model for the propagation of signal and noise in concatenated erbium-doped fibre amplifiers (EDFAs) [16]. They studied the signal and ASE propagation through a cascade of N identical amplifiers with optical filters after each of the amplifiers to filter out the broadband ASE. The model only describes a unidirectional system and does not take into account the Rayleigh backscattering of the light along the fibre links. In this chapter, we will expand from Giles and Desurvire's model to study signal and ASE propagation in an open cascade of EDFAs. The system studied is bidirectional and we take the Rayleigh backscattering into account.

In section 3.1 we give a brief description of the system under study, we then present our model in section 3.2, followed by a study of the optical SNR at the receiver end in section 3.3, some numerical applications in section 3.4, and results of computer simulations in section 3.5.

3.1 System description

The transmission system under study, shown in Figure 3.1, comprises a series of EDFAs concatenated with transmission fibre. The amplifiers are not necessarily all the same. No filters or isolators are present so as to allow bidirectional transmission of signals. In such a system, the full spectrum of the ASE is allowed to build up along the way and Rayleigh backscattering of signal and ASE is present along the fibre links. Notions of Rayleigh scattering are presented in appendix A. We present a model for the transmission of both contra-propagating signals (the two signals are launched at opposite ends of the transmission system and propagate in opposite directions; co-propagating signals would be propagating in the same direction) and ASE as well as the backscattered light along the system. With such a model, we can try to assess the impact of Rayleigh backscattering and broadband ASE in a bidirectional system as well as try to optimize the system parameters. We will also present equations for the received power and optical signal-to-noise ratio at each receiver.

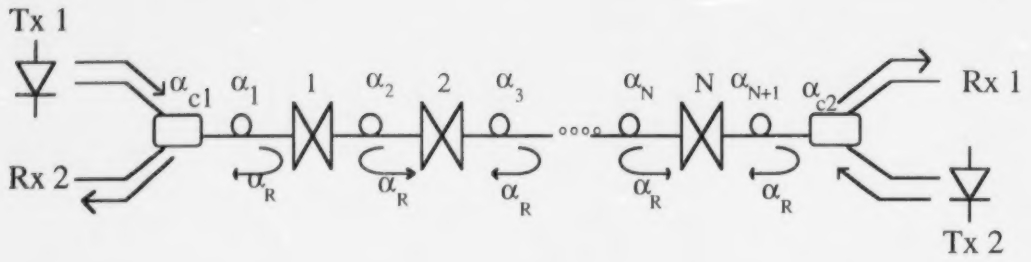

Figure 3.1 - System under study - α_i : loss of the ith transmission fibre link ; α_R : Rayleigh backscattering coefficient; α_{c1},α_{c2} : coupling losses; Tx : transmitter; Rx : receiver.

3.2 Transmission model

To characterize signal and ASE propagation in an open cascade of EDFAs, we have first to look at the propagation of the different components of the light in the system: signal, ASE, and backscattered light. For simplicity, we will follow the derivation of the model for a cascade of three amplifiers and then generalize to a cascade of N amplifiers. Throughout this thesis we define the forward-propagating signal as light propagating from amplifier 1 to amplifier N, the backward signal propagates from amplifier N to amplifier 1.

3.2.1 System equations for a cascade of three amplifiers

We present here a derivation of the system equation for a cascade of only three amplifiers. This serves to illustrate how signal and ASE propagate along the cascade and to show how we achieve the derivation of the general N-amplifier cascade model. A bidirectional cascade of three optical amplifiers is shown in Figure 3.2. Signals with different powers are launched at each end of the system: P_f in the forward direction and P_b in the backward direction. Transmission fibre links the amplifiers together and we consider Rayleigh backscattering along the fibre to be present; the model is restricted to exclude double Rayleigh backscattering where light undergoes two Rayleigh scattering events and winds up travelling in the same direction as it started out in.

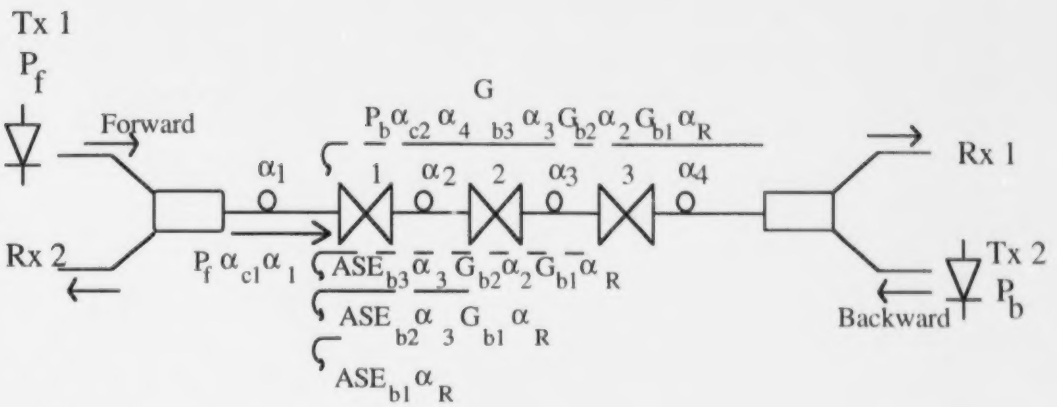

Figure 3.2 - Propagation of signal and noise in a three amplifier cascade

There are four distinct components of the forward input power to an amplifier in a bidirectional cascade (Figure 3.2 for reference):

1) Propagation of P_f in the forward direction from its transmitter to amplifier i;
2) Propagation of P_b in the backward direction from its transmitter through amplifier i, and then Rayleigh backscattered into the input of amplifier i;
3) Emission and propagation of forward ASE from all previous amplifiers (amplifier 1 to amplifier i-1) to amplifier i;
4) Emission and propagation of backward ASE from all the amplifiers then backscattered into the input of amplifier i.

The forward input power to the first amplifier is then given by

$$P_{fin,1}(\nu) = P_f(\nu)\alpha_{c1}\alpha_1 + P_b(\nu)\alpha_{c2}\alpha_4 G_{b3}(\nu)\alpha_3 G_{b2}(\nu)\alpha_2 G_{b1}(\nu)\alpha_R + ASE_{b1}(\nu)\alpha_R + ASE_{b2}(\nu)\alpha_2 G_{b1}(\nu)\alpha_R + ASE_{b3}(\nu)\alpha_3 G_{b2}(\nu)\alpha_2 G_{b1}(\nu)\alpha_R \quad \textbf{(3.1)}$$

Where $ASE_{fi}(\nu)=2n_{sp,fi}(\nu)h\nu\Delta\nu(G_{fi}(\nu)-1)$ and $ASE_{bi}(\nu)=2n_{sp,bi}(\nu)h\nu\Delta\nu(G_{bi}(\nu)-1)$ are the forward and backward ASE spectra generated by the ith amplifier in the cascade.

Now taking a look at the forward input power to the second amplifier, we get

$$P_{fin,2}(\nu) = P_f(\nu)\alpha_{c1}\alpha_1 G_{f1}(\nu)\alpha_2 + P_b\alpha_{c2}\alpha_4 G_{b3}(\nu)\alpha_3 G_{b2}(\nu)\alpha_R$$
$$+ P_b(\nu)\alpha_{c2}\alpha_4 G_{b3}(\nu)\alpha_3 G_{b2}(\nu)\alpha_2 G_{b1}(\nu)\alpha_R G_{f1}(\nu)\alpha_2 + ASE_{f1}(\nu)\alpha_2$$
$$+ASE_{b1}(\nu)\alpha_R G_{f1}(\nu)\alpha_2 + ASE_{b2}(\nu)\alpha_R + ASE_{b2}(\nu)\alpha_2 G_{b1}(\nu)\alpha_R G_{f1}(\nu)\alpha_2$$
$$+ASE_{b3}(\nu)\alpha_3 G_{b2}(\nu)\alpha_R + ASE_{b3}(\nu)\alpha_3 G_{b2}(\nu)\alpha_2 G_{b1}(\nu)\alpha_R G_{f1}(\nu)\alpha_2$$

(3.2)

In the same way, we can derive an expression for the forward input power to the last amplifier in the link.

$$P_{fin,3}(\nu) = P_f(\nu)\alpha_{c1}\alpha_1 G_{f1}(\nu)\alpha_2 G_{f2}(\nu)\alpha_3 + P_b(\nu)\alpha_{c2}\alpha_4 G_{b3}(\nu)\alpha_R$$
$$+P_b(\nu)\alpha_{c2}\alpha_4 G_{b3}(\nu)\alpha_3 G_{b2}(\nu)\alpha_R G_{f2}(\nu)\alpha_3$$
$$+P_b(\nu)\alpha_{c2}\alpha_4 G_{b3}(\nu)\alpha_3 G_{b2}(\nu)\alpha_2 G_{b1}(\nu)\alpha_R G_{f1}(\nu)\alpha_2 G_{f2}(\nu)\alpha_3$$
$$+ASE_{f1}(\nu)\alpha_2 G_{f2}(\nu)\alpha_3 + ASE_{f2}(\nu)\alpha_3 + ASE_{b1}(\nu)\alpha_R G_{f1}(\nu)\alpha_2 G_{f2}(\nu)\alpha_3$$
$$+ASE_{b2}(\nu)\alpha_R G_{f2}(\nu)\alpha_3 + ASE_{b2}(\nu)\alpha_2 G_{b1}(\nu)\alpha_R G_{f1}(\nu)\alpha_2 G_{f2}(\nu)\alpha_3$$
$$+ASE_{b3}(\nu)\alpha_R + ASE_{b3}(\nu)\alpha_3 G_{b2}(\nu)\alpha_R G_{f2}(\nu)\alpha_3$$
$$+ASE_{b3}(\nu)\alpha_3 G_{b2}(\nu)\alpha_2 G_{b1}(\nu)\alpha_R G_{f1}(\nu)\alpha_2 G_{f2}(\nu)\alpha_3$$

(3.3)

We can write the input power to each amplifier in a shorter form if we realize that there is a pattern that enables us to use summations and products. An analysis for the backward input power to each amplifier can also be derived in a similar fashion. Here are the system equations for a cascade of three amplifiers.[1] The next section will look at the general case of an N amplifier cascade.

$$P_{fin,1}(\nu) = P_f(\nu)\alpha_{c1}\alpha_1 + P_b(\nu)\alpha_{c2}\alpha_R \prod_{j=1}^{3}[\alpha_{j+1} G_{bj}(\nu)] + ASE_{b1}(\nu)\alpha_R$$
$$+ \sum_{j=2}^{3}\{ASE_{bj}(\nu)\alpha_R \prod_{k=1}^{j-1}[\alpha_{k+1} G_{bk}(\nu)]\}$$

(3.4)

---

[1] The reader should take note that we used the following definition throughout this paper: a sum (Σ) or product (Π) with illegal limits (upper limit smaller than lower limit) is assumed to be equal to one.

$$P_{fin,2}(\nu)= P_f(\nu)\alpha_{c1}\alpha_1 G_{f1}(\nu)\alpha_2 + P_b(\nu)\alpha_{c2}\alpha_R \prod_{j=2}^{3}[\alpha_{j+1}G_{bj}(\nu)]\{1+\alpha_2^2 G_{b1}(\nu)G_{f1}(\nu)\}$$

$$+\{ASE_{f1}(\nu)\alpha_2\}+\sum_{j=1}^{2}\{ASE_{bj}(\nu)\alpha_R \prod_{k=j}^{1}[\alpha_{k+1}G_{fk}(\nu)]\{1+\sum_{p=1}^{j-1}\{\prod_{m=p}^{j-1}[\alpha_{m+1}^2 G_{fm}(\nu)G_{bm}(\nu)]\}\}\}$$

$$+ASE_{b3}(\nu)\alpha_R\alpha_3 G_{b2}(\nu)\{1+\alpha_2^2 G_{f1}(\nu)G_{b1}(\nu)\}$$

(3.5)

$$P_{fin,3}(\nu)= P_f(\nu)\alpha_{c1}\alpha_1 \prod_{j=1}^{2}[G_{fj}(\nu)\alpha_{j+1}]$$

$$+ P_b(\nu)\alpha_{c2}\alpha_R\alpha_4 G_{b3}(\nu)\{1+\sum_{j=1}^{2}\{\prod_{k=j}^{2}[\alpha_{k+1}^2 G_{bk}(\nu)G_{fk}(\nu)]\}\}$$

$$+\sum_{j=1}^{2}\{ASE_{fj}(\nu)\prod_{k=j+1}^{3}[\alpha_k]\prod_{m=j+1}^{2}[G_{fm}(\nu)]$$

$$+\sum_{j=1}^{3}\{ASE_{bj}(\nu)\alpha_R \prod_{k=j}^{2}[\alpha_{k+1}G_{fk}(\nu)]\{1+\sum_{p=1}^{j-1}\{\prod_{m=p}^{j-1}[\alpha_{m+1}^2 G_{fm}(\nu)G_{bm}(\nu)]\}\}\}$$

(3.6)

$$P_{bin,1}(\nu)= P_b(\nu)\alpha_{c2}\alpha_4 \prod_{j=2}^{3}[G_{fj}(\nu)\alpha_j]$$

$$+P_f(\nu)\alpha_{c1}\alpha_R\alpha_1 G_{f1}(\nu)\{1+\sum_{m=2}^{3}\{\prod_{k=2}^{m}[\alpha_k^2 G_{fk}(\nu)G_{bk}(\nu)]\}\}$$

$$+\sum_{j=2}^{3}\{ASE_{bj}(\nu)\prod_{k=2}^{j}[\alpha_k]\prod_{m=2}^{j-1}[G_{bm}(\nu)]\} \qquad \textbf{(3.7)}$$

$$+\sum_{j=1}^{3}ASE_{fj}(\nu)\alpha_R\{1+\sum_{p=j+1}^{3}\{\prod_{m=j+1}^{p}[\alpha_m^2 G_{fm}(\nu)G_{bm}(\nu)]\}\}$$

$$P_{bin,2}(\nu)= P_b(\nu)\alpha_{c2}\alpha_4 G_{b3}(\nu)\alpha_3 + P_f(\nu)\alpha_{c1}\alpha_R \prod_{j=1}^{2}[\alpha_j G_{fj}(\nu)]\{1+\alpha_3^2 G_{f3}(\nu)G_{b3}(\nu)\}$$

$$+ASE_{b3}(\nu)\alpha_3 + ASE_{f1}(\nu)\alpha_R\alpha_2 G_{f2}(\nu)\{1+\alpha_3^2 G_{f3}(\nu)G_{b3}(\nu)$$

$$+\sum_{j=2}^{3}\{ASE_{fj}(\nu)\alpha_R\{1+\sum_{p=j+1}^{3}\{\prod_{m=j+1}^{p}[\alpha_m^2 G_{fm}(\nu)G_{bm}(\nu)]\}\}\}$$

(3.8)

$$P_{bin,3}(\nu)= P_b(\nu)\alpha_{c2}\alpha_3 + P_f(\nu)\alpha_{c1}\alpha_R \prod_{j=1}^{3}[\alpha_j G_{fj}(\nu)] + P_f(\nu)\alpha_{c1}\alpha_R \prod_{j=1}^{3}[\alpha_j G_{fj}(\nu)]$$

$$+\sum_{j=1}^{2}\{ASE_{fj}\alpha_R \prod_{k=j+1}^{3}[\alpha_k G_{fk}(\nu_f)]\} + ASE_{f3}(\nu)\alpha_R$$

(3.9)

3.2.2 Propagation model for a cascade of N amplifiers

We will now derive a model for the propagation of signal and ASE in a bidirectional cascade of an arbitrary number N erbium-doped fibre amplifiers. The approach is very similar to what we did in the previous section for a cascade of three amplifiers, but now we have an undefined number of amplifiers. Deriving the equations here is just a matter of expanding the equations of section 3.2.1 to the general case of an N amplifier cascade.

The system under study is shown in Figure 3.1. The contribution to the forward input to the ith amplifier in the chain due to various sources is given by:

- Propagation of forward signal :

$$P_{fsig,i}(\nu)= P_f(\nu)\alpha_{c1}\alpha_1 \prod_{j=1}^{i-1}[G_{fj}(\nu)\alpha_{j+1}] \qquad \textbf{(3.10)}$$

- Rayleigh backscattering of backward signal :

$$RB_{bsig,i}(\nu) = P_b(\nu)\alpha_{c2}\alpha_R \prod_{j=i}^{N}[\alpha_{j+1}G_{bj}(\nu)]\{1+\sum_{m=1}^{i-1}\{\prod_{k=m}^{i-1}[\alpha_{k+1}^2 G_{bk}(\nu)G_{fk}(\nu)]\}\}$$

(3.11)

- Generation and propagation of forward ASE :

$$P_{fASE,1}(\nu) = 0$$

$$P_{fASE,i}(\nu)=\sum_{j=1}^{i-1}\{2n_{sp}h\nu\Delta\nu(G_{fj}(\nu)-1)\prod_{k=j+1}^{i}[\alpha_k]\prod_{m=j+1}^{i-1}[G_{fm}(\nu)]\} \qquad 2\le i\le N$$

(3.12)

- Rayleigh backscattering of backward ASE :

$$RB_{bASE,i}(\nu) = \sum_{j=1}^{i}\{2n_{sp}h\nu\Delta\nu(G_{bj}(\nu)-1)\alpha_R\prod_{k=j}^{i-1}[\alpha_{k+1}G_{fk}]\{1+$$

$$\sum_{p=1}^{j-1}\{\prod_{m=p}^{j-1}[\alpha_{m+1}^2 G_{fm}(\nu)G_{bm}(\nu)]\}\}$$

$$+\sum_{j=i+1}^{N}\{2n_{sp}h\nu\Delta\nu(G_{bj}(\nu)-1)\alpha_R\prod_{k=i}[\alpha_{k+1}G_{bk}]\{1+$$

$$\sum_{p=1}^{i-1}\{\prod_{m=p}^{i-1}[\alpha_{m+1}^2 G_{fm}(\nu)G_{bm}(\nu)]\}\}$$

(3.13)

- Total forward input to the ith amplifier :

$$P_{fin,i} = P_{fsig,i} + RB_{bsig,i} + P_{fASE,i} + RB_{bASE,i} \qquad \textbf{(3.14)}$$

The contribution to the backward input power to the ith amplifier due to various sources is given by:

- Propagation of backward signal :

$$P_{bsig,i}(\nu)=P_b(\nu)\alpha_{c2}\alpha_{N+1}\prod_{j=i+1}^{N}[G_{bj}(\nu)\alpha_j] \quad \textbf{(3.15)}$$

- Rayleigh backscattering of forward signal :

$$RB_{fsig,i}(\nu)=P_f\alpha_{c1}\alpha_R\prod_{j=1}^{i}[\alpha_j G_{fj}(\nu)]\{1+\sum_{m=i+1}^{N}\{\prod_{k=i+1}^{m}[\alpha_k^2 G_{fk}(\nu)G_{bk}(\nu)]\}\} \quad \textbf{(3.16)}$$

- Generation and propagation of backward ASE :

$$P_{bASE,i}(\nu)=\sum_{j=i+1}^{N}\{2n_{sp}h\nu\Delta\nu(G_{bj}(\nu)-1)\prod_{k=i+1}^{j}[\alpha_k]\prod_{m=i+1}^{j-1}[G_{bm}(\nu)]\} \qquad 1\le i\le N-1$$

$$P_{bASE,N}(\nu) = 0$$

(3.17)

- Raleigh backscattering of forward ASE :

$$\begin{aligned}RB_{fASE,i}(\nu) = &\sum_{j=1}^{i-1}\{2n_{sp}h\nu\Delta\nu(G_{fj}(\nu)-1)\alpha_R\prod_{k=j+1}^{i}[\alpha_k G_{fk}(\nu)]\{1+\\ &\sum_{p=i+1}^{N}\{\prod_{m=i+1}^{p}[\alpha_m^2 G_{fm}(\nu)G_{bm}(\nu)]\}\}\\ &+\sum_{j=i}^{N}\{2n_{sp}h\nu\Delta\nu(G_{fj}(\nu)-1)\alpha_R\prod_{k=j+1}^{i}[\alpha_k G_{bk}(\nu)]\{1+\\ &\sum_{p=j+1}^{N}\{\prod_{m=j+1}^{p}[\alpha_m^2 G_{fm}(\nu)G_{bm}(\nu)]\}\}\end{aligned}$$

(3.18)

- Total backward input power to the ith amplifier :

$$P_{bin,i} = P_{bsig,i} + RB_{fsig,i} + P_{bASE,i} + RB_{fASE,i} \quad \textbf{(3.19)}$$

The total input power to each amplifier is the sum of the forward and backward output power.

$$P_{in,i} = P_{fin,i} + P_{bin,i} \quad (3.20)$$

The equations presented in this section are the base for the system propagation model. One can use this model to study the influence of Rayleigh backscattering and ASE build-up on the performance of the system or to evaluate the influence of some system parameters such as amplifier gain, inter-amplifier link loss, signal power and wavelength. Computer programs based on the model equations can be written to find numerical solutions or to generate simulations of a bidirectional cascade of fibre amplifiers. We present some examples of numerical applications in section 3.4.

3.3 Optical signal to noise ratio at the receiver end

After propagating through the cascade of amplifiers, both signals reach their respective receivers. We will here look at the optical signal to noise ratio at the receiver end.

The forward propagating signal will reach receiver 1 at one end of the cascade while the backward propagating signal will reach receiver 2 at the other end. The received power can be expressed as

$$REC_1(\nu) = P_{fin,N}(\nu) G_{fN}(\nu) \alpha_{N+1} \alpha_{c2} + ASE_{f,N} \alpha_{N+1} \alpha_{c2} + P_b(\nu) \alpha_{c2}^2 \alpha_R \quad (3.21)$$

$$REC_2(\nu) = P_{bin,1}(\nu) G_{b1}(\nu) \alpha_1 \alpha_{c1} + ASE_{b,1} \alpha_1 \alpha_{c1} + P_f(\nu) \alpha_{c1}^2 \alpha_R \quad (3.22)$$

Using equations (3.10) to (3.19), we get

$$REC_1(\nu)=\{P_f(\nu)\alpha_{c1}\alpha_1\prod_{j=1}^{N-1}[G_{fj}(\nu)\alpha_{j+1}]$$
$$+P_b(\nu)\alpha_{c2}\alpha_R\alpha_{N+1}G_{bN}(\nu)\{1+\sum_{m=1}^{N-1}\{\prod_{k=m}^{N-1}[\alpha_{k+1}^2G_{bk}(\nu)G_{fk}(\nu)]\}\}$$
$$+\sum_{j=1}^{N-1}\{2n_{sp}h\nu\Delta\nu(G_{fj}(\nu)-1)\prod_{k=j+1}^{N}[\alpha_k]\prod_{m=j+1}^{N-1}[G_{fm}(\nu)]\}$$
$$+\sum_{j=1}^{N}\{2n_{sp}h\nu\Delta\nu(G_{bj}(\nu)-1)\alpha_R\prod_{k=j}^{N-1}[\alpha_{k+1}G_{fk}(\nu)]\{1+\sum_{p=1}^{j-1}\{\prod_{m=p}^{j-1}[\alpha_{k+1}^2G_{bk}(\nu_b)G_{fk}(\nu_b)]\}\}\}G_{fN}(\nu)\alpha_{N+1}\alpha_{c2}$$
$$+2n_{sp}h\nu\Delta\nu(G_{fN}(\nu)-1)\alpha_{N+1}\alpha_{c2}+P_b(\nu)\alpha_{c2}\alpha_R$$

(3.23)

$$REC_2(\nu)=\{P_b(\nu)\alpha_{c2}\alpha_{N+1}\prod_{j=2}^{N}[G_{bj}(\nu)\alpha_j]+P_f(\nu)\alpha_{c1}\alpha_R\alpha_1G_{f1}(\nu)\{1+\sum_{j=2}^{N}\{\prod_{k=2}^{j}[\alpha_k^2G_{fk}(\nu)G_{bk}(\nu)]\}\}$$
$$+\sum_{j=2}^{N}\{2n_{sp}h\nu\Delta\nu(G_{bj}(\nu)-1)\prod_{k=2}^{j}[\alpha_k]\prod_{m=2}^{j-1}[G_{bm}(\nu)]\}$$
$$+\sum_{j=1}^{N}\{2n_{sp}h\nu\Delta\nu(G_{fj}(\nu)-1)\alpha_R\{1+\sum_{p=j+1}^{N}\{\prod_{m=j+1}^{p}[\alpha_m^2G_{fm}(\nu_f)G_{bm}(\nu_f)]\}\}\}G_{b1}(\nu)\alpha_1\alpha_{c1}$$
$$+2n_{sp}h\nu\Delta\nu(G_{b1}(\nu)-1)\alpha_1\alpha_{c1}+P_f(\nu)\alpha_{c1}\alpha_R$$

(3.24)

If we use a filter of bandwidth B_o in front of the receiver to filter out the second signal and the broadband ASE, we can express the received signal and inband ASE as:

$$REC_{1,signal}=P_f(\nu_f)\alpha_{c1}\alpha_{c2}\alpha_1\prod_{j=1}^{N}[G_{fj}(\nu_f)\alpha_{j+1}] \qquad (3.25)$$

$$REC_{1,ASE}=\{\sum_{j=1}^{N-1}\{2n_{sp}h\nu_fB_o(G_{fj}(\nu_f)-1)\prod_{k=j+1}^{N}[\alpha_k]\prod_{m=j+1}^{N-1}[G_{fm}(\nu_f)]\}$$
$$+\sum_{j=1}^{N}\{2n_{sp}h\nu_fB_o(G_{bj}(\nu_f)-1)\alpha_R\prod_{k=j}^{N-1}[\alpha_{k+1}G_{fk}(\nu_m)]\{1+\sum_{p=1}^{j-1}\{\prod_{m=p}^{j-1}[\alpha_{m+1}^2G_{fm}(\nu_f)G_{bm}(\nu_f)]\}\}\}G_{fN}(\nu_f)\alpha_{N+1}\alpha_{c2}$$
$$+2n_{sp}h\nu_fB_o(G_{fN}(\nu_f)-1)\alpha_{N+1}\alpha_{c2}$$

(3.26)

$$REC_{2,signal} = P_b(\nu_b)\alpha_{c1}\alpha_{c2}\alpha_{N+1}\prod_{j=1}^{N}[G_{bj}\alpha_j] \qquad (3.27)$$

$$REC_{2,ASE} = \{\sum_{j=2}^{N}\{2n_{sp}h\nu_b B_o(G_{bj}(\nu_b)-1)\prod_{k=2}^{j}[\alpha_k]\prod_{m=2}^{j-1}[G_{bm}(\nu_b)]\}$$
$$+\sum_{j=1}^{N}\{2n_{sp}h\nu_b B_o(G_{fj}(\nu_b)-1)\alpha_R\{1+\sum_{p=j+1}^{N}\{\prod_{m=j+1}^{p}[\alpha_m^2 G_{fm}(\nu_b)G_{bm}(\nu_b)]\}\}\}G_{fN}(\nu_f)\alpha_{N+1}\alpha_{c2}$$
$$+2n_{sp}h\nu_b(G_{bl}(\nu_b)-1)\alpha_l\alpha_{cl}$$

(3.28)

The received optical signal power to ASE power ratio is given by

$$SAR = \frac{REC_{signal}}{REC_{ASE}} \qquad (3.29)$$

Equation (3.29) represents the ratio of the received signal power to amplified spontaneous emission power. The signal to noise ratio at the receiver also includes shot noise, thermal noise and beat noises in addition to the amplified spontaneous noise [4].

$$\sigma_{shot}^2 = 2eB_e\eta(I_s + I_N) \qquad (3.30)$$

$$\sigma_{th}^2 = \frac{4k_B T B_e}{R} \qquad (3.31)$$

$$\sigma_{s-sp}^2 = 4\eta^2 I_s I_N \frac{B_e}{B_o} \qquad (3.32)$$

$$\sigma_{sp-sp}^2 = 2\eta^2 I_N^2 \frac{(2B_o - B_e)B_e}{B_o^2} \qquad (3.33)$$

where

$$I_s = \frac{eREC_{sig}}{h\nu_{sig}} \quad \text{and} \quad I_N = \frac{eREC_{ASE}}{h\nu_N} \qquad (3.34)$$

and B_e is the detector electronic bandwidth, e is the electric charge, η is the quantum efficiency of the detector, B_o is the optical bandwidth, k_B is Boltzmann's constant (k_B =

1.38×10^{-23} J/K), h is Planck's constant ($h=6.626 \times 10^{-34}$ J·s), T is an absolute temperature, and R is the load resistor of the detection circuit. The SNR at the receiver is then given by:

$$SNR = \frac{(\eta I_s)^2}{\sigma^2_{shot} + \sigma^2_{s-sp} + \sigma^2_{sp-sp} + \sigma^2_{th}} \qquad (3.35)$$

3.4 Numerical applications

3.4.1 Simple system simulation

A simple simulation of a bidirectional cascade of optical amplifiers can be done by using the results from our model and the equation for amplifier gain used by Giles and Desurvire [16].

$$G = G_o \exp[(1-G)\frac{P_{in}}{P_{sat}}]$$

$$\text{where } P_{sat} = P_{out} \text{ for } G = \frac{G_o}{e} \qquad (3.36)$$

assuming G>>1

This equation assumes local homogeneous saturation of the gain and uniform pumping of the amplifier. A numerical solution can be found by iteration using the two following equations:

$$P_{in,i} = P_{fin,i} + P_{bin,i} \qquad (3.37)$$

$$G_i = G_{0i} \exp[(1-G_i)P_{in,i}/P_{sat,i}] \qquad (3.38)$$

One has first to assume values for the gain of each amplifier, then use our model to compute the input power to each amplifier. The next step is to perform numerical root-solving on equation (3.38) to find values for the gain of each amplifier, and then iterate again until a solution is reached.

This simulation has limited accuracy since it uses a simple approximation for the amplifier gain. Better results would be obtained by using a complete fibre amplifier model. The next

section presents a numerical application of our model in conjunction with a more complete fibre amplifier model.

3.4.2 Erbium-doped fibre amplifier cascade model

In previous sections, we derived a system characterization model giving the input power to each amplifier in the link as a function of the launched power from the transmitter ends and the generated ASE. We can express the input power to each amplifier as a function of the output power of the previous and following amplifiers in the chain.

As shown in Figure 3.3, the input power to a given amplifier in the system is the sum of the forward output from the previous amplifier in the chain times the loss of the fibre link between the two amplifiers, the backward output from the following amplifier times the loss of the fibre link between the two amplifiers, and the backscattering of both outputs of the amplifier under study.

Figure 3.3 - Propagation of light from one amplifier to the next

The input power to each amplifier is then given by

$$P_{in,i} = P_{fout,i-1}\alpha_i + (P_{fout,i} + P_{bout,i})\alpha_R + P_{bout,i+1}\alpha_{i+1}$$
$$\text{where } P_{fout,0} = P_f\alpha_{c1} \text{ and } P_{bout,N+1} = P_b\alpha_{c2} \qquad \textbf{(3.39)}$$

We used equation (3.39) together with a complete erbium-doped fibre amplifier model that uses the propagation equations in the erbium-doped fibre to compute the output power and residual pump of the amplifier [25]. Our model thus simulates the propagation of the signals at the system level while the model presented in [25] simulates the propagation of

light in the erbium-doped fibre. The flow chart in Figure 3.4 shows how this EDFA computer simulation works.

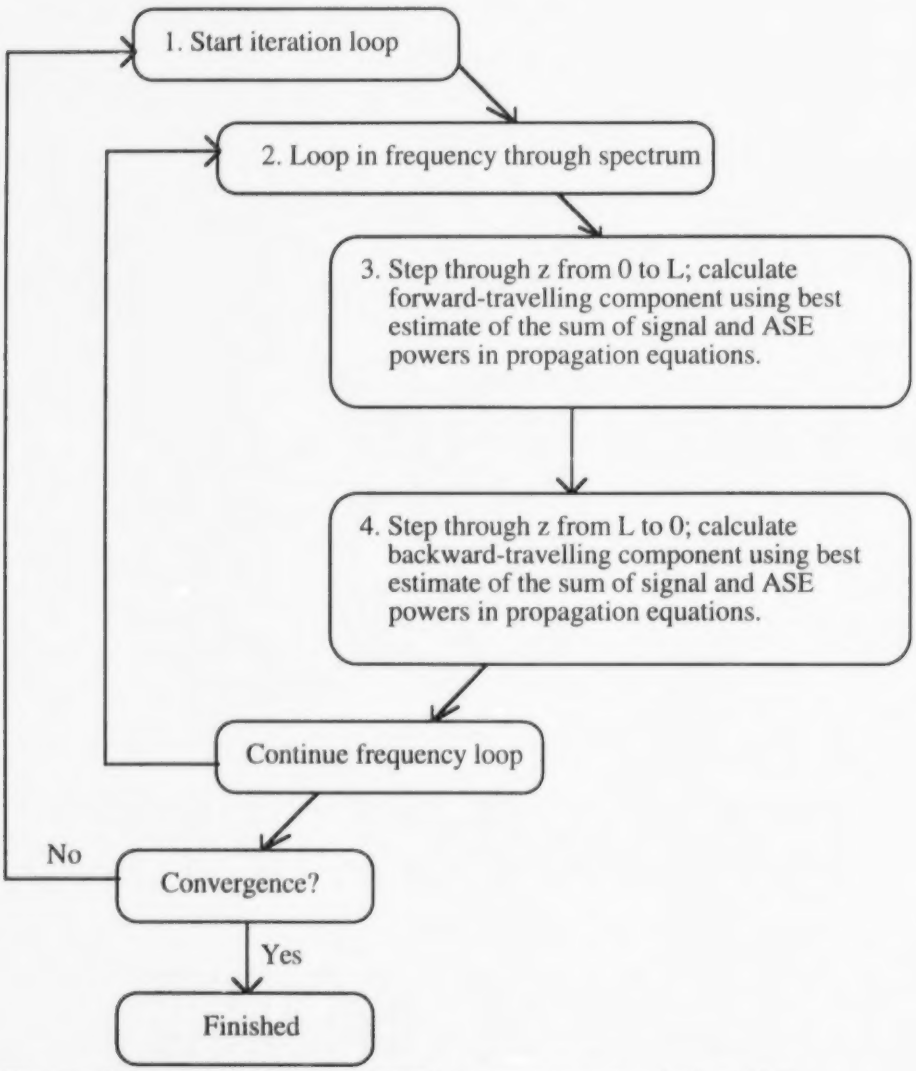
1. Start iteration loop
2. Loop in frequency through spectrum
3. Step through z from 0 to L; calculate forward-travelling component using best estimate of the sum of signal and ASE powers in propagation equations.
4. Step through z from L to 0; calculate backward-travelling component using best estimate of the sum of signal and ASE powers in propagation equations.
Continue frequency loop
No
Convergence?
Yes
Finished

Figure 3.4 - Flow chart of EDFA computer simulation [25]

A fourth order Runge-Kutta technique taking 50 steps in z is used to solve the equations for signal, ASE and pump propagation over the entire spectrum of operation of the amplifier. For each iteration, estimates of each component are taken to be the results of the previous iteration; zero is taken as an estimate for the first iteration.

We use the EDFA model in [25] as an element of a system computer simulation. By combining equation (3.39), from our signal and noise bidirectional propagation model, and the amplifier model in [25], we developed a bidirectional system simulation illustrated by the flow chart in Figure 3.5.

A computer simulation was coded in C language based on the flow chart in Figure 3.5. The power spectral density of the input power to the first amplifier is fed in the EDFA simulation from [25], which gives, at the output, the power spectral density of the output power of amplifier one. The forward input power spectrum is zero except for the forward propagating signal at λ_f; the backward input power spectrum is assumed to be zero in this first iteration. The output spectrum of amplifier one is then used in equation (3.39) to compute the input power spectrum to the second amplifier. We repeatedly use the simulation in [25] and equation (3.39) to compute the input and output power spectral densities of each amplifier from the first one to the last one. The same process is then repeated from the last amplifier to the first one. An overall loop iterates over the whole system for a fixed number of iterations. As a rule of thumb, we usually use twice as many iterations as there are amplifiers in the system under study. We present some simulation results in the next section. It should be noted that the amplifier simulation developed in [25] simulates the propagation and amplification of light in the erbium-doped fibre only. Assorted insertion losses from wavelength multiplexers, fusion splices, connectors, and couplers have to be taken into account when simulating the transmission system. The simulation code is presented in appendix B.

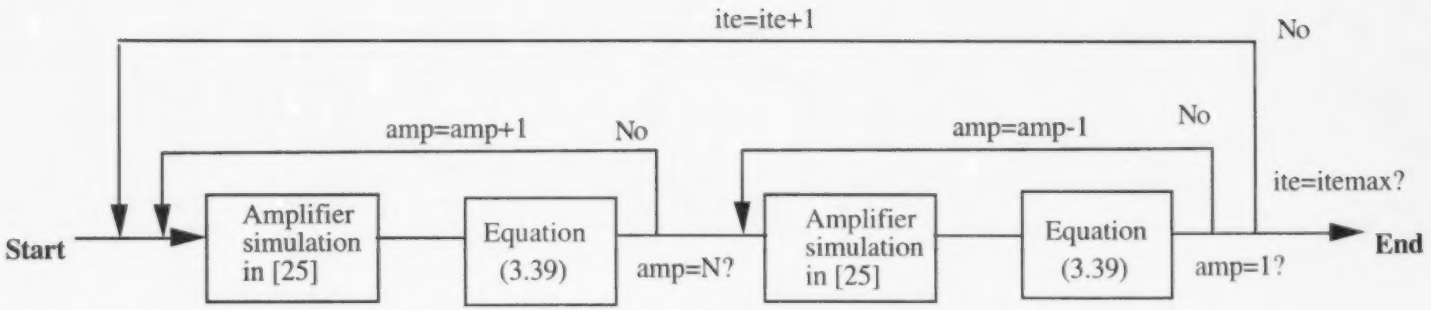

Figure 3.5 - Flow chart of bidirectional transmission system computer simulation

3.5 Simulation of bidirectional transmission systems

The bidirectional transmission system computer simulation described in section 3.4.2 was used to simulate a cascade of three erbium-doped fibre amplifiers under bidirectional transmission. We studied the performance of the system by simulating the ASE spectrum, signal power, inband ASE power, and optical signal to noise ratio at each stage. The effect of variations in system parameters such as signal wavelength and power, inter-amplifier link loss, amplifier position, and Rayleigh backscattering was also studied.

A basic bidirectional transmission cascade of three amplifiers is shown in Figure 3.6. All the following results were obtained with variations of the set-up in Figure 3.6. In chapter 4 we will present experimental results obtained in the lab for the corresponding simulation cases.

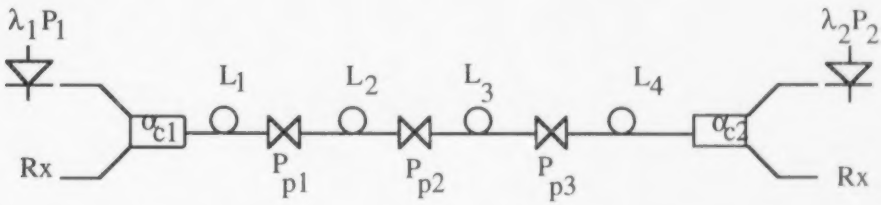

Figure 3.6 - Bidirectional transmission cascade of three amplifiers

The system parameters for each simulation case are given in Table 3.1.

System parameters	Case 1	Case 2	Case 3	Case 4	Case 5	Case 6	Case 7	Case 8	Case 9
λ_1 [nm]	1543	1543	1543	1543	1543	1538	1538	1538	1543
λ_2 [nm]	1551	1540	1551	1551	1551	1540	1540	1540	1551
P_1 [dBm]	-20	-20	-10	-5	-10	-8	-7	-7	-10
P_2 [dBm]	-20	-20	-10	-5	-10	-8	-6	-6	-10
α_{c1} [dB]	1	1	1	1	1	1	1	1	1
α_{c2} [dB]	1	1	1	1	1	1	1	1	1
L_1 [dB]	0	0	0	0	0	0	8.8	8.8	0
L_2 [dB]	14.2	14.2	14.2	14.2	19.2	19.2	14.2	14.1	14.2
L_3 [dB]	16.4	16.4	16.4	16.4	20.8	20.8	16.4	16.4	16.4
L_4 [dB]	0	0	0	0	0	0	9.3	9.3	0
Pump power[mW]									
1	22	22	22	22	22	22	22	22	22
2	50	50	50	50	50	50	50	50	50
3	50	50	50	50	50	50	50	50	50
Pump direction									
1	forward	forward	forward	forward	forward	forward	forward	forward	backward
2	forward	forward	forward	forward	forward	forward	forward	forward	forward
3	forward	forward	forward	forward	forward	forward	forward	forward	forward
α_{Rf} [dB]									
1	0	0	0	0	0	0	-33.2	0	0
2	-31.5	-31.5	-31.5	-31.5	-31.5	-31.5	-31.5	0	0
3	-31.5	-31.5	-31.5	-31.5	-31.5	-31.5	-31.5	0	0
4	0	0	0	0	0	0	-33.2	0	0
α_{Rb} [dB]									
1	0	0	0	0	0	0	-33.2	0	0
2	-31.5	-31.5	-31.5	-31.5	-33.2	-33.2	-31.5	0	0
3	-31.5	-31.5	-31.5	-31.5	-33.2	-33.2	-31.5	0	0
4	0	0	0	0	0	0	-33.2	0	0

Table 3.1 - Basic bidirectional transmission system simulation parameters

In the following sections, we will study the influence of the various system parameters with the nine cases listed in Table 3.1.

3.5.1 Signal wavelength

The erbium-doped fibre gain bandwidth extends from 1530 nm to 1560 nm. Technically, a system like the one in Figure 3.6 could transmit any signal falling within the amplifier gain bandwidth. We saw in chapter 2 that there is a large variation in gain throughout this bandwidth, so one might want to choose carefully the wavelength of the signals to be transmitted. In this section, we will study two variations of the system in Figure 3.6.

The two cases studied here, cases 1 and 2, are the same except for the wavelength of signal 2 (table 3.1). Simulation of these two systems will allow us to study the influence of wavelength separation between the transmitted signals.

Figures 3.7 and 3.8 show the forward and backward output spectra at each stage in the system for simulation case 1. Figures 3.9 and 3.10 display results for the simulation case 2. We can see on these graphs the propagation and Rayleigh backscattering of the two signals (at 1540 nm, 1543 nm, and 1551 nm), and the ASE build-up along the system. Figures 3.11 to 3.16 show the signal power, gain, and signal to ASE ratio respectively for both simulation cases.

According to results shown in Figure 2.8, there is about a 1 dB difference in small signal gain between signals at 1540 nm and 1543 nm, and a 6 dB difference between signals at 1543 nm and 1551 nm. It is thus not surprising to see in Figures 3.11, 3.12, 3.14, and 3.15 that there is a bigger difference between the signal output power and gain of the two signals in simulation case 1 than in simulation case 2. The signal to ASE ratio characteristic for the 1543 nm signal is almost the same in both cases. This suggests that the second signal is of lesser importance in saturating the amplifiers compared to the 1543 nm signal and the accumulating ASE.

3.5.2 Signal power

We have seen before that the amplifier gain varies with the input power. What effect will a variation in launched signal power have in cascaded amplifiers? To try to answer that question, we have compared three cases where the only variable parameter is the launched signal power. We are looking here at case 1, where $P_1=P_2=$ -20 dBm, case 3, where $P_1=P_2=$ -10 dBm, and case 4 where $P_1=P_2=$ -5 dBm.

Figures 3.17 to 3.22 show the signal output power, gain, and signal to ASE ratio for cases 3 and 4. Results for case 1 have already been presented.

Looking at the results in Figures 3.12, 3.18, and 3.19 for the gain at each amplifier, it is not surprising to see that we get higher gain for lower launched signal power since amplifier gain decreases with increasing input power. For case 1, where the signal is launched at a power of -20 dBm, the gain is at its highest for both signals. The gain for the 1543 nm signal is then between 12 dB and 20 dB. The inter-amplifier losses, at 14.2 dB and 16.4 dB, are then comparable to the gain and the signal builds up along the cascade, as seen in Figure 3.11. The gain of the 1551 nm signal being between 7 dB to 12 dB, the output signal power decreases along the cascade of amplifiers. When the signal power is increased to -10 dBm, as in case 3, the gain of both signals is reduced but the output signal power is increased while the signal to ASE ratio is improved. For a launched signal power of -5 dBm, as in case 4, the gain is further reduced and the signal to ASE ratio improved. The gain of the signal at 1551 nm is now below 10 dB and cannot compensate for the inter-amplifier loss anymore, the output signal power at 1551 nm thus decreases at every stage.

The above results show that a system where $L_iG_i>>1$ will more likely permit a constant output power at every stage. This is best achieved for system with signals in a narrow wavelength bandwidth since the amplifier gain varies with wavelength while the inter-amplifier loss does not.

3.5.3 Inter-amplifier link length

In this section, we vary the fibre link length between each in-line amplifier. The amplifiers should operate less in saturation in a configuration with larger inter-amplifier link losses. We will look at simulation cases 3 and 5 where the link losses are:

Case 3 :	L_1=0	L_2=14.2	L_3=16.4	L_4=0
Case 5 :	L_1=0	L_2=19.2	L_3=20.8	L_4=0

The results for signal power, gain, and signal to ASE ratio for simulation case 5 are shown in Figures 3.23 to 3.25 respectively. The signal at 1551 nm decreases rapidly in power at each stage, its gain being much too low (7 to 11 dB) to compensate for the inter-amplifier loss of 19 to 20 dB. In general, one should design a transmission system in which the inter-amplifier loss is not greater than the small signal gain of the signal propagating

through the system. In the case of multi-wavelength systems, the inter-amplifier loss should be comparable to the smallest small signal gain of all signals.

3.5.4 Amplifier position

Optical amplifiers can be used in a transmission system either as pre/post or in-line amplifiers. Pre/post amplifiers are placed before the receiver/after the transmitter to increase sensitivity and boost the signal before transmission respectively. In-line amplifiers are placed in the link with transmission fibre on either side and compensate for transmission and splitting losses.

Here, in cases 6 and 7, we compare a system with three in-line amplifiers to a system with two pre/post amplifiers and an in-line one. Figures 3.26 to 3.28 show results for simulation case 6 while Figures 3.29 to 3.31 show results for case 7. The total transmission distance is 150 km in case 6 and 170 km in case 7.

According to results in Figures 3.26 to 3.31, the pre/post amplifiers case 6 yields higher gain, larger signal output power, and larger signal to ASE ratio than the in-line amplifiers case 7. There thus seems to be, from the simulation results, a slight advantage to use pre/post configuration even if in the cases studied here, the transmission distance was 20 km less in the pre/post case than in the in-line case.

3.5.5 Rayleigh backscattering

Rayleigh scattering is a natural phenomenon occurring in glass fibres. The influence of Rayleigh backscattered light can be reduced by the use of optical isolators in a transmission system. Since we are not using optical isolators in our bidirectional transmission system, we are interested in looking at the influence of Rayleigh backscattering on the system performance. To do so, we study simulation cases 7 and 8 where the Rayleigh backscattering is respectively present and absent. A transmission system where Rayleigh backscattering is absent is achieved by replacing the transmission fibre with attenuators of equivalent loss.

Figures 3.32 to 3.34 show simulation results for case 8. We can see in Figure 3.29 to 3.34 that the presence of Rayleigh backscattering reduces the gain and output signal power of each amplifier and introduces a penalty to the system.

3.5.6 Pumping scheme

Up to now in this chapter, we have simulated systems with all the amplifiers pumped in the same direction. It can be interesting to see if a different pumping scheme could make a difference. An alternative to all forward or all backward pumping in a cascade of amplifiers is symmetrical pumping where each amplifier is pumped in the direction towards the nearest transmitter. In case 9, we are simulating the same system as in case 3 but with a different pumping scheme. We cannot really talk about symmetry of pumping in an amplifier system with an odd number of amplifiers since the middle amplifier is as close to one transmitter as the other. We have to choose a pumping direction for the middle amplifier and we chose forward pumping in case 9. The only difference between cases 3 and 9 is thus the pumping direction of amplifier 1.

The results for case 9 are presented in Figures 3.35 to 3.37. Comparing those results to the results for case 3 shown in Figures in 3.17 to 3.19, we see very little variation between the two pumping schemes. We saw in chapter 2 that forward and backward output ASE powers in an inverted fibre will be almost equal. The same goes for signal gain in a co-propagating signal and pump amplifier and a contra-propagating signal and pump amplifier: an inverted amplifier will give very similar signal gain in both cases. Thus we would not expect much difference between two systems with different pumping schemes if the amplifiers are inverted. In this case, amplifier 1 has lower power than the other two and its backward ASE is larger than its forward ASE (which is not the case for the other amplifiers). The small differences between the results of cases 3 and 9 are caused by the fact that amplifier 1 will launch more ASE in the system when pumped in the backward direction than when pumped in the forward direction. This has the effect of lowering the signal to ASE ratio in case 9. We expect the difference between the results in cases 3 and 9 would be smaller if all three amplifiers were pumped with high power.

3.6 Summary

In this chapter, we presented the derivation of a signal and noise propagation model for bidirectional transmission systems with EDFAs. We also studied some characteristics of bidirectional systems with optical amplifiers by looking at a set of computer simulation cases.

In the next chapter, we will look at the performance of a bidirectional transmission system in more detail by studying results of experimental work and comparing the data obtained to the computer simulation results.

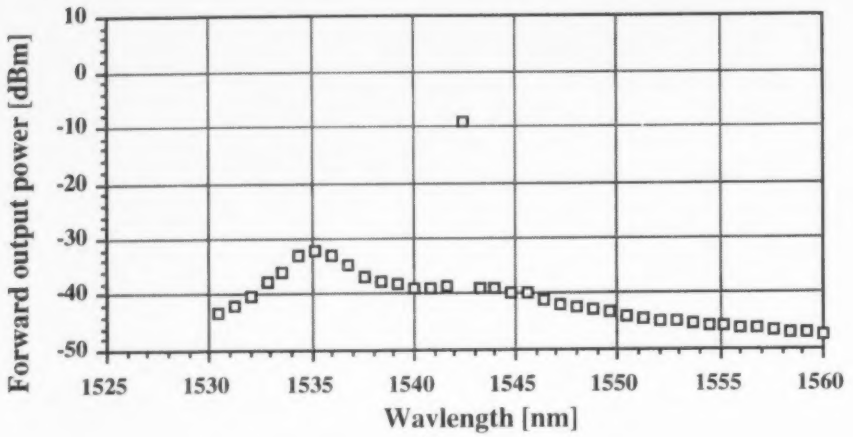

(a)

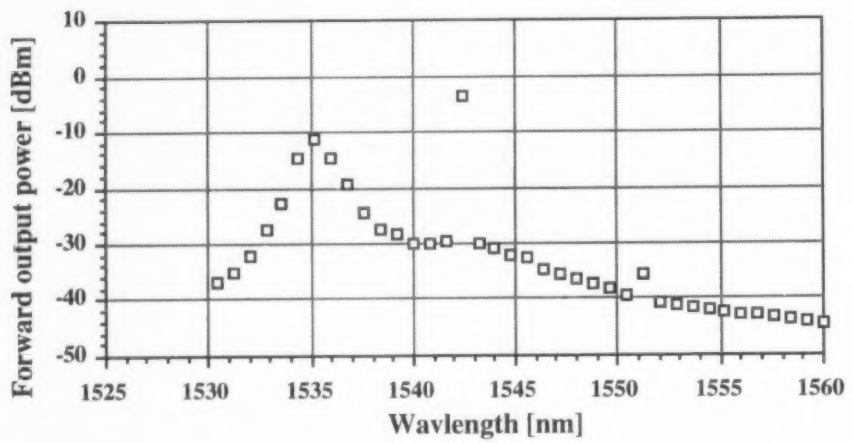

(b)

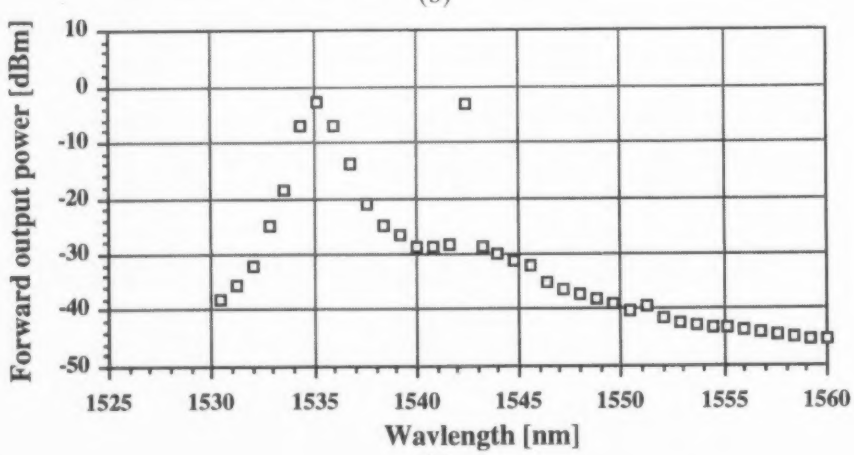

(c)

Figure 3.7 - Forward output spectra for simulation case 1. (a) Amplifier 1, (b) amplifier 2, (c) amplifier 3.

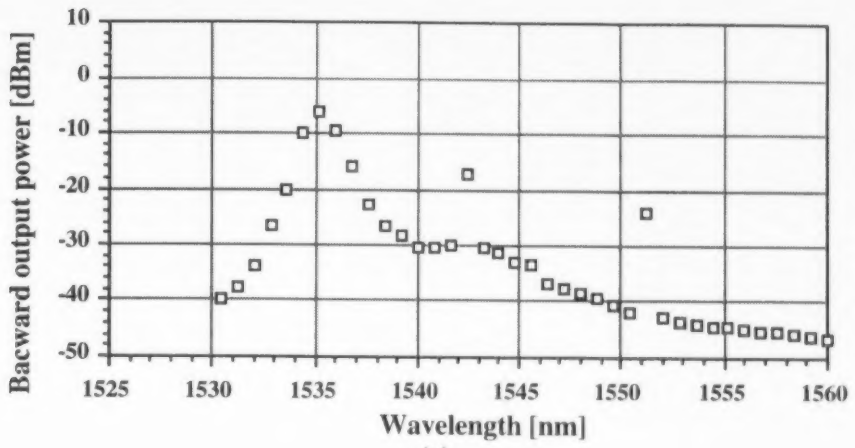

(a)

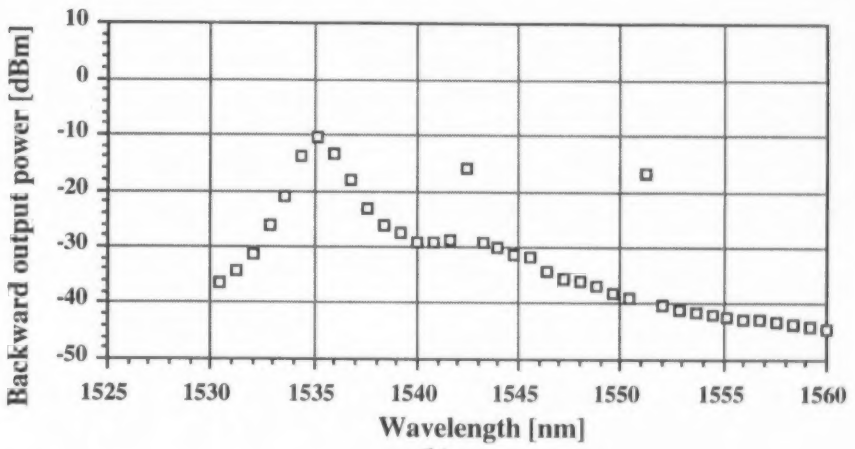

(b)

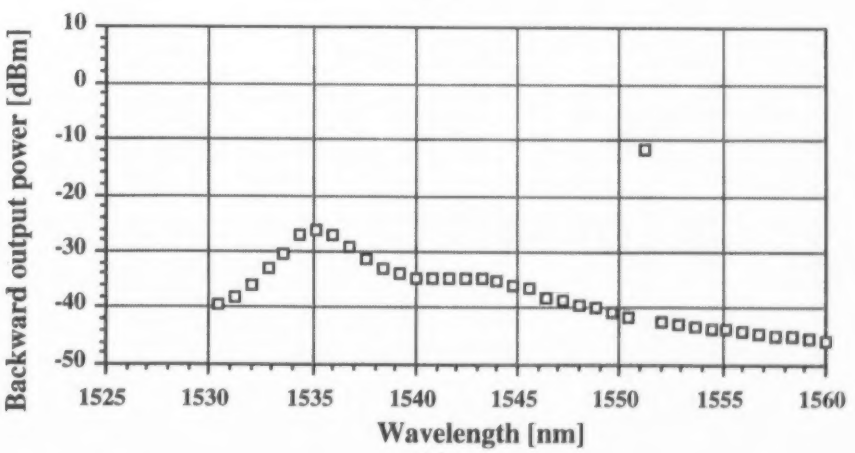

(c)

Figure 3.8 - Backward output power for simulation case 1. (a) Amplifier 1, (b) amplifier 2, (c) amplifier 3

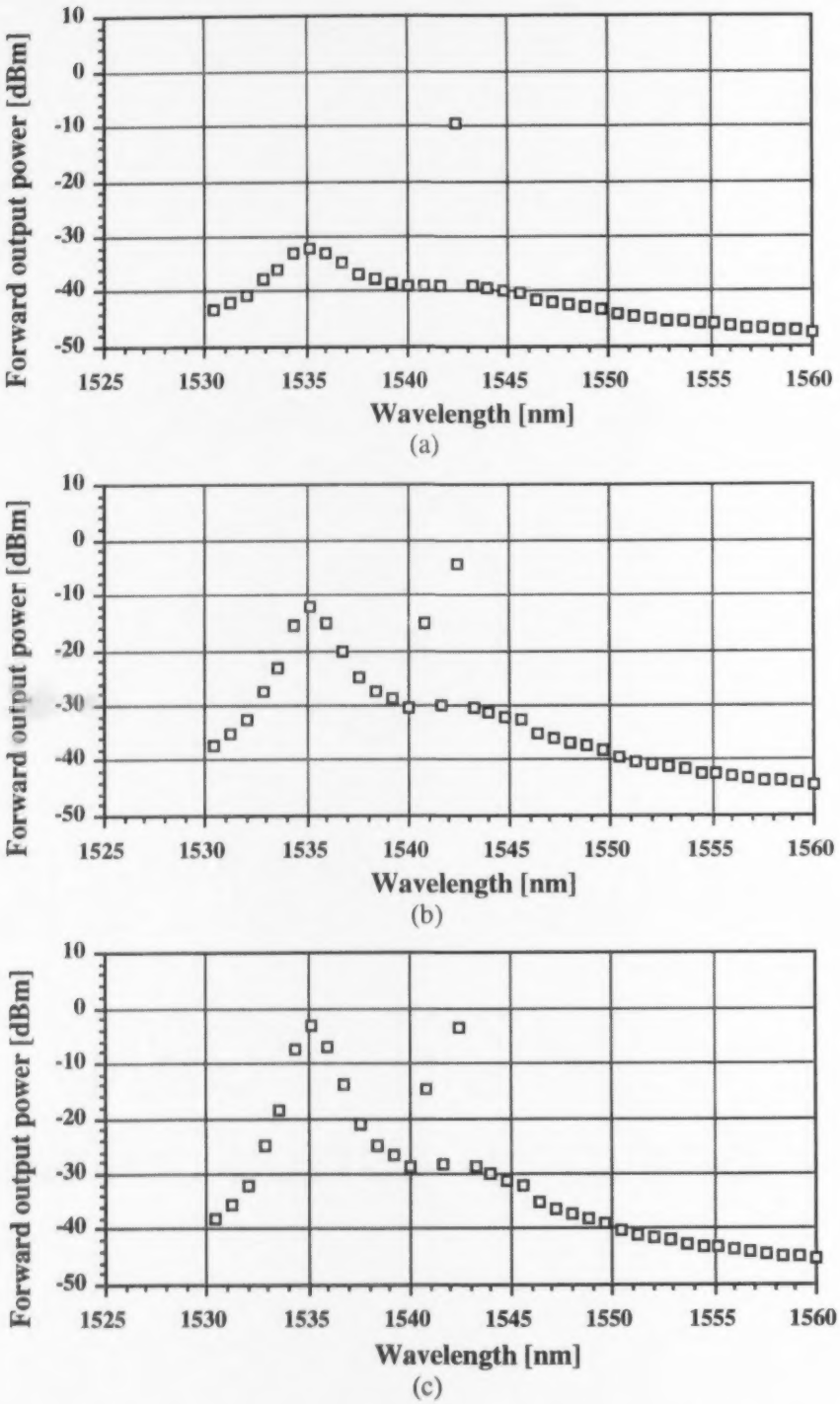

Figure 3.9 - Forward output spectra for simulation case 2. (a) Amplifier 1, (b) amplifier 2, (c) amplifier 3.

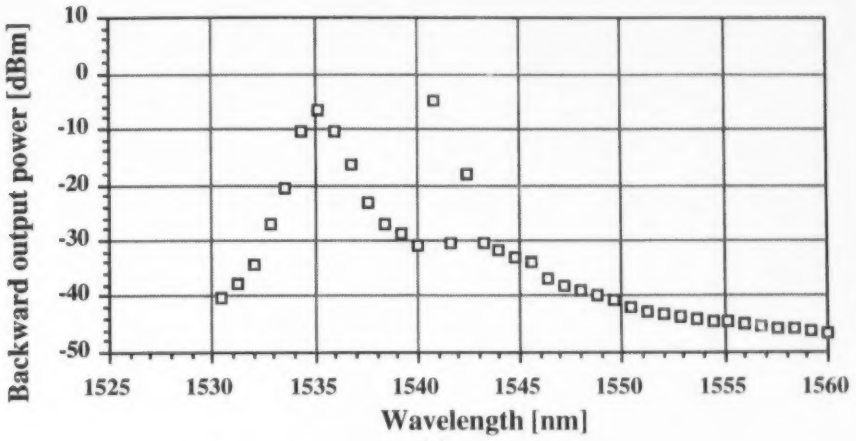

(a)

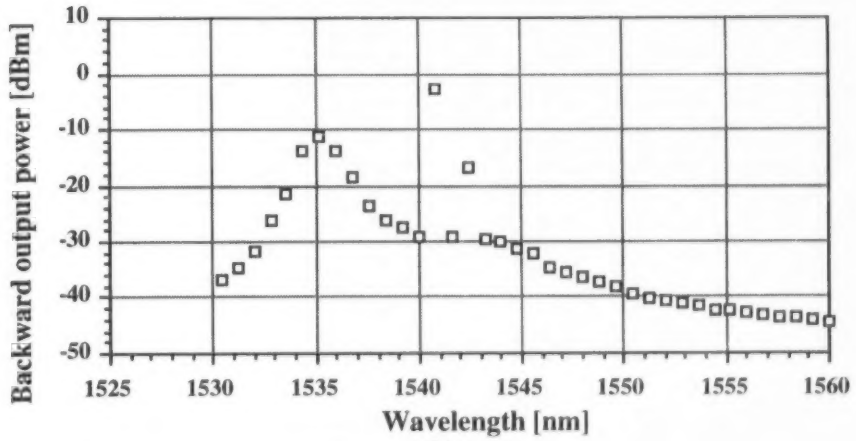

(b)

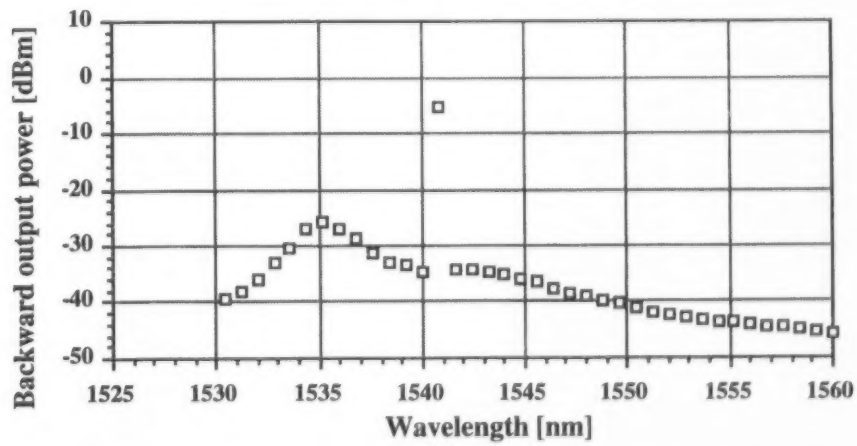

(c)

Figure 3.10 - Backward output spectra for simulation case 2. (a) Amplifier 1, (b) amplifier 2, (c) amplifier 3

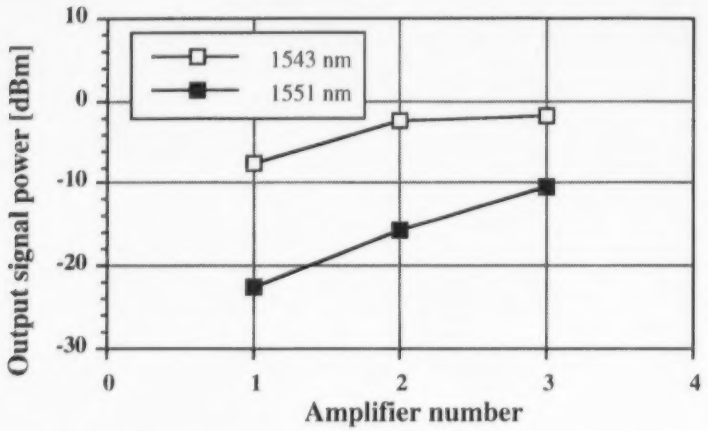

Figure 3.11 - Output signal power at each amplifier for simulation case 1

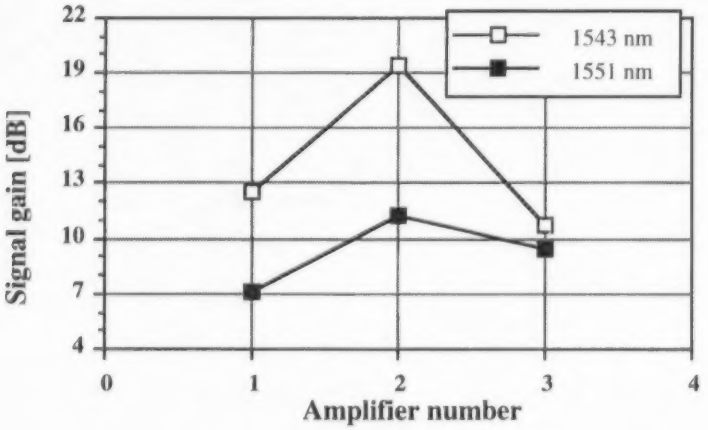

Figure 3.12 - Signal gain of each amplifier for simulation case 1

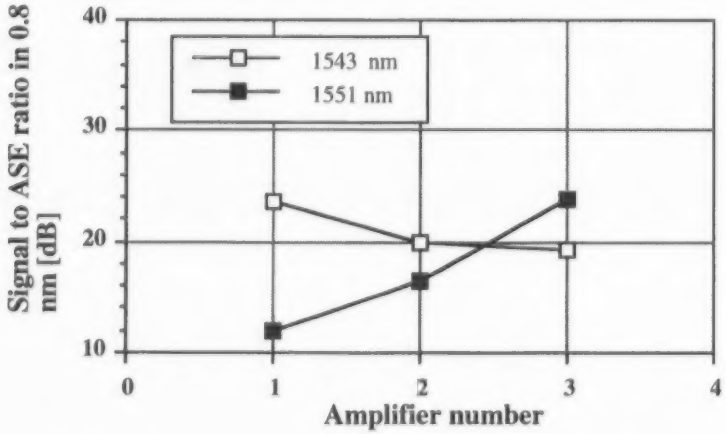

Figure 3.13 - Signal to ASE ratio at each amplifier in case 1

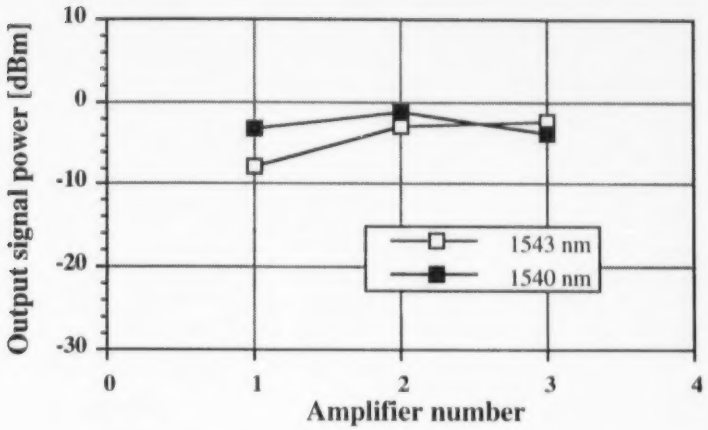

Figure 3.14 - Output signal power at each amplifier for simulation case 2

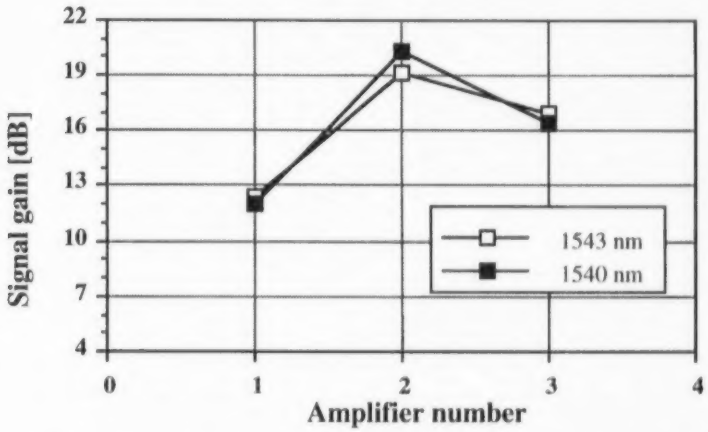

Figure 3.15 - Signal gain of each amplifier for simulation case 2

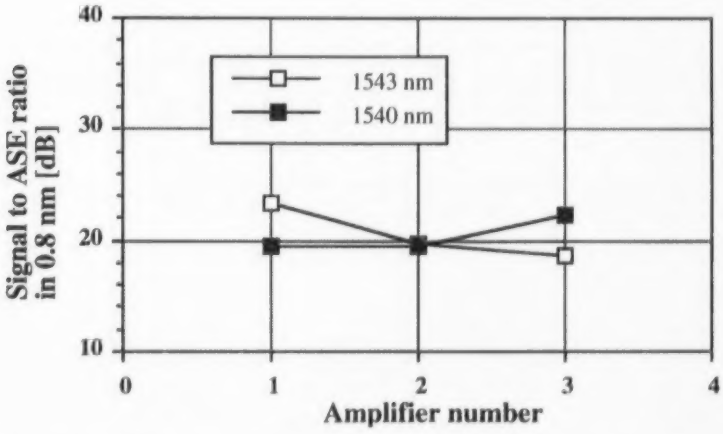

Figure 3.16 - Signal to ASE ratio at each amplifier for simulation case 2

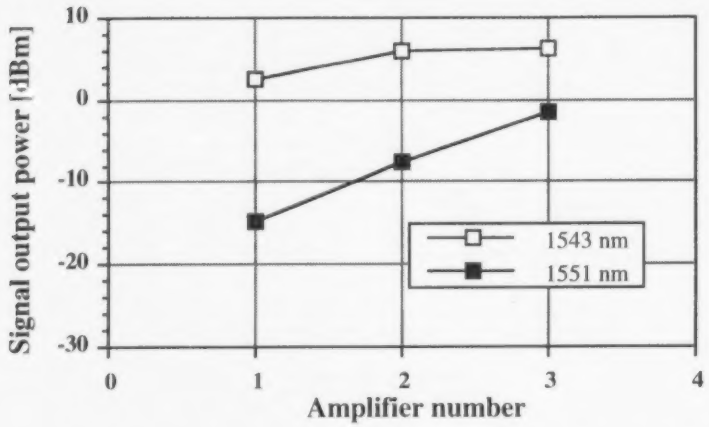

Figure 3.17 - Output signal power at each amplifier for simulation case 3

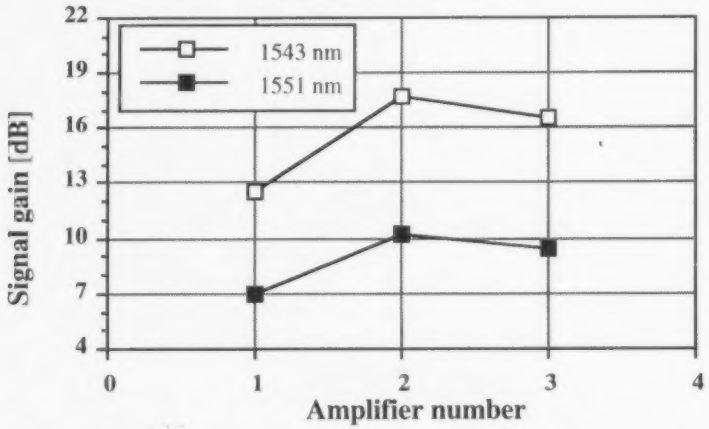

Figure 3.18 - Signal gain of each amplifier for simulation case 3

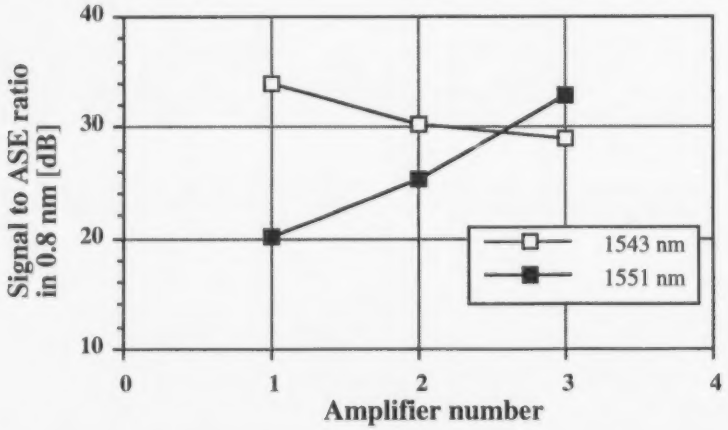

Figure 3.19 - Signal to ASE ratio at each amplifier for simulation case 3

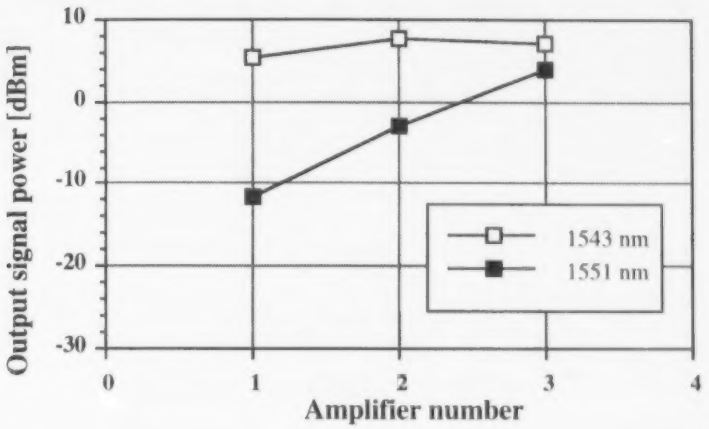

Figure 3.20 - Output signal power at each amplifier for simulation case 4

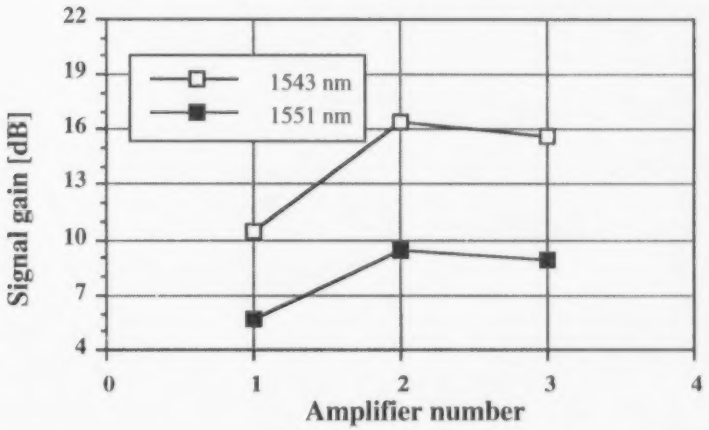

Figure 3.21 - Signal gain of each amplifier for simulation case 4

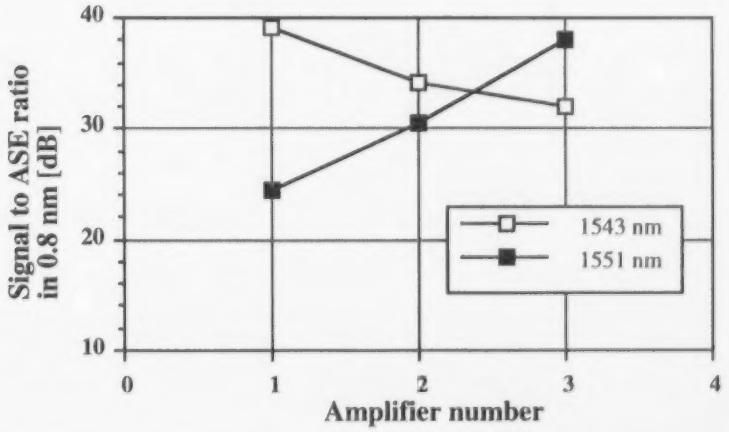

Figure 3.22 - Signal to ASE at each amplifier for simulation case 4

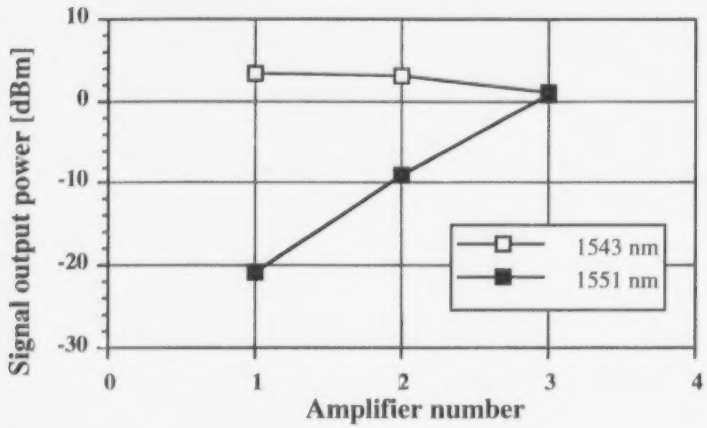

Figure 3.23 - Output signal power at each amplifier for simulation case 5

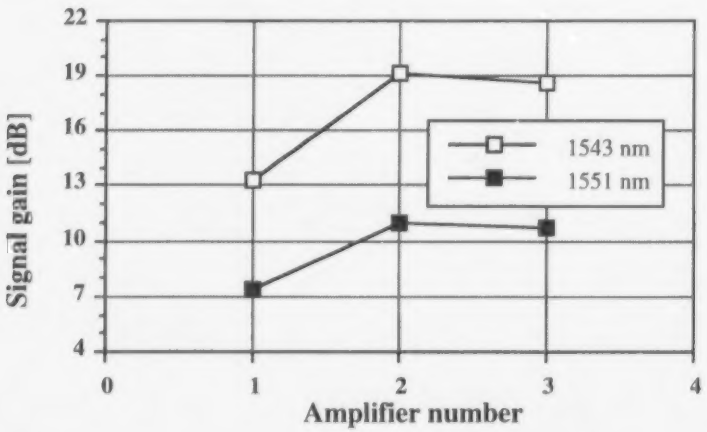

Figure 3.24 - Signal gain of each amplifier for simulation case 5

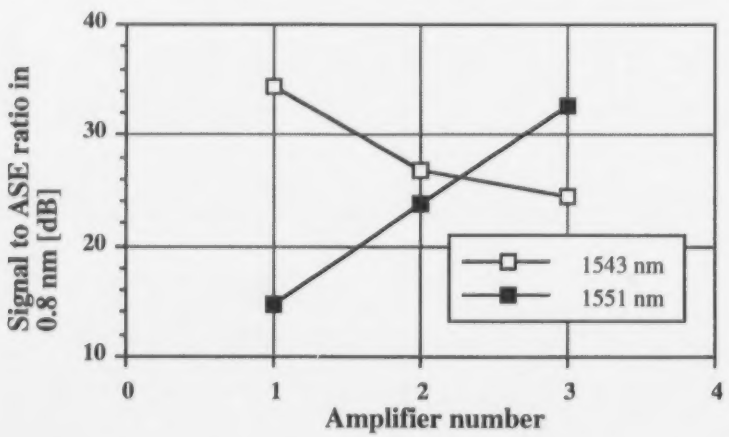

Figure 3.25 - Signal to ASE ratio at each amplifier for simulation case 5

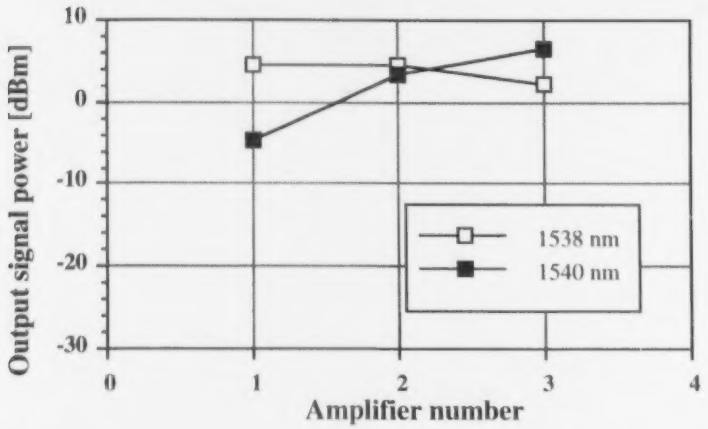

Figure 3.26 - Output signal power at each amplifier for simulation case 6

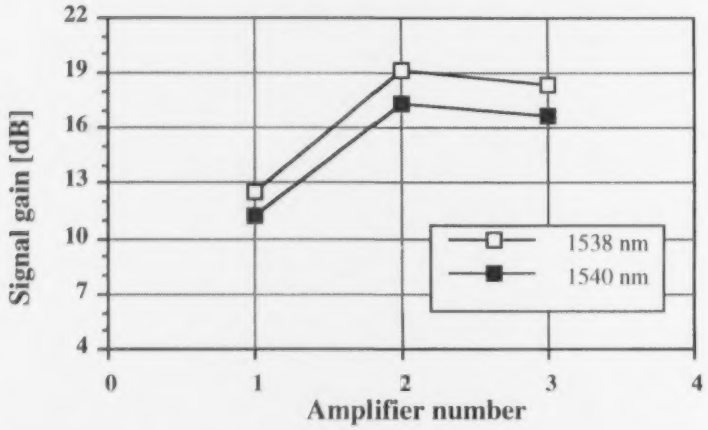

Figure 3.27 - Signal gain of each amplifier for saturation case 6

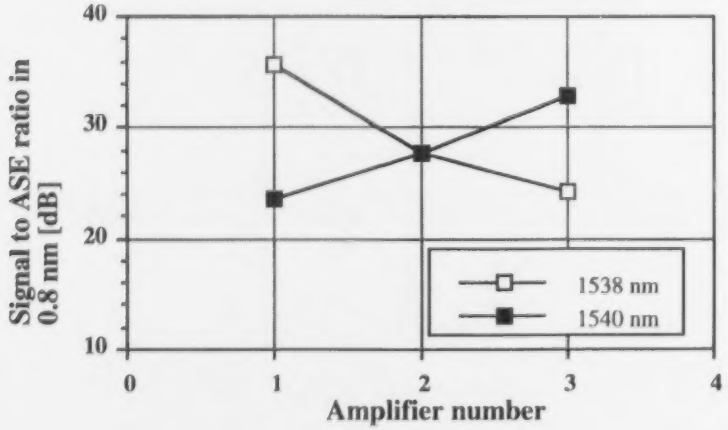

Figure 3.28 - Signal to ASE ratio at each amplifier for simulation case 6

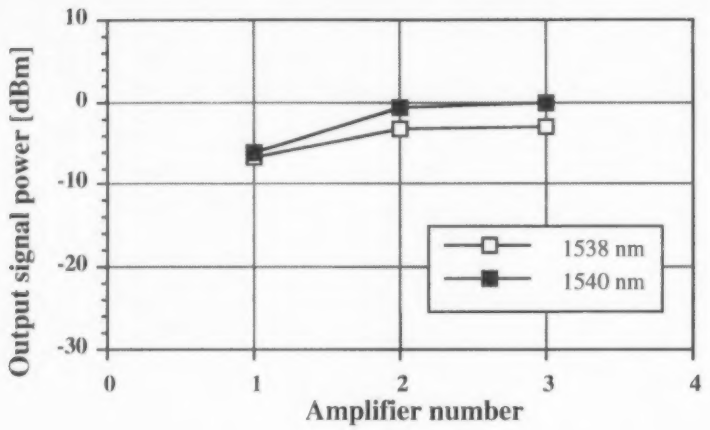

Figure 3.29 - Output signal power at each amplifier for simulation case 7

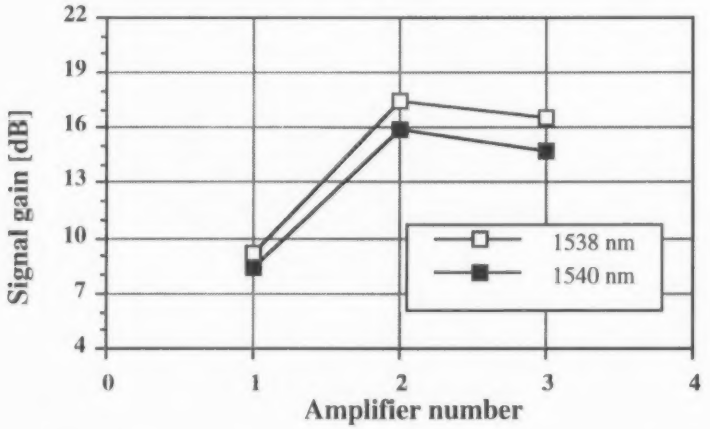

Figure 3.30 - Signal gain at each amplifier for simulation case 7

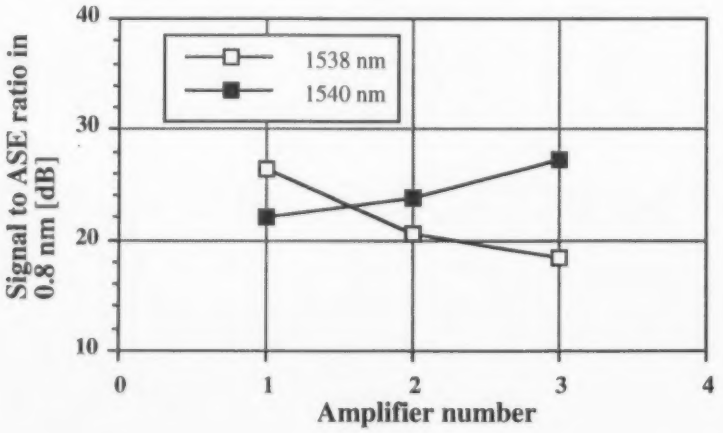

Figure 3.31 - Signal to ASE at each amplifier for simulation case 7

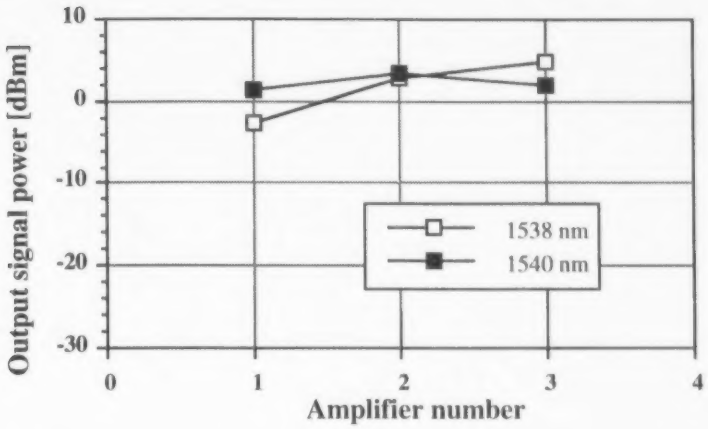

Figure 3.32 - Output signal power at each amplifier for simulation case 8

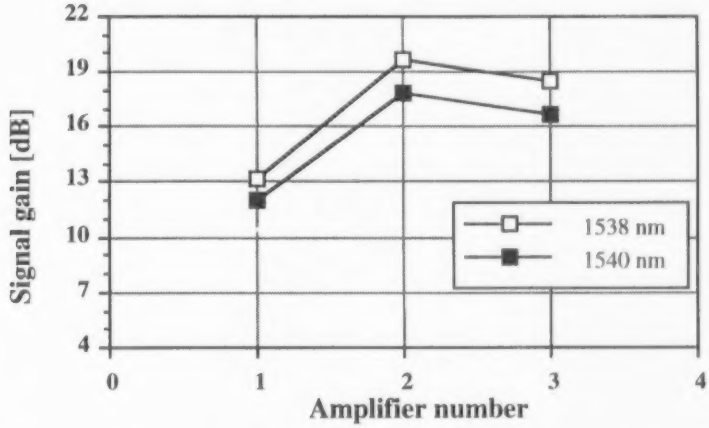

Figure 3.33 - Signal gain of each amplifier for simulation case 8

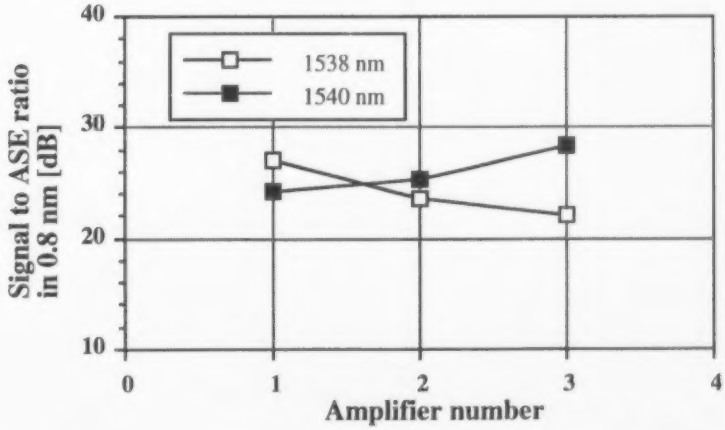

Figure 3.34 - Signal to ASE ratio at each amplifier for simulation case 8

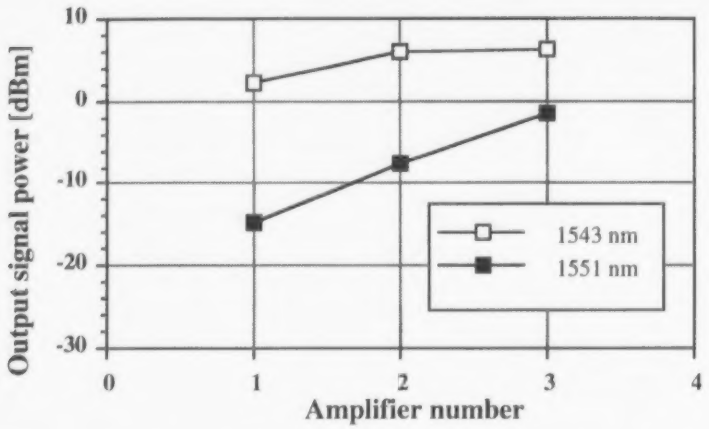

Figure 3.35 - Output signal power at each amplifier for simulation case 9

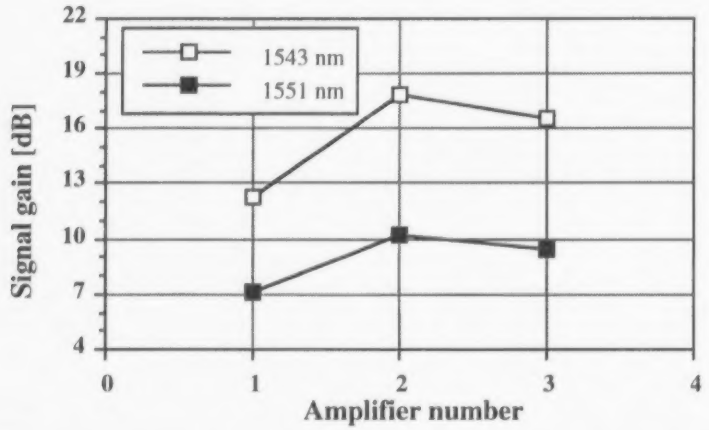

Figure 3.36 - Signal gain of each amplifier for simulation case 9

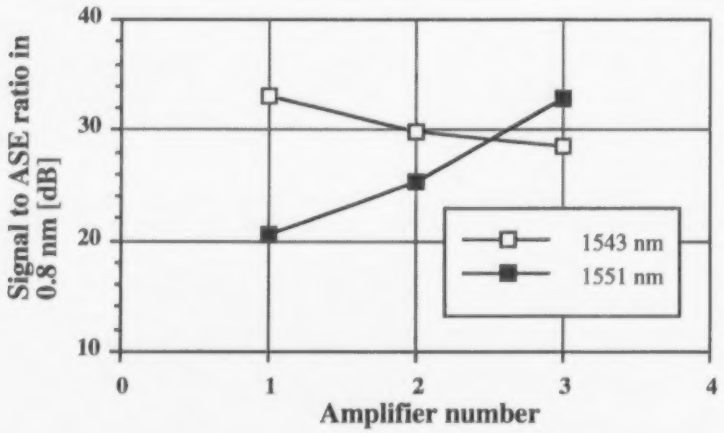

Figure 3.37 - Signal to ASE ratio at each amplifier for simulation case 9

4. Bidirectional transmission experiments

In chapter 2 we saw experimental results of the behaviour of an EDFA. In chapter 3 we developed a model for signal and ASE propagation in bidirectional transmission systems with cascaded EDFAs and simulated such a system. Here, in chapter 4, we will look at experimental results for the bidirectional transmission of two signals through an optical system including three EDFAs as either pre/post, or in-line amplifiers. We will look at the propagation and accumulation of signal and ASE at each stage of the transmission system for different operating conditions and will compare the results to analyze optical bidirectional transmission systems with EDFAs.

In the following sections, we will present the characteristics of the equipment available (laser sources, EDFAs, optical filters,...), describe the setup used to obtain the experimental data, and analyze the data collected.

4.1 Optical sources

Four different optical sources were available for us to use. All four lasers were used for multi-wavelength transmission and study of the variations in performance of the system with signal wavelength. The operating characteristics of all four sources are listed in Table 4.1.

Laser source	1	2	3	4
Type	DFB	DFB	DFB	DFB
Emission wavelength [nm]	1538	1540	1543	1551
Maximum output power [dBm]	-3.7	-3.1	9.0	7.0

Table 4.1 - Optical source characteristics

The laser sources at 1540 and 1543 nm are in the flat portion of the amplifier gain spectrum (see Figure 2.8), they thus have a similar small signal gain. The laser at 1538 nm is part way up the main emission peak at 1535 nm and will experience more gain through an amplifier than the other sources. Finally, the last source emits at 1551 nm which is in the part of the amplifier spectrum where the gain is smallest. These four available optical

sources enable us to examine a good portion of the amplifier gain spectrum in our experiments.

4.2 Erbium-doped fibre amplifiers

A total of three amplifiers were built here at **TR***Labs* and used for the experimental work of this thesis. The erbium-doped fibre was produced by the National Optics Institute (NOI) from a design provided by **TR***Labs*. Erbium-doped fibre amplifiers were built with this doped fibre, wavelength division multiplexers, and a pump laser as shown in Figure 1.2. The erbium-doped fibre properties are given in Table 4.2 while the EDFAs' characteristics are listed in Table 4.3. The erbium-doped fibre absorption and emission cross-sections are given in Figure 4.1. The emission cross-section data provided by NOI was slightly modified to better correspond to the actual behaviour of the amplifiers, especially for the dip around 1540 nm and the peak at 1535 nm. The simulations in chapter 3 were done with the modified cross-sections.

EDF type	N.A.	Core diameter	Core dopants	Er content	Al content
S.N. 920331	0.145	5.2 µm	Ge/P/Al/Er	163 ppm molar	8630 ppm molar

Table 4.2 - Erbium-doped fibre properties

EDFA	1	2	3
Number	302	303	001
Type of fibre	920331	920331	920331
Fibre length [m]	31.0	31.0	29.4
Pump wavelength [nm]	977	978	977
Maximum pump power [mW]	28[2]	70	80

Table 4.3 - Erbium-doped fibre amplifiers' characteristics

[2] The maximum available power out of the laser in amplifier #302 is much lower than the other ones because of deteriorated coupling between the chip and the fibre pigtail.

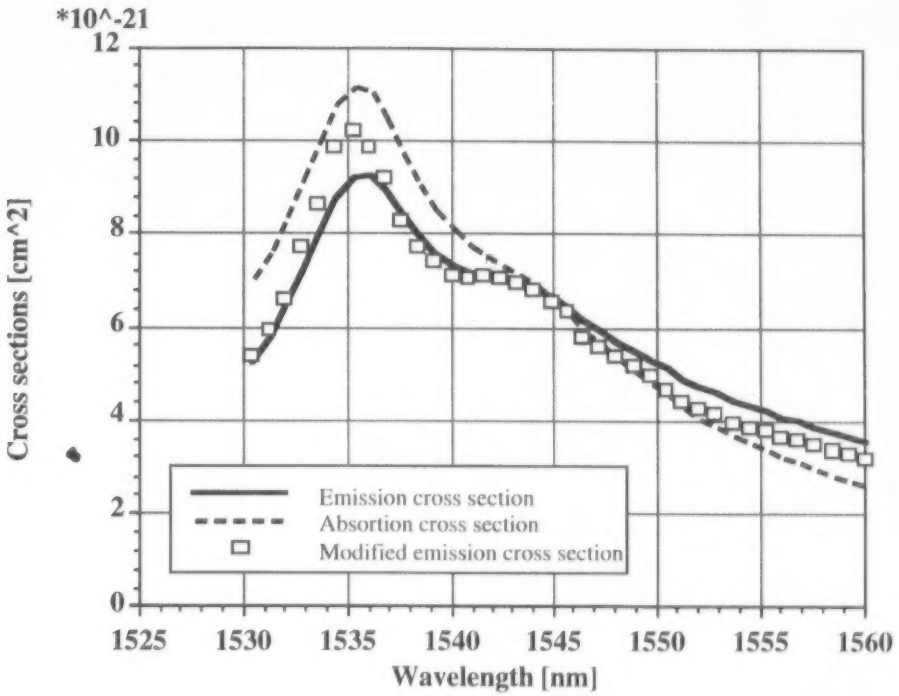

Figure 4.1 - Emission and absorption cross sections of erbium-doped fibre

4.3 Bidirectional transmission experimental setup

The setup used to collect data on bidirectional transmission in a cascade of three EDFAs is shown in Figure 4.2. One laser source is at each end of the transmission link and is isolated from the light coming from the contra-propagating signal by a circulator. The three amplifiers are separated by spools of transmission fibre and used either as in-line or pre/post amplifiers. A 90/10 directional coupler is attached to the entrance and exit of each amplifier to provide monitoring ports for both input and output power at each stage in the system. Signal output power, inband ASE, and gain were measured at each output port of the amplifiers with the method presented in chapter 2 which consists in using polarization controllers and splitters to separate signal and ASE at the output of the amplifier. Amplifier input and output spectra were measured utilizing a monochromator to scan the entire spectrum. The monochromator was used with a constant resolution width of 0.14 nm for every scanning interval used. This setup has been used to study the performance of bidirectional transmission systems with EDFAs by varying parameters such as signal

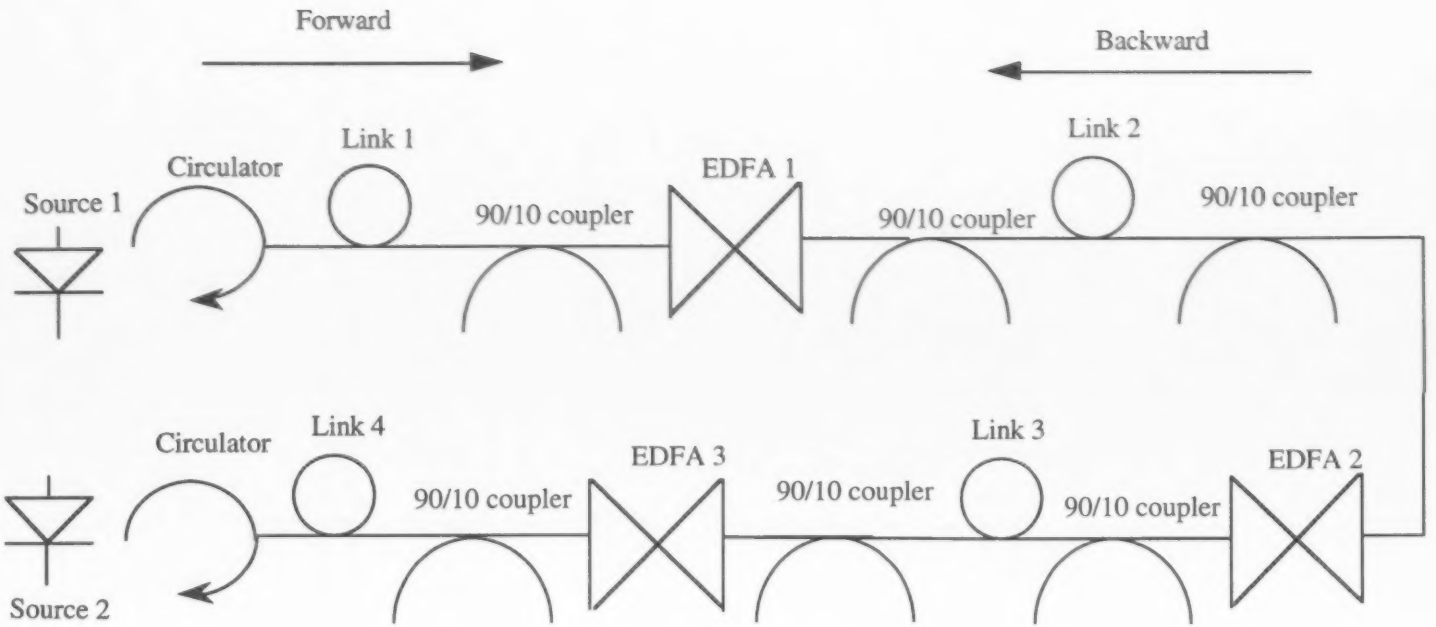

Figure 4.2 - Bidirectional transmission experimental setup

wavelength, signal power, fibre link length, amplifier position, and Rayleigh backscattering in a similar fashion to the computer study presented in chapter 3.

Each experimental case used a variation of the setup in Figure 4.2. The parameters corresponding to each case, such as the two signal wavelengths and launched power as well as the inter amplifier total loss and transmission fibre link length, are listed in Table 4.4. Total inter amplifier link losses include the transmission loss of the fibre and the insertion loss of connectors and couplers.

Parameters	**Case 1**	**2**	**3**	**4**	**5**	**6**	**7**	**8**	**9**
λ_1 [nm]	1543	1543	1543	1543	1543	1538	1538	1538	1543
λ_2 [nm]	1551	1540	1551	1551	1551	1540	1540	1540	1540
P_1 [dBm]	-19.2	-19.2	-9.2	-4.2	-9.2	-7	-7	-7	-6
P_2 [dBm]	-18.5	-18.5	-9.2	-3.5	-9.2	-6	-6	-6	-6
L_1 [dB]	0.8	0.8	0.8	0.8	0.8	0.8	8.8	8.8	8.8
L_2 [dB]	14.2	14.2	14.2	14.2	19.2	19.2	14.2	14.1	14.2
L_3 [dB]	16.4	16.4	16.4	16.4	21.8	20.8	16.4	16.4	16.4
L_4 [dB]	1.5	1.5	1.5	1.5	1.5	1.5	9.3	9.3	9.3
$Link_1$ [km]	-	-	-	-	-	-	35	-	35
$Link_2$ [km]	50	50	50	50	75	75	50	-	50
$Link_3$ [km]	50	50	50	50	75	75	50	-	50
$Link_4$ [km]	-	-	-	-	-	-	35	-	35
Pump [mW]									
1	22	22	22	22	22	22	22	22	22
2	50	50	50	50	50	50	50	50	50
3	50	50	50	50	50	50	50	50	50

Table 4.4 - Experimental parameters for each case

4.4 Bidirectional transmission experimental results

In the rest of this chapter, we will present the experimental results obtained for cases 1 to 9, discuss and compare them to each other and analyze the effect of signal wavelength, signal power, fibre link length, amplifier position, and Rayleigh backscattering on the performance of the system much like what was done for the computer simulation results in chapter 3. The forward and backward input and output spectra of each amplifier as well as the signal gain, output power and signal to ASE ratio are presented in Figures 4.3 to 4.47 on the following pages. Refer to these graphs and Table 4.4 while reading the rest of this chapter. As a reminder, the forward signal propagates from amplifier 1 to amplifier 3 and the backward signal propagates from amplifier 3 to amplifier 1.

4.4.1 Signal wavelength

Erbium-doped fibre amplifiers have a gain bandwidth of about 30 nm. Technically, signals at any wavelength in that bandwidth can be transmitted in a multi wavelength system. We will see in this section that some limitations to the choice of signal wavelength arise from the variations in performance of an optical bidirectional transmission system with signal wavelength.

To assess the impact of the launched signal wavelength on system performance, we will compare results from cases 1 and 2, cases 5 and 6, and cases 7 and 9.

In cases 1 and 2, we have an example of two amplifiers used as pre/post amplifiers and one used as an in-line amplifier. The experimental conditions and setup parameters are the same except that the backward propagating signal (λ_2) is set at a different wavelength: 1551 nm in case 1 and 1540 nm for case 2.

Let us try to understand the results obtained for cases 1 and 2. We have to point out is that, and this is true for every case studied in this chapter, the small signal gain at all wavelengths is substantially lower for amplifier 1 (#302) than for the two other amplifiers in the cascade. We found out, after the experimental work was completed, that the coupling between the fibre pigtail and the pump laser chip has degraded and that a fraction of the total pump power is available at the output of the pigtail fibre. It is important to remember

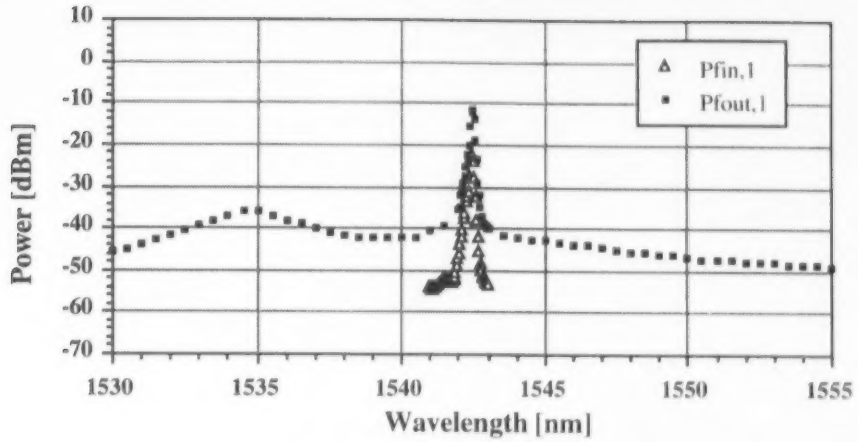

(a)

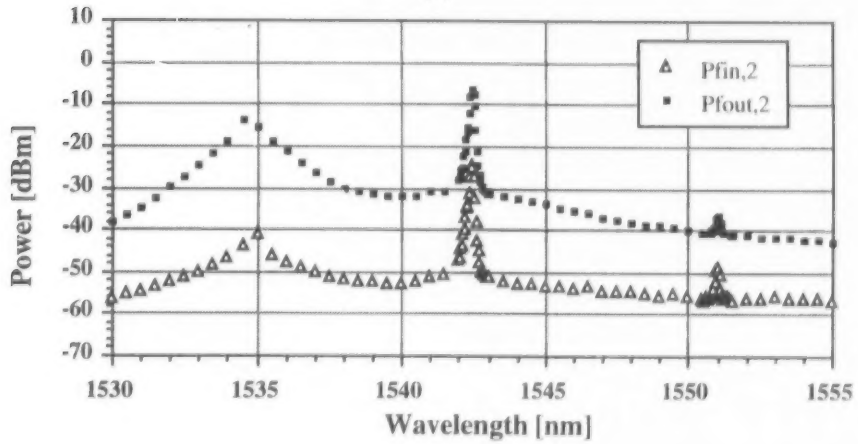

(b)

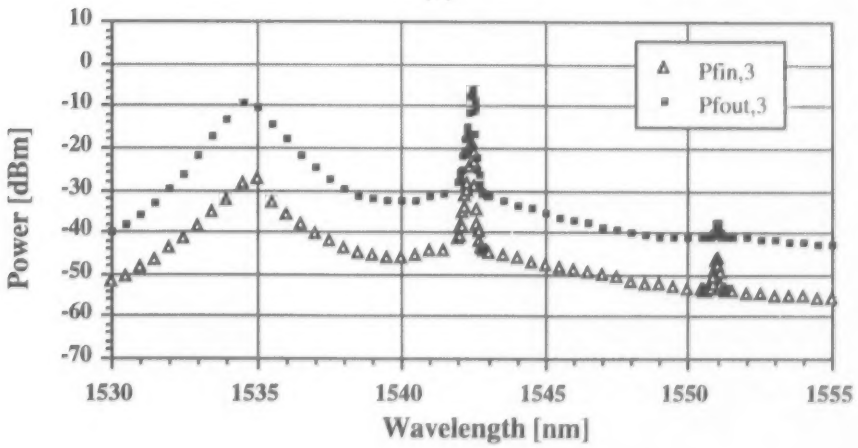

(c)

Figure 4.3 - Forward input and output spectra for experimental case 1. (a) Amplifier 1, (b) amplifier 2, (c) amplifier 3

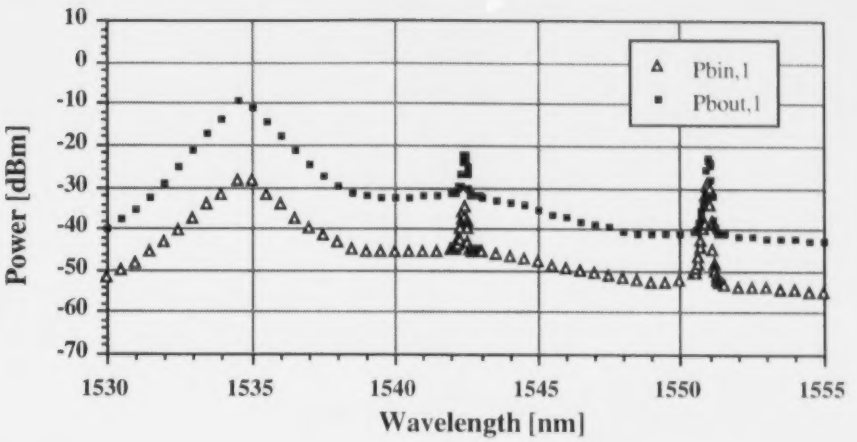

(a)

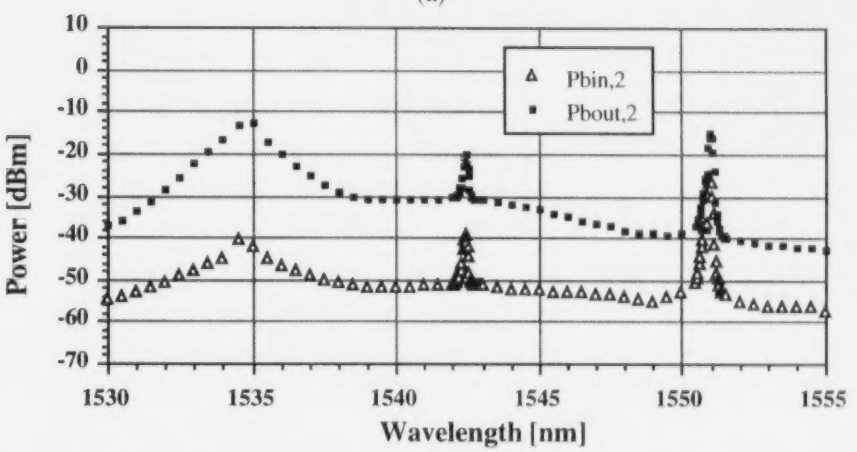

(b)

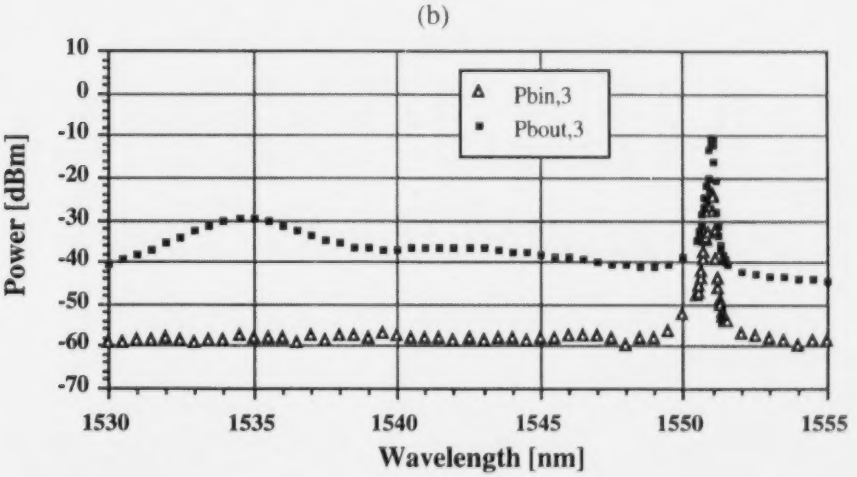

(c)

Figure 4.4 - Backward input and output spectra for experimental case 1. (a) Amplifier 1, (b) amplifier 2, (c) amplifier 3

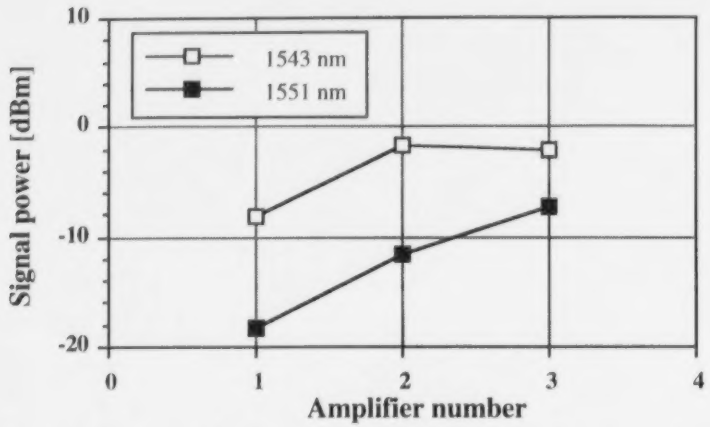

Figure 4.5 - Output signal power at each amplifier for experimental case 1

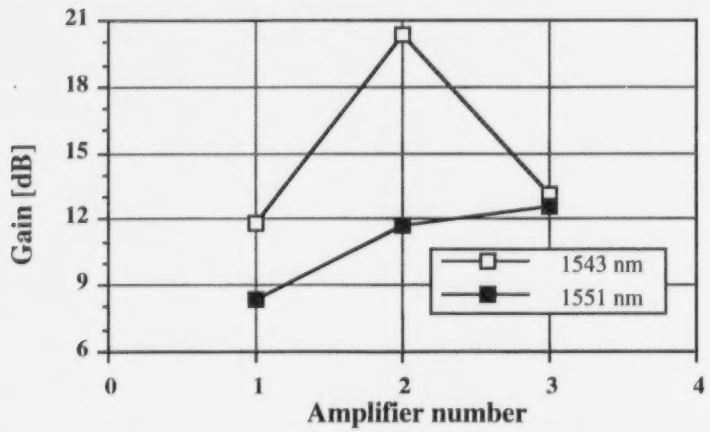

Figure 4.6 - Signal gain at each amplifier for experimental case 1

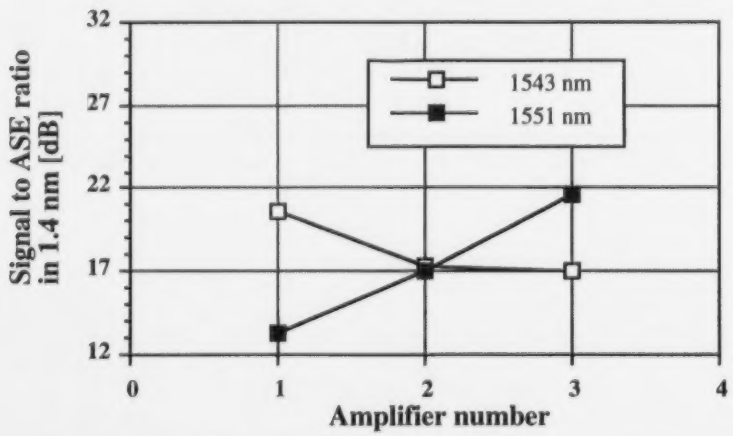

Figure 4.7 - Signal to ASE ratio at each amplifier for experimental case 1

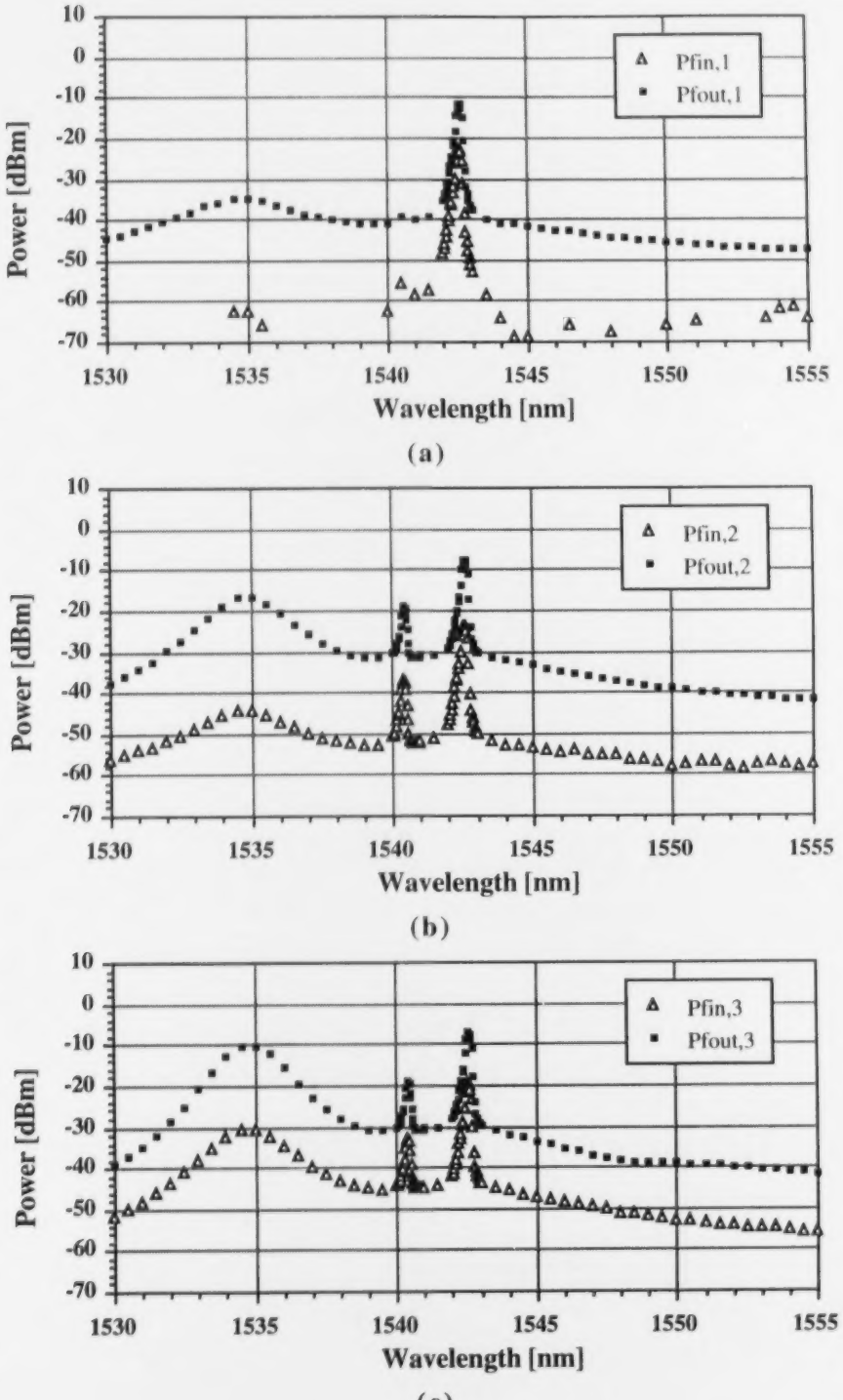

Figure 4.8 - Forward input and output spectra for experimental case 2. (a) Amplifier 1, (b) amplifier 2, (c) amplifier 3

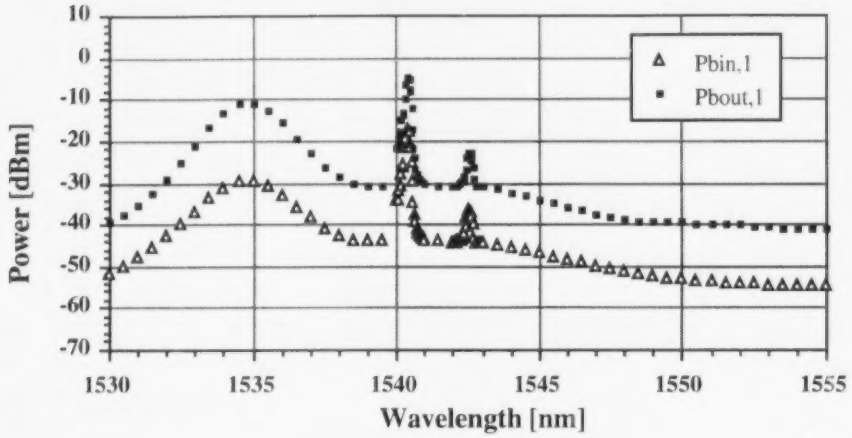

(a)

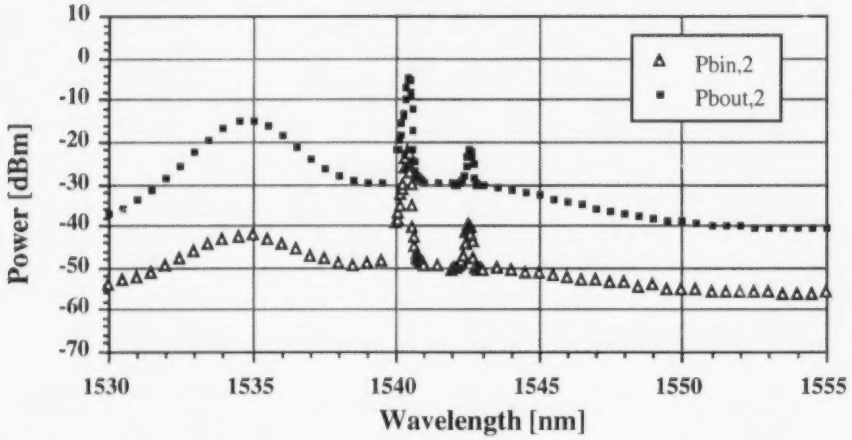

(b)

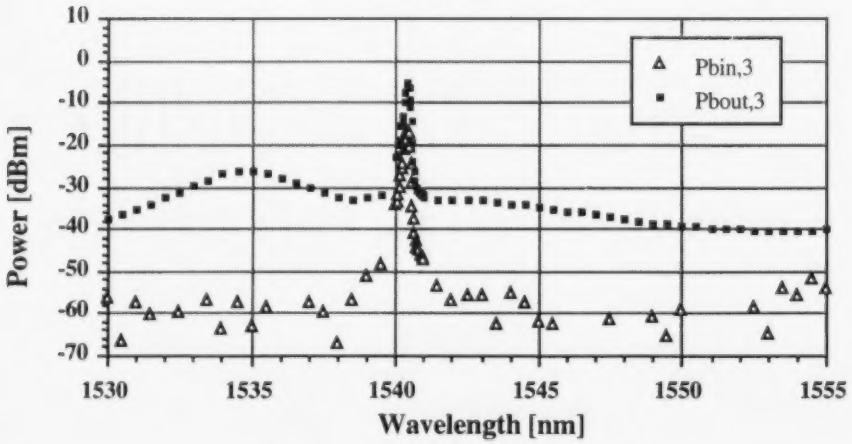

(c)

Figure 4.9 - Backward input and output spectra for experimental case 2. (a) Amplifier 1, (b) amplifier 2, (c) amplifier 3

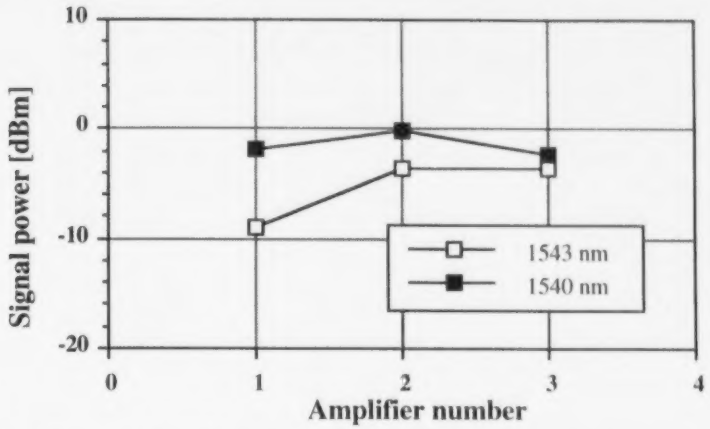

Figure 4.10 - Output signal power at each amplifier for experimental case 2

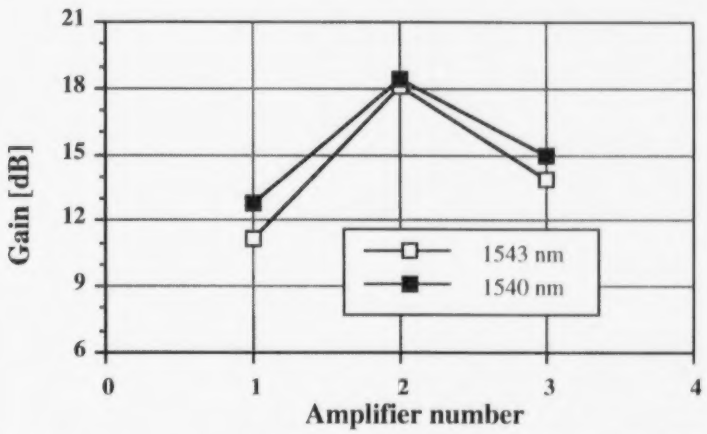

Figure 4.11 - Signal gain at each amplifier for experimental case 2

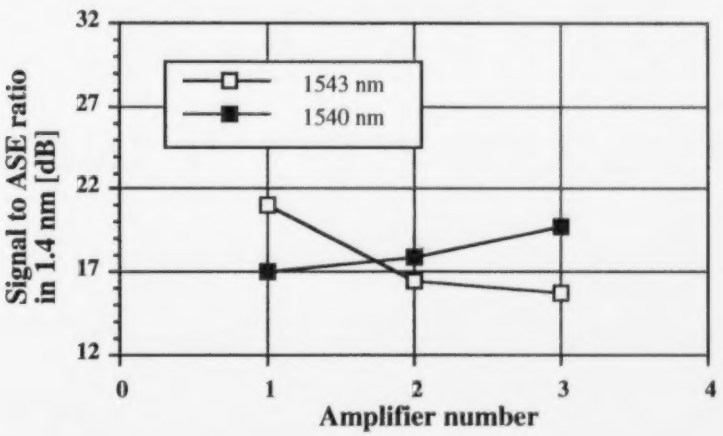

Figure 4.12 - Signal to ASE ratio at each amplifier for experimental case 2

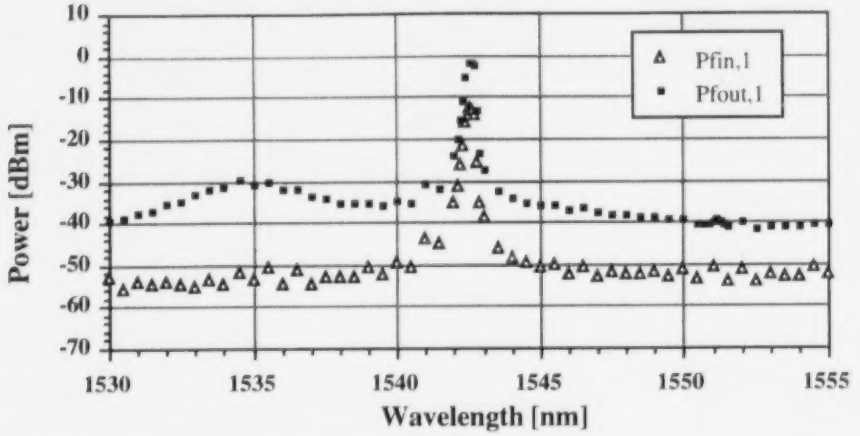

(a)

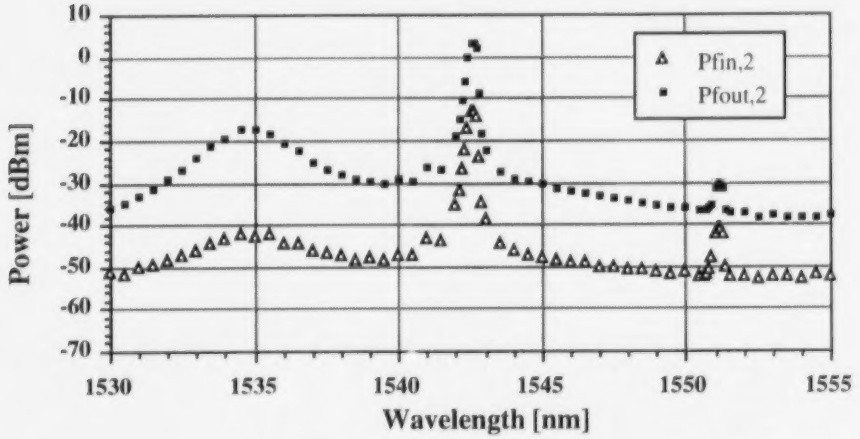

(b)

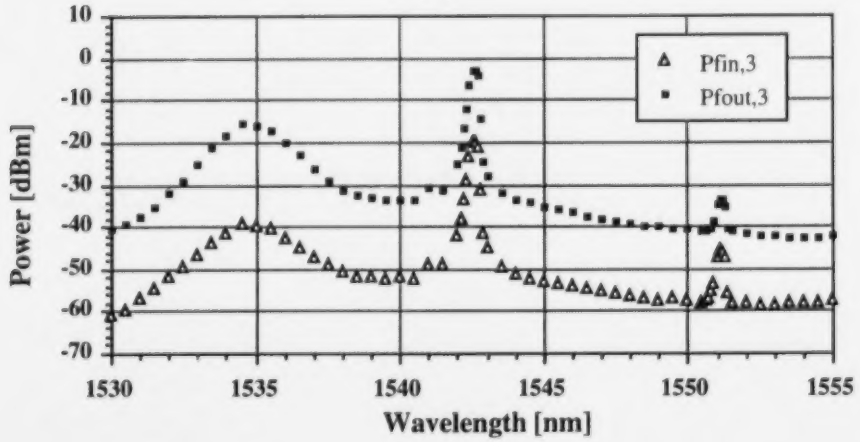

(c)

Figure 4.13 - Forward input and output spectra for experimental case 3. (a) Amplifier 1, (b) amplifier 2, (c) amplifier 3

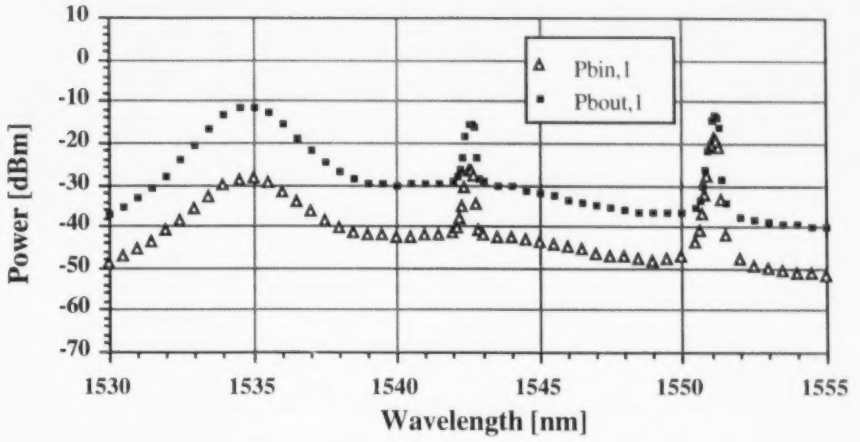

(a)

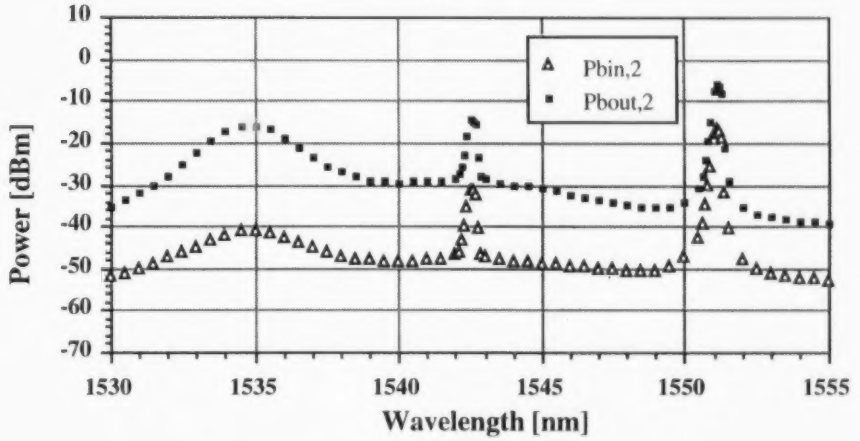

(b)

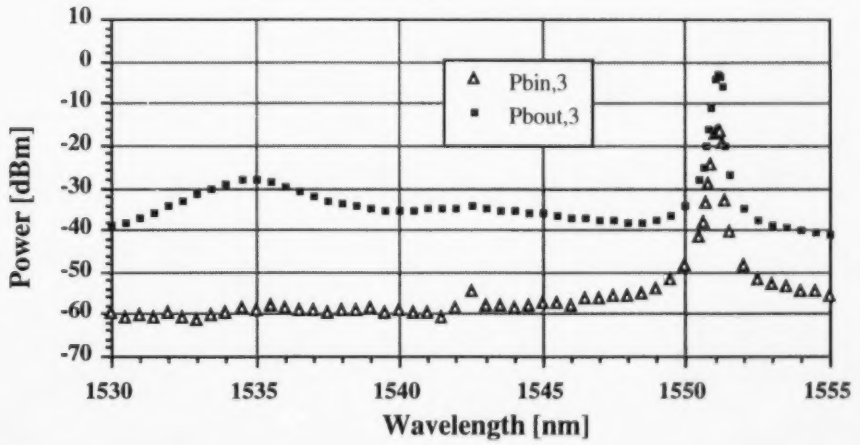

(c)

Figure 4.14 - Backward input and output spectra for experimental case 3. (a) Amplifier 1, (b) amplifier 2, (c) amplifier 3

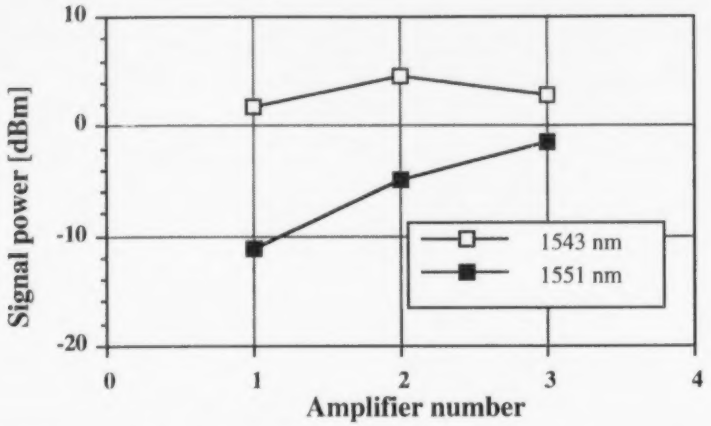

Figure 4.15 - Output signal power of each amplifier in experimental case 3

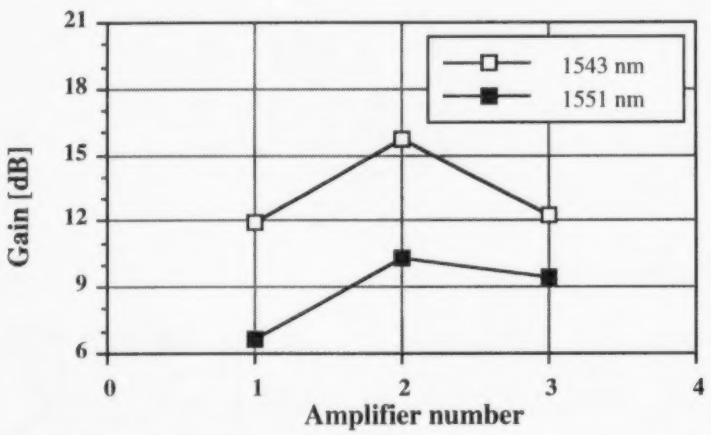

Figure 4.16 - Signal gain for at each amplifier in experimental case 3

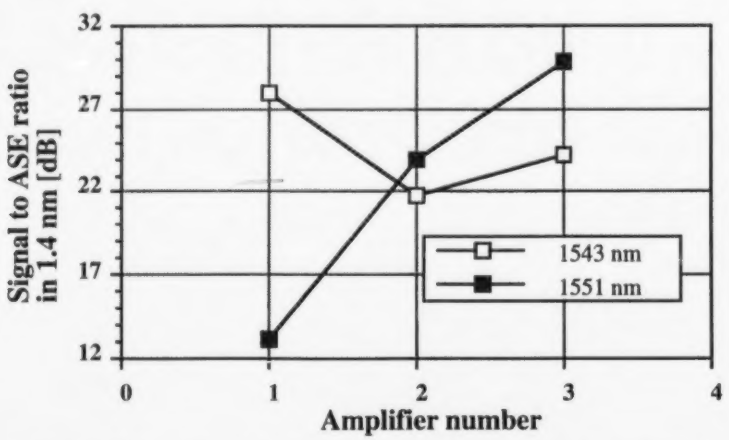

Figure 4.17 - Signal to ASE ratio at each amplifier for experimental case 3

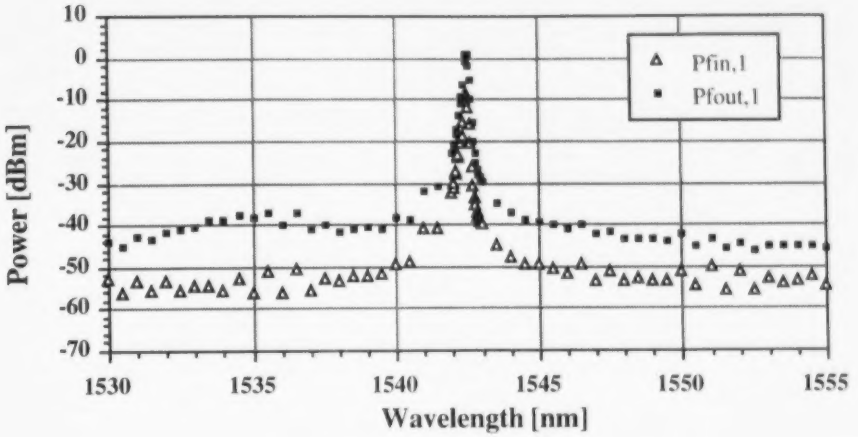

(a)

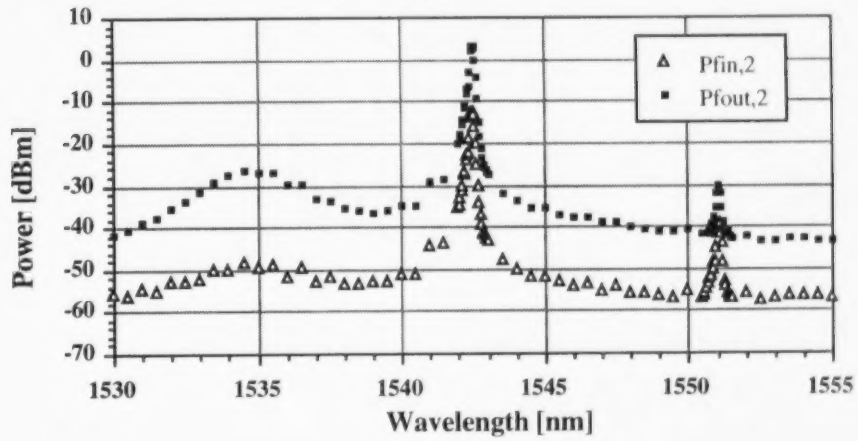

(b)

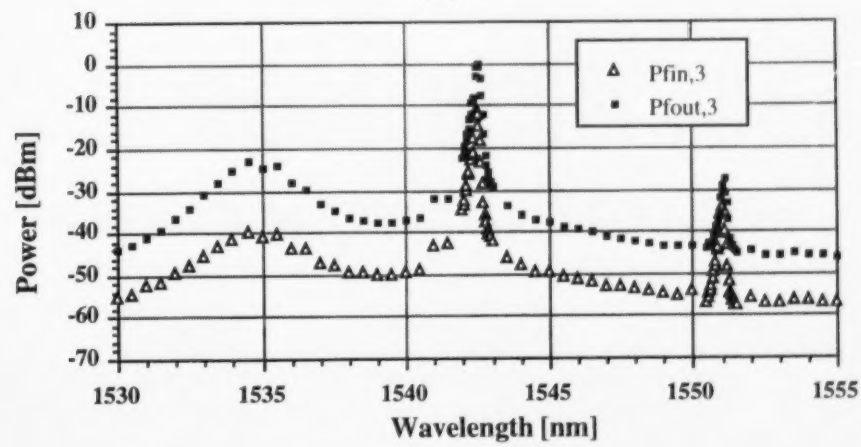

(c)

Figure 4.18 - Forward input and output spectra for experimental case 4. (a) Amplifier 1, (b) amplifier 2, (c) amplifier 3

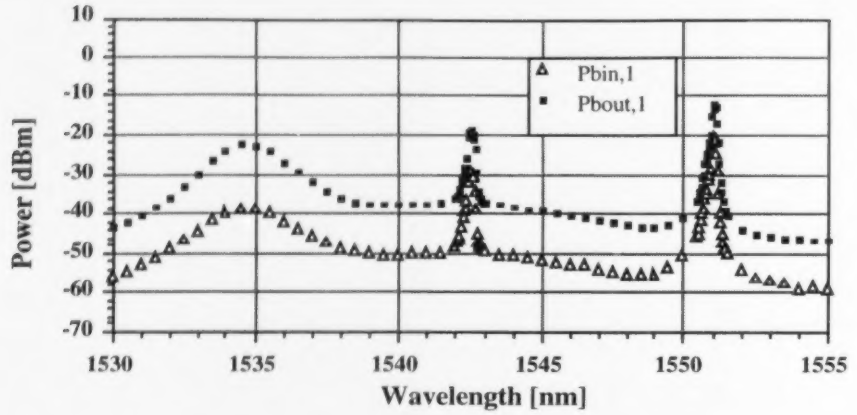

(a)

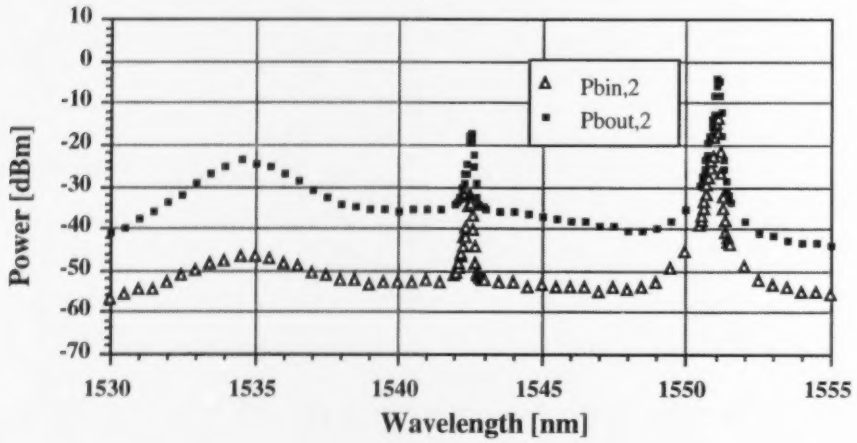

(b)

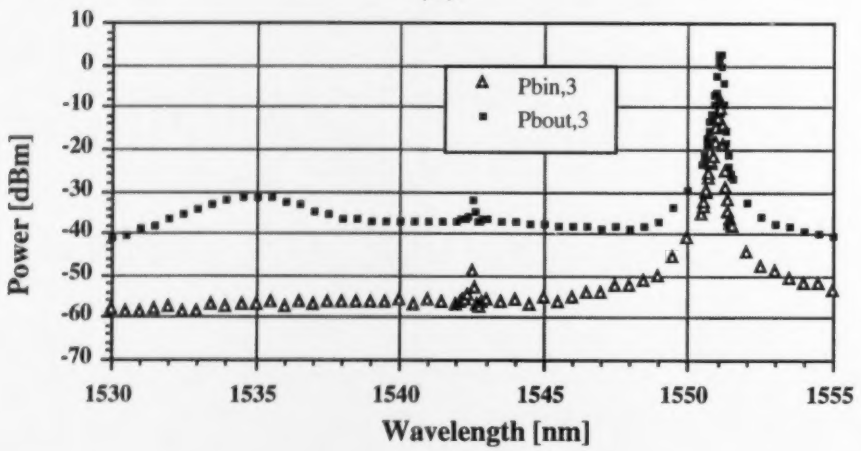

(c)

Figure 4.19 - Backward input and output spectra for experimental case 4. (a) Amplifier 1, (b) amplifier 2, (c) amplifier 3

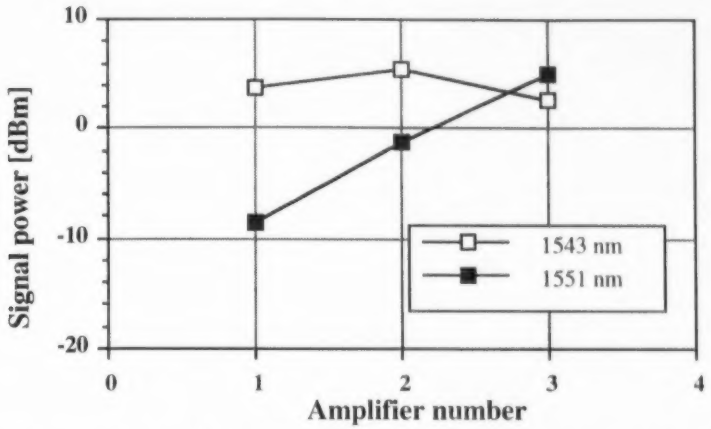

Figure 4.20 - Output signal power at each amplifier for experimental case 4

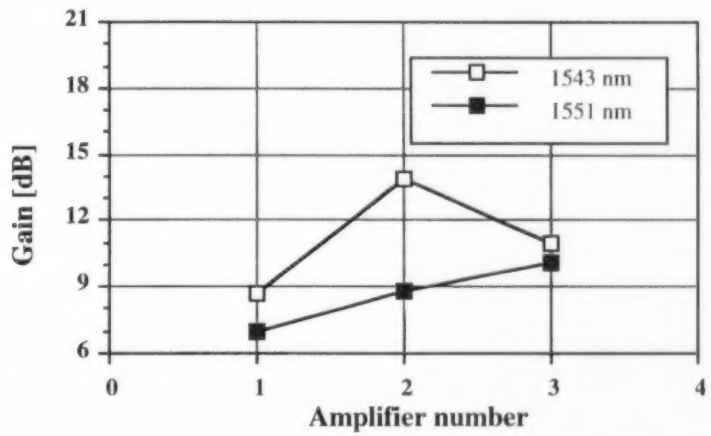

Figure 4.21 - Signal gain at each amplifier for experimental case 4

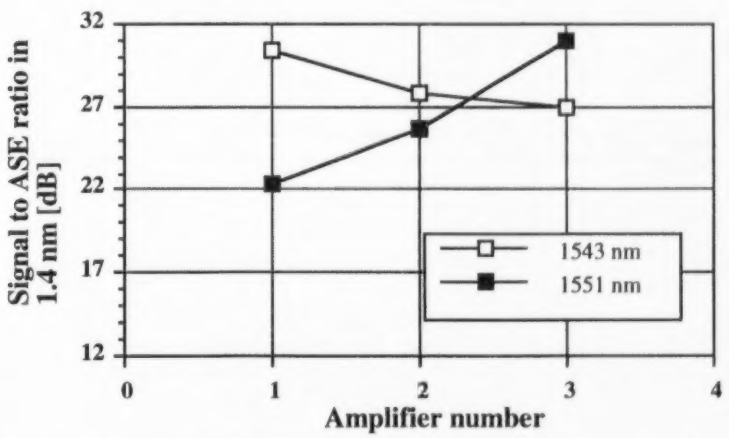

Figure 4.22 - Signal to ASE ratio at each amplifier for experimental case 4

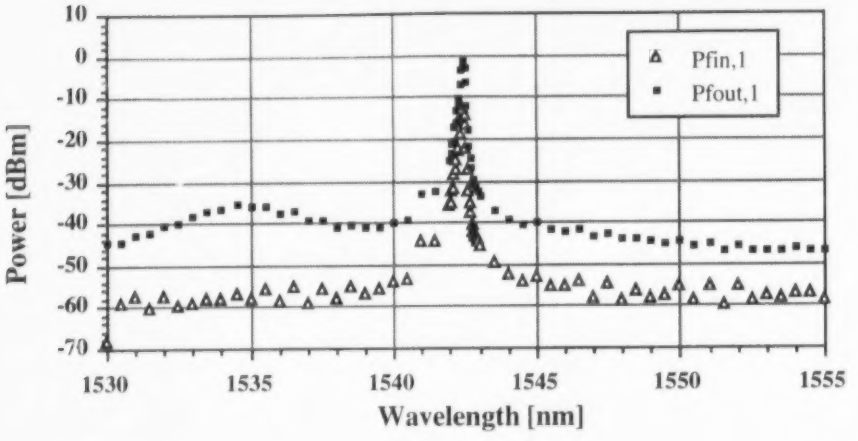

(a)

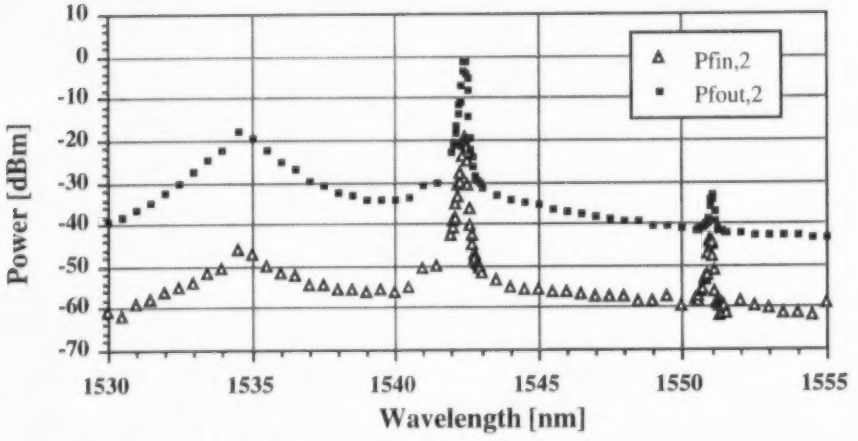

(b)

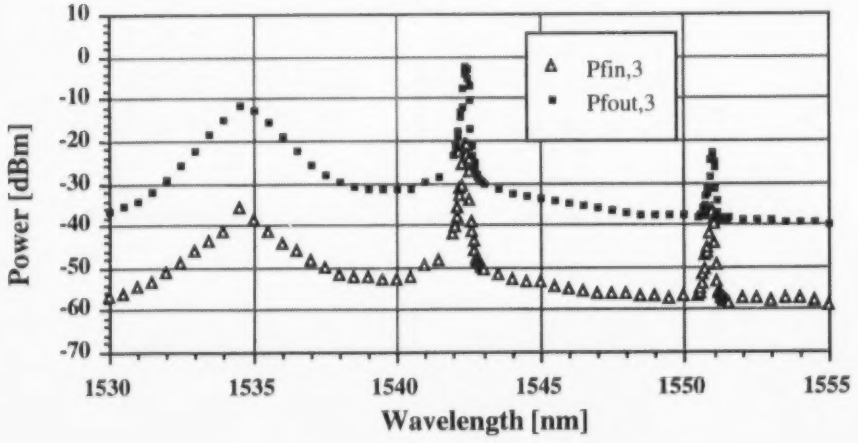

(c)

Figure 4.23 - Forward input and output spectra for experimental case 5. (a) Amplifier 1, (b) amplifier 2, (c) amplifier 3

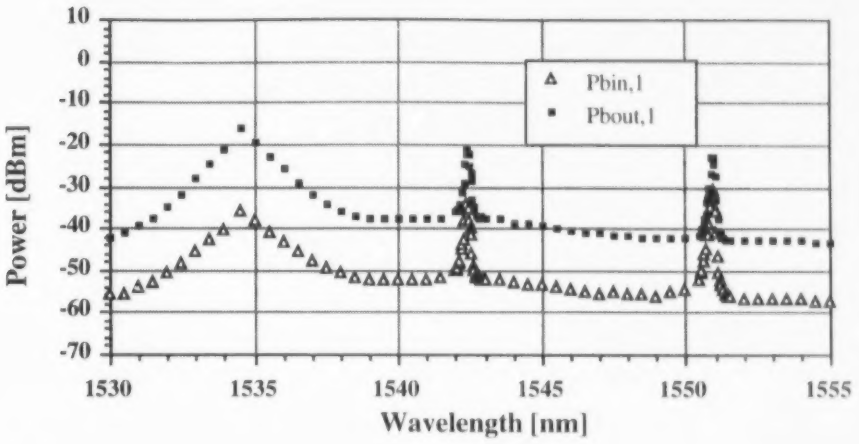

(a)

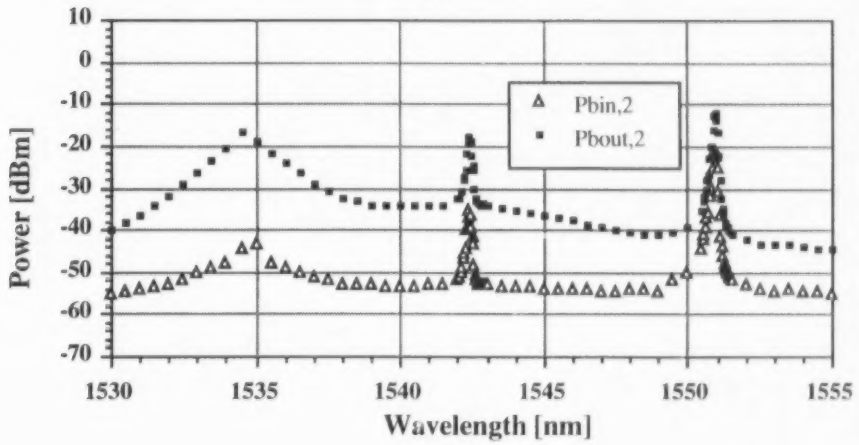

(b)

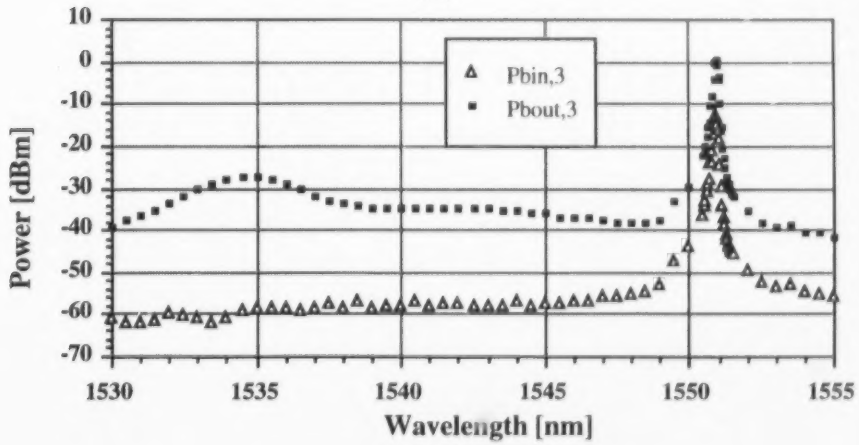

(c)

Figure 4.24 - Backward input and output spectra for experimental case 5. (a) Amplifier 1, (b) amplifier 2, (c) amplifier 3

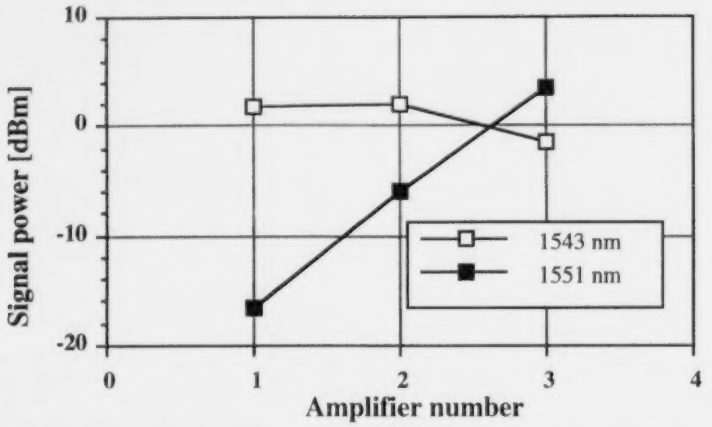

Figure 4.25 - Output signal power at each amplifier for experimental case 5

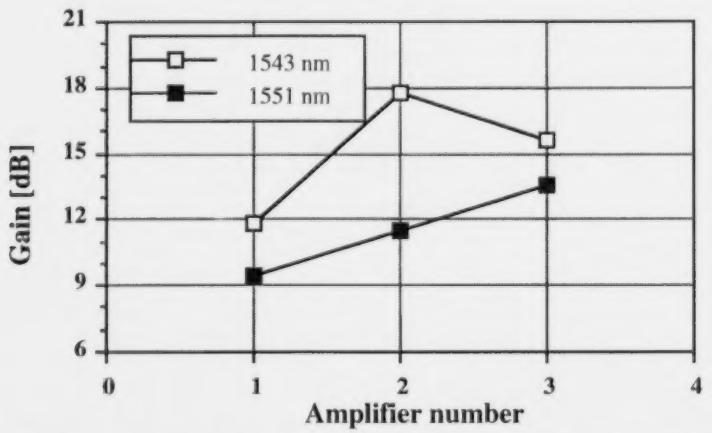

Figure 4.26 - Signal gain at each amplifier in experimental case 5

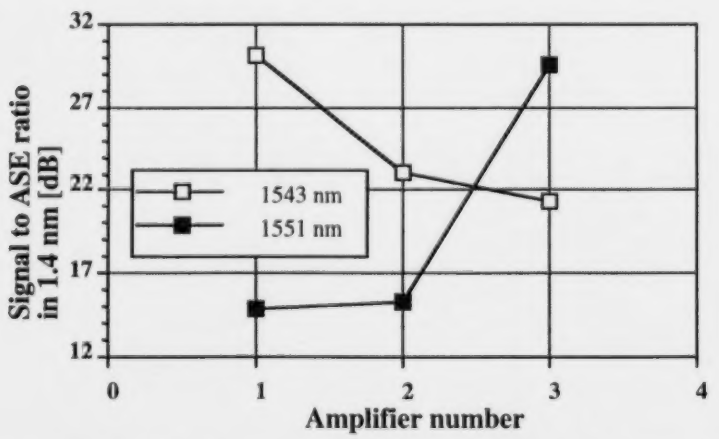

Figure 4.27 - Signal to ASE ratio at each amplifier in experimental case 5

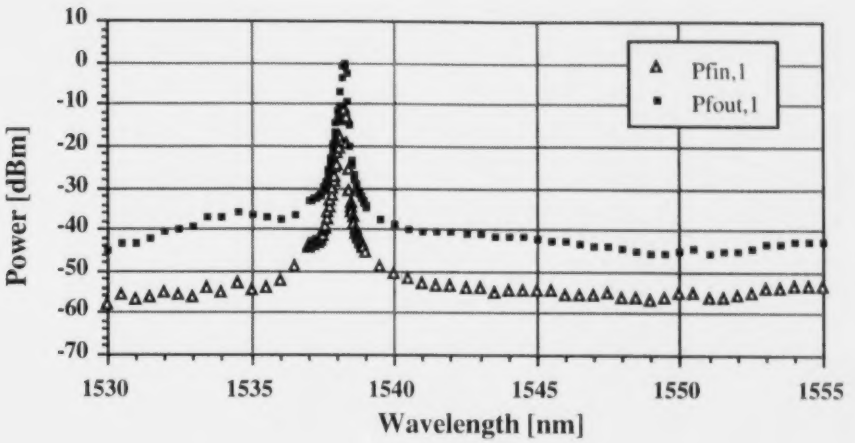

(a)

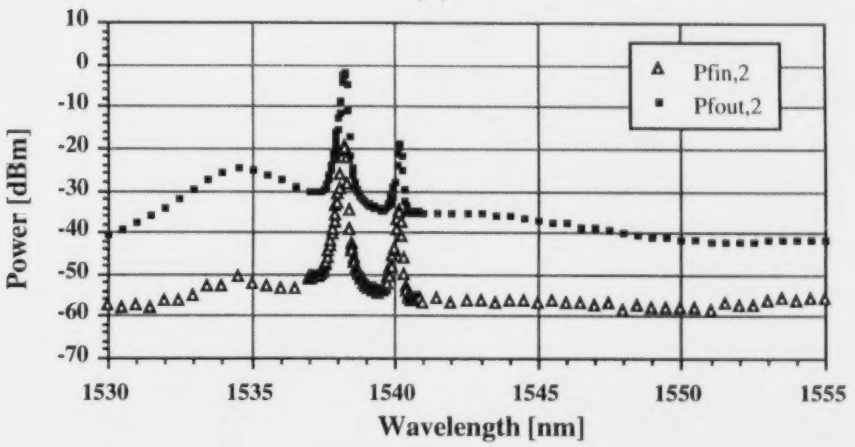

(b)

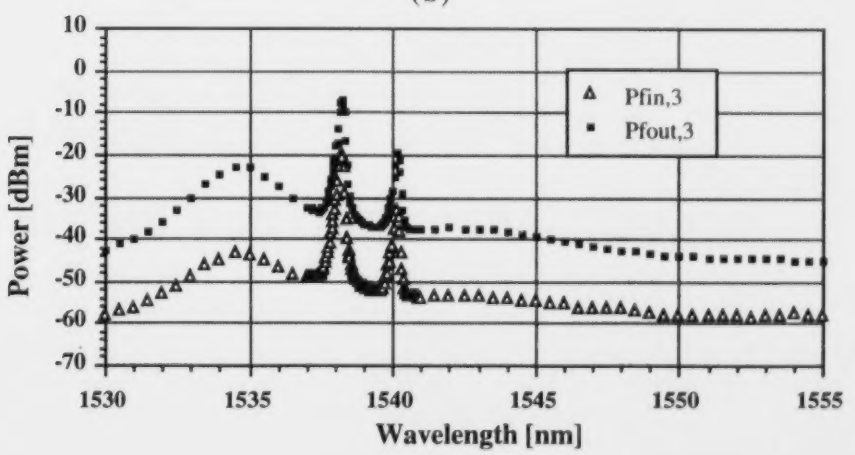

(c)

Figure 4.28 - Forward input and output spectra for experimental case 6. (a) Amplifier 1, (b) amplifier 2, (c) amplifier 3

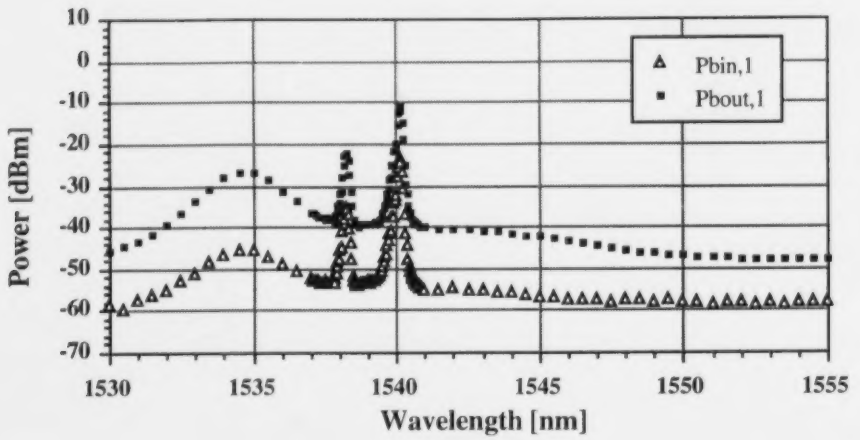

(a)

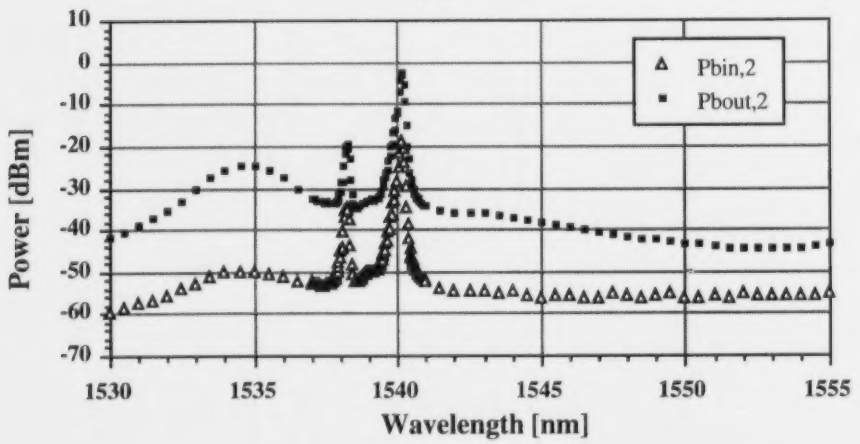

(b)

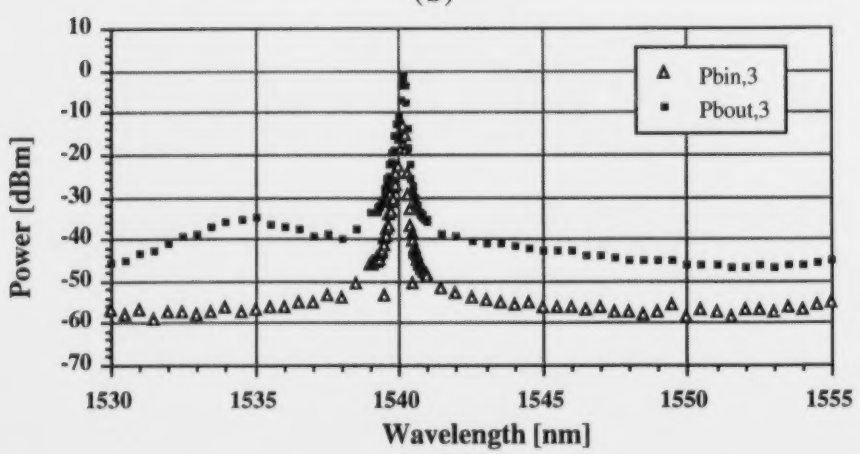

(c)

Figure 4.29 - Backward input and output spectra for experimental case 6. (a) Amplifier 1, (b) amplifier 2, (c) amplifier 3

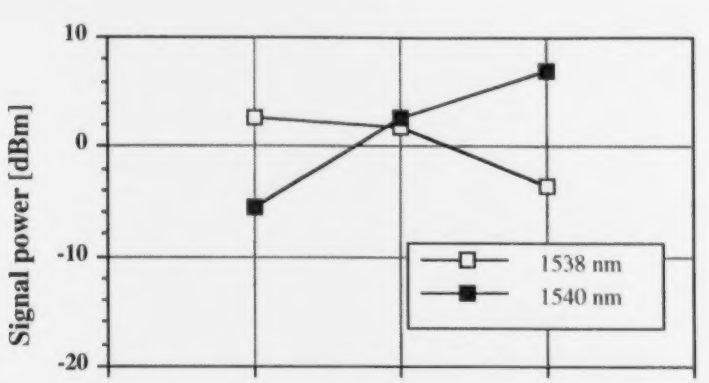

Figure 4.30 - Output signal power at each amplifier for experimental case 6

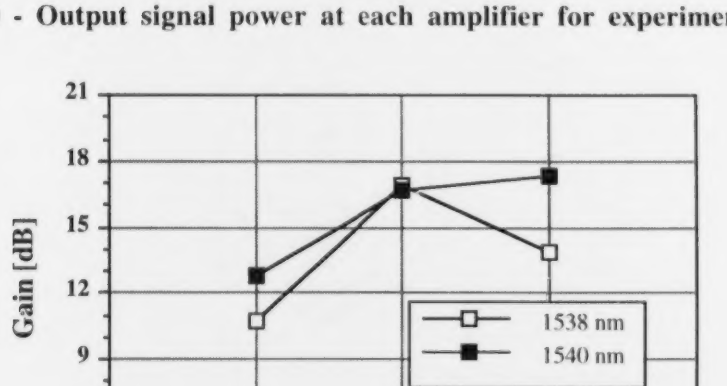

Figure 4.31 - Signal gain at each amplifier for experimental case 6

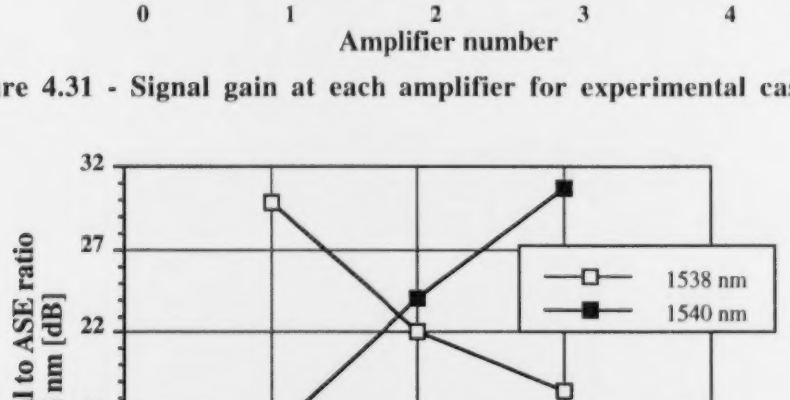

Figure 4.32 - Signal to ASE ratio at each amplifier for experimental case 6

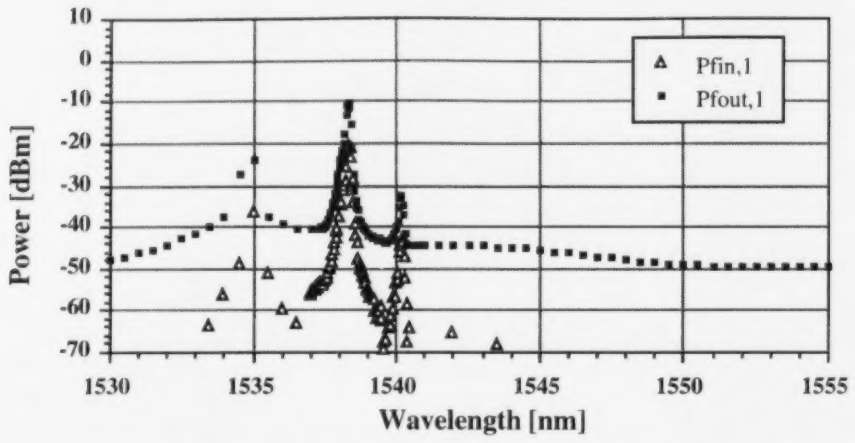

(a)

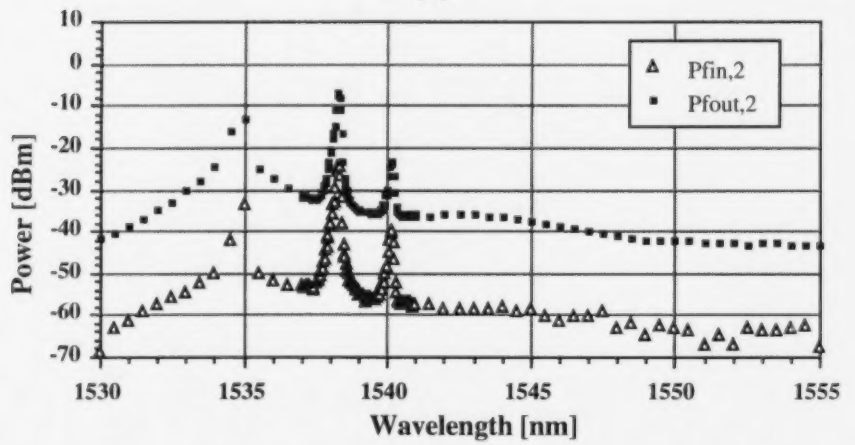

(b)

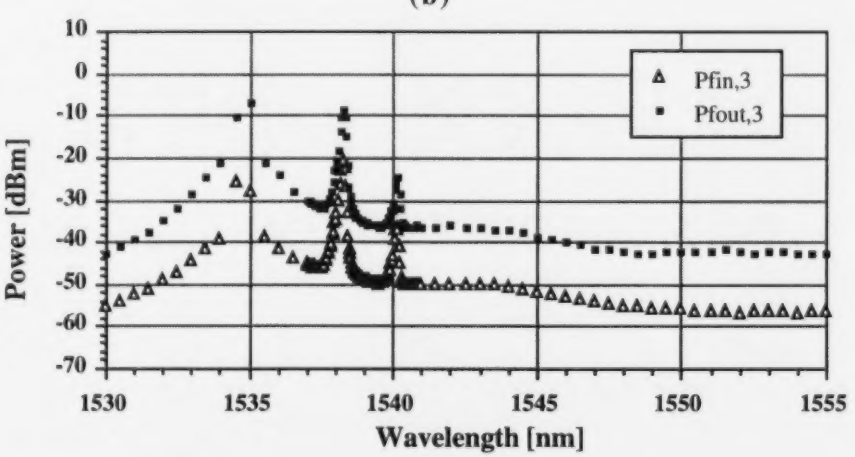

(c)

Figure 4.33 - Forward input and output spectra for experimental case 7. (a) Amplifier 1, (b) amplifier 2, (c) amplifier 3

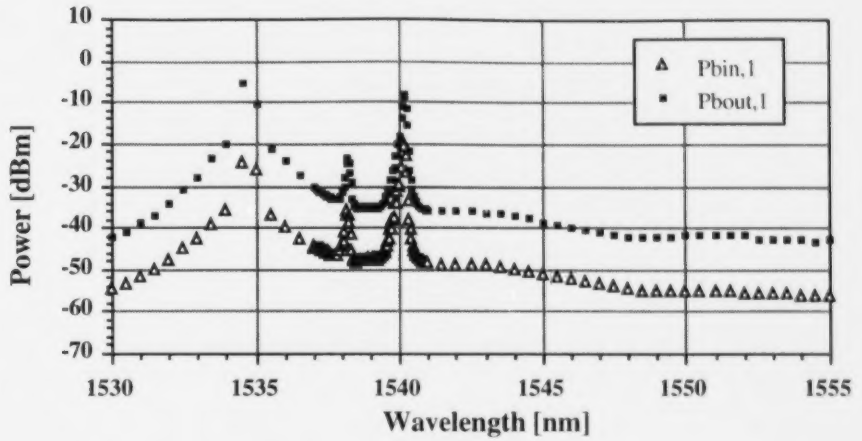

(a)

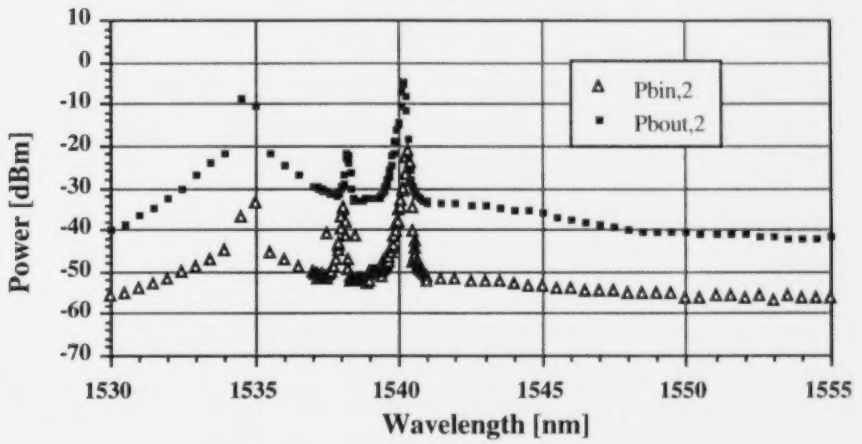

(b)

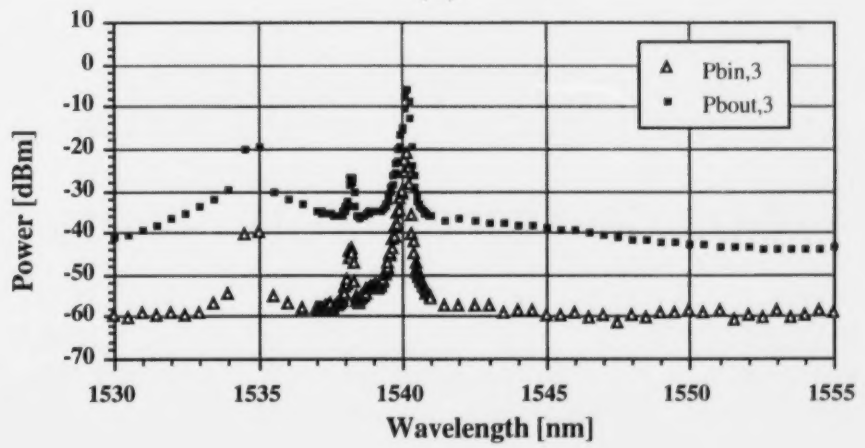

(c)

Figure 4.34 - Backward input and output spectra for experimental case 7. (a) Amplifier 1, (b) amplifier 2, (c) amplifier 3

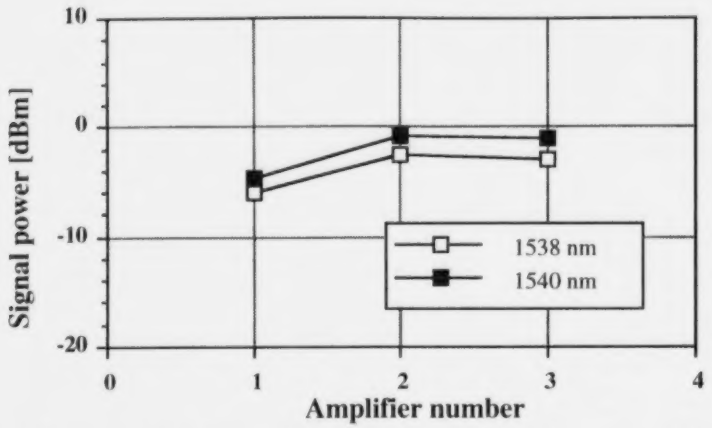

Figure 4.35 - Output signal power at each amplifier for experimental case 7

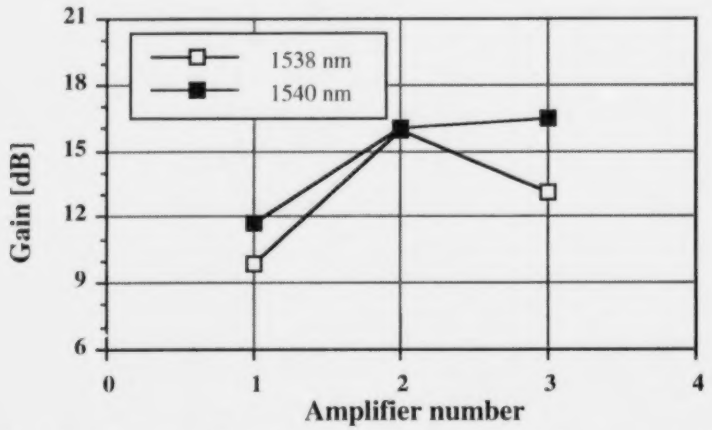

Figure 4.36 - Signal gain at each amplifier for experimental case 7

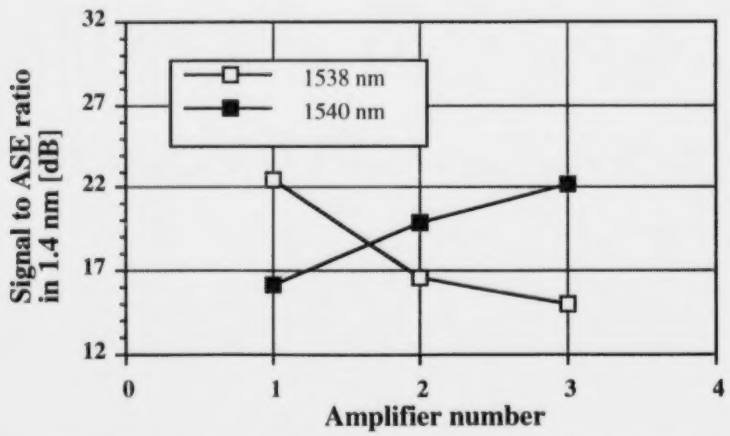

Figure 4.37 - Signal to ASE ratio at each amplifier for experimental case 7

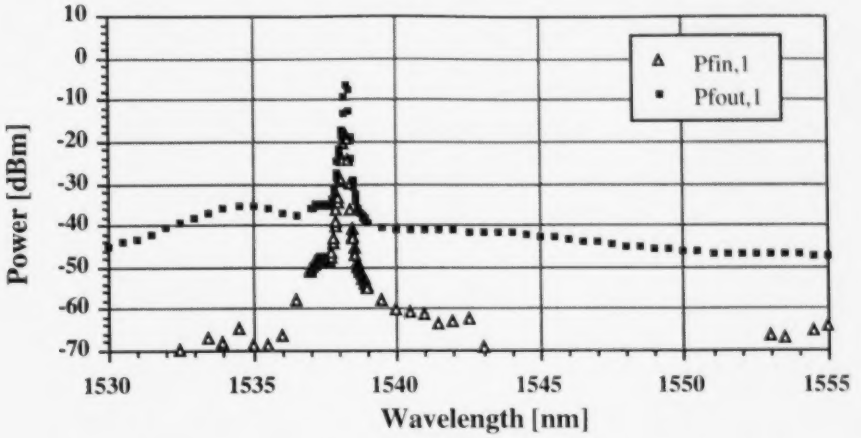

(a)

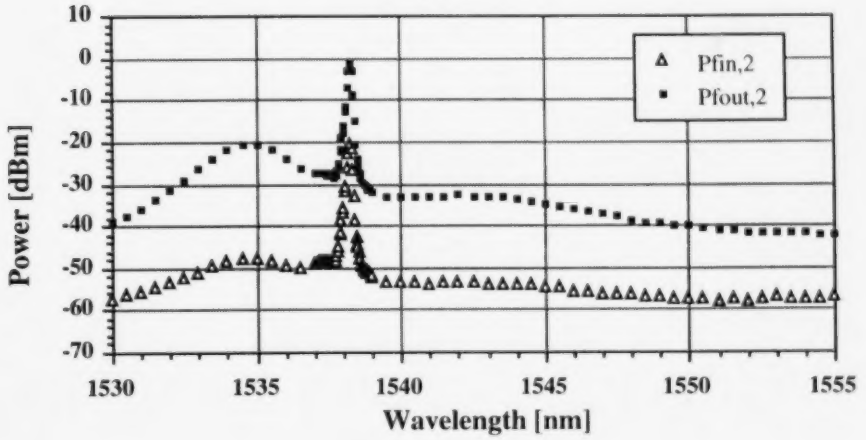

(b)

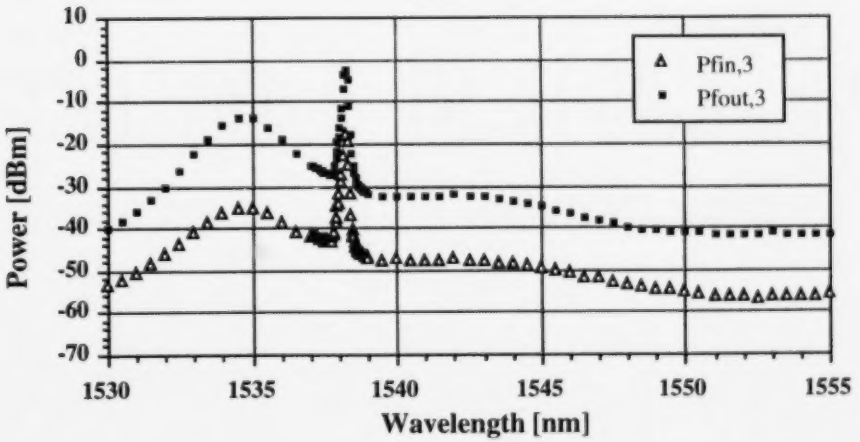

(c)

Figure 4.38 - Forward input and output spectra for experimental case 8. (a) Amplifier 1, (b) amplifier 2, (c) amplifier 3

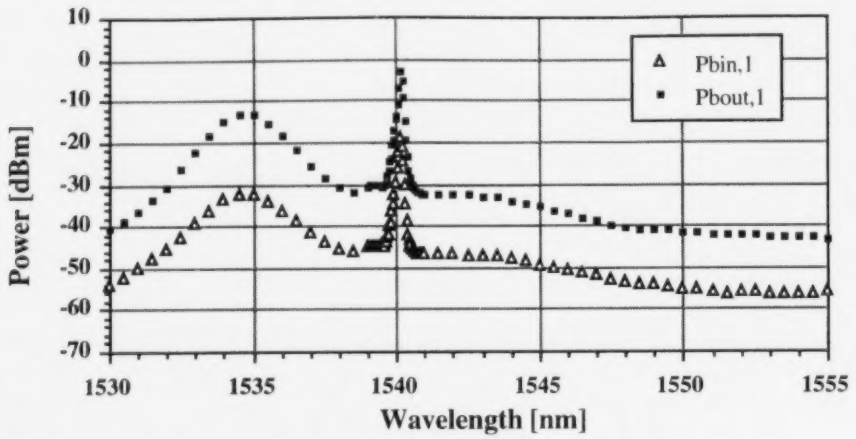

(a)

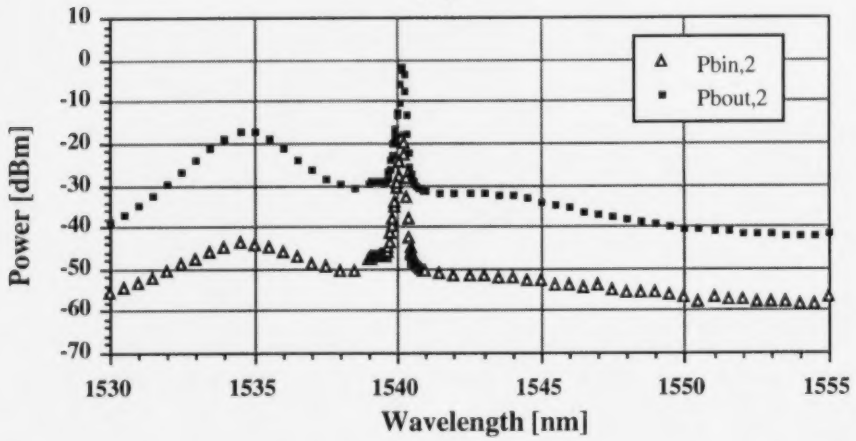

(b)

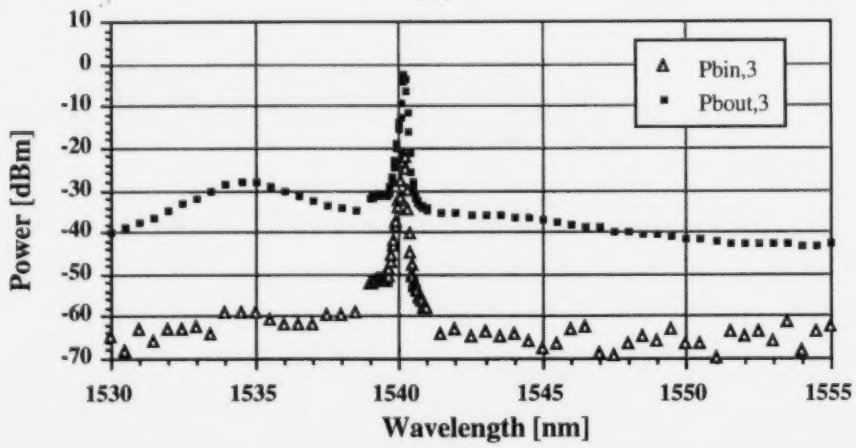

(c)

Figure 4.39 - Backward input and output spectra for experimental case 8. (a) Amplifier 1, (b) amplifier 2, (c) amplifier 3

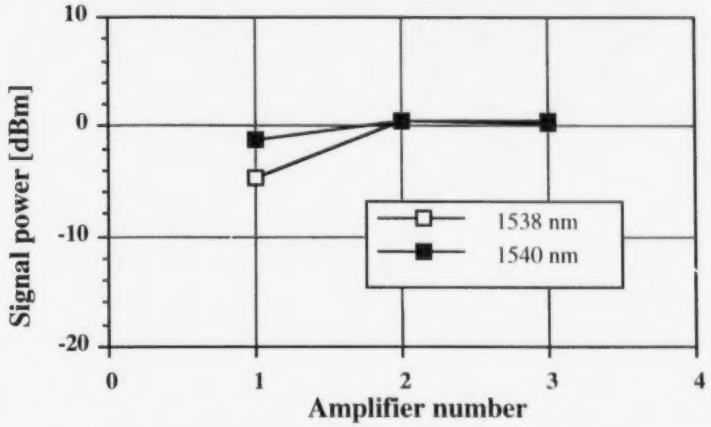

Figure 4.40 - Output signal power at each amplifier for experimental case 8

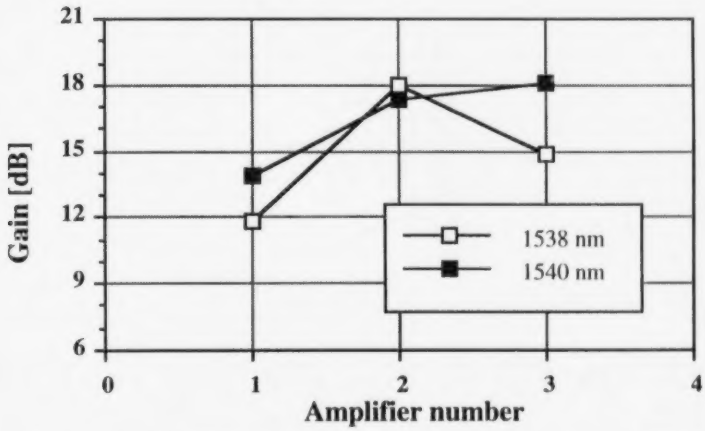

Figure 4.41 - Signal gain at each amplifier for experimental case 8

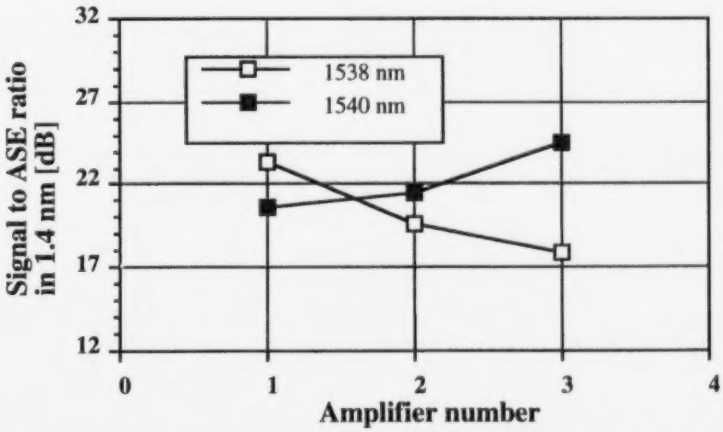

Figure 4.42 - Signal to ASE ratio at each amplifier for experimental case 8

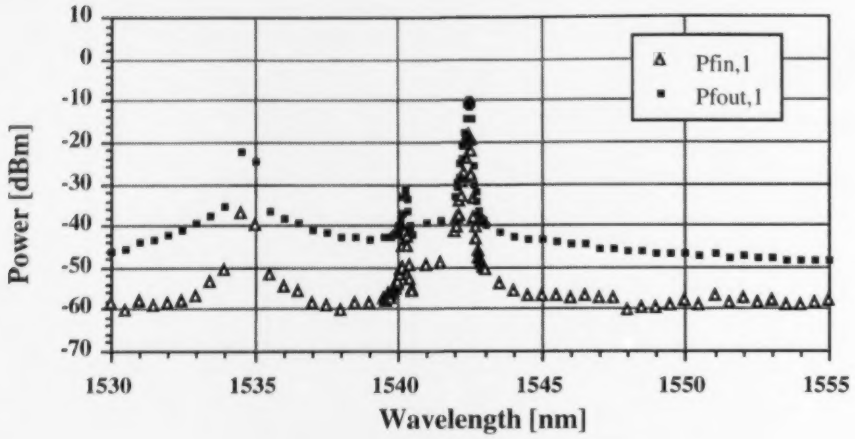

(a)

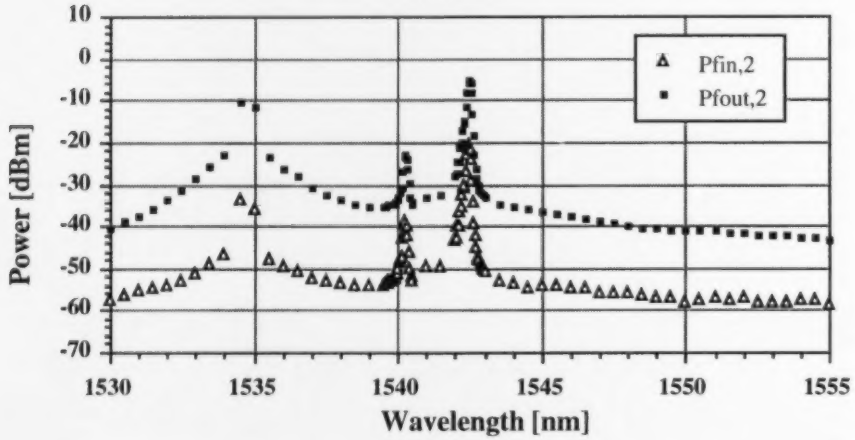

(b)

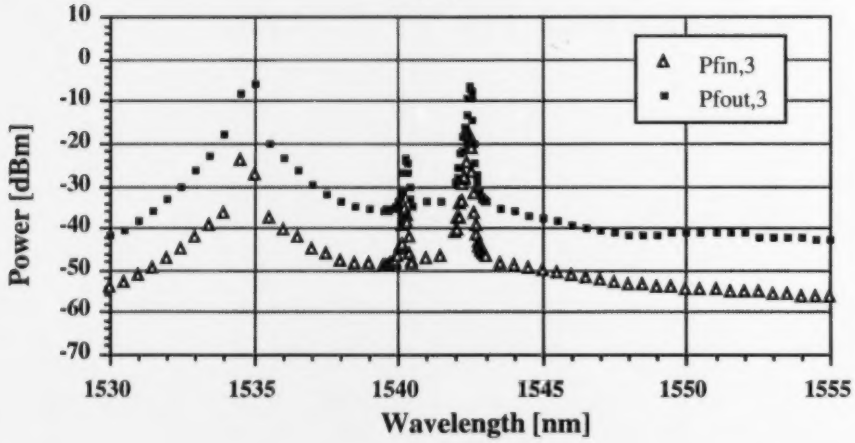

(c)

Figure 4.43 - Forward input and output spectra for experimental case 9. (a) Amplifier 1, (b) amplifier 2, (c) amplifier 3

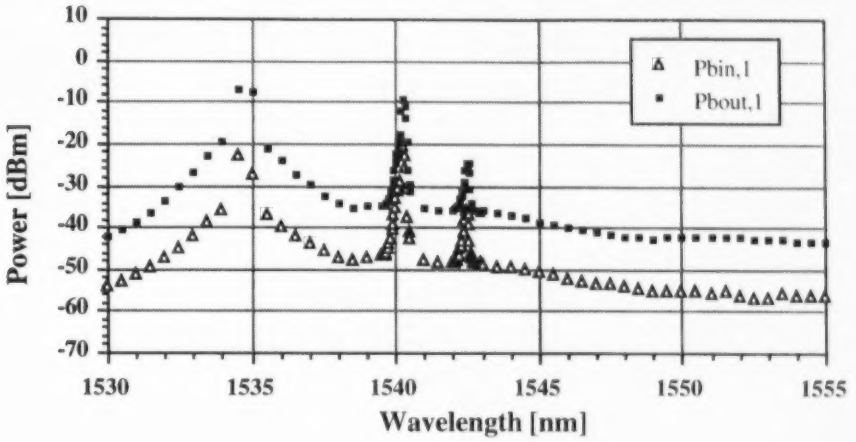

(a)

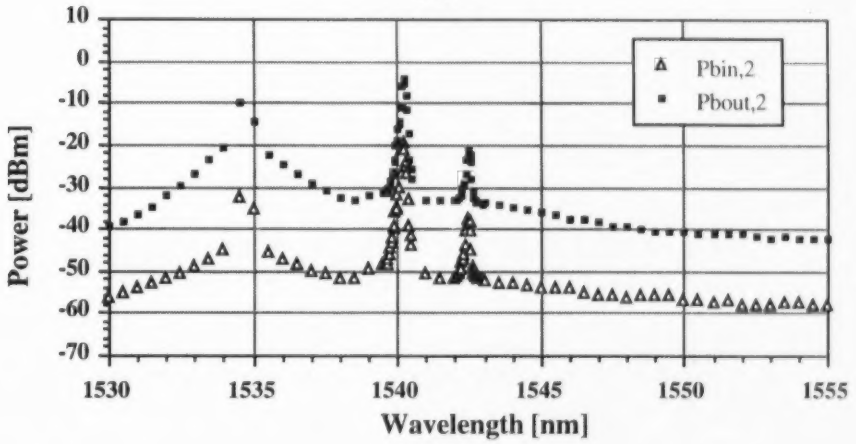

(b)

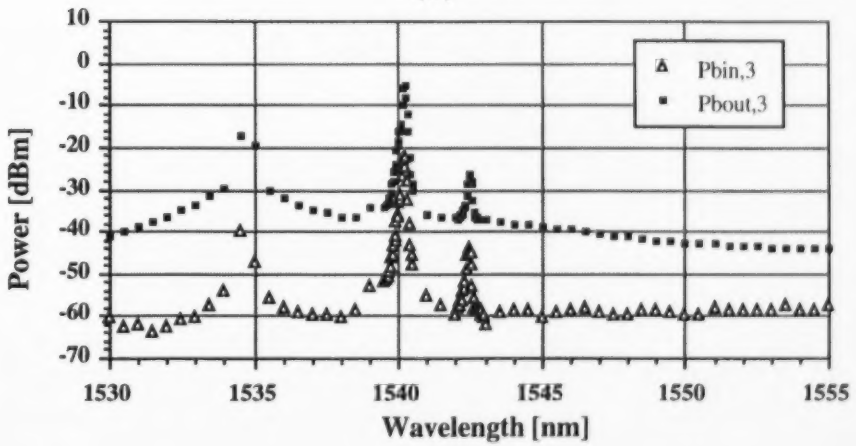

(c)

Figure 4.44 - Backward input and output spectra for experimental case 9. (a) Amplifier 1, (b) amplifier 2, (c) amplifier 3

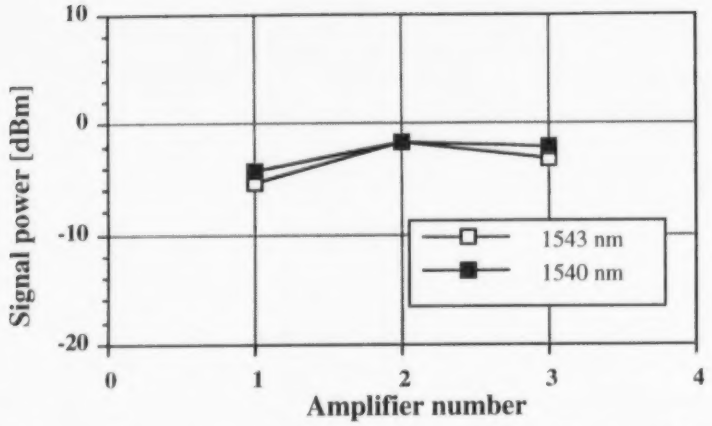

Figure 4.45 - Output signal power at each amplifier for experimental case 9

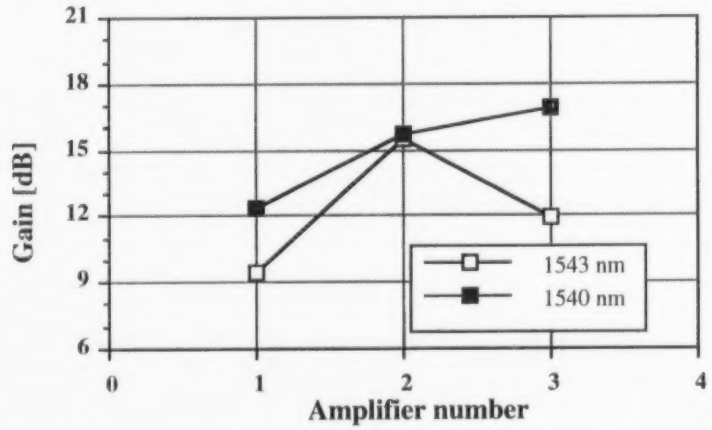

Figure 4.46 - Signal gain at each amplifier for experimental case 9

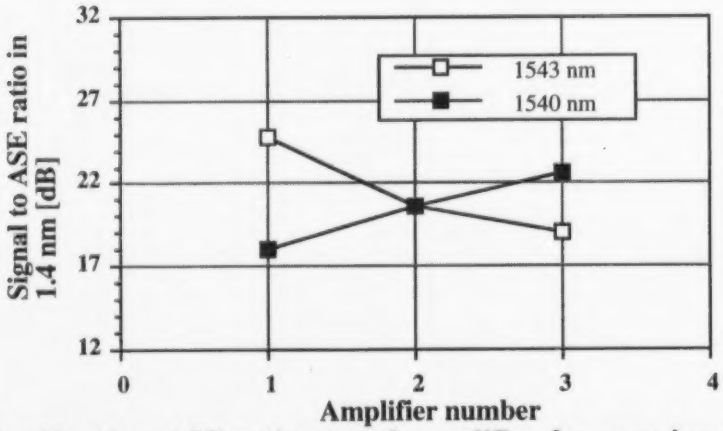

Figure 4.47 - Signal to ASE ratio at each amplifier for experimental case 9

in analyzing the experimental data collected that the transmission system is not symmetric since amplifier 1 has much lower gain than the other two.

We can see in case 1 that the signal at 1543 nm increases from stage 1 to stage 3. One could expect its gain to decrease since we have seen in chapter 2 that the signal gain decreases with increasing signal power. The fact is that the amplifier gain is controlled not only by the signal power but by the total input power to the amplifier, which includes the propagating signal and the accu.nulating ASE. The gain compression that each signal experiences is due to the effect of both propagating signals and the ASE accumulation in both directions. Rayleigh backscattered light is likely to play a role in the compression of the 1551 nm signal since the backscattered 1543 nm signal power is of the same order of magnitude as the propagating 1551 nm signal power (Figure 4.4).

We saw in chapter 2 that gains of signals at different wavelengths have different compression behaviours. We can see for example in Figure 2.7 that the gain of a signal at 1536 nm will saturate for lower input powers than the gain of a signal at 1544 nm. Figure 2.16 also tells us that a signal gain will be more or less compressed depending on the wavelength of the other signals present in the system. This explains the fact that the 1543 nm signal experiences different amounts of gain compression in case 1 and in case 2 since the second signal is at different wavelengths in those two cases.

We will now compare two others cases, 5 and 6. We are looking here at a longer transmission distance than in the cases mentioned above and shorter wavelengths in case 6 than in case 2. We will not attempt to compare gain and output power of signals since they are at different wavelengths but rather look at the differences in system performance for two different sets of wavelengths.

The obvious problem arising from a system transmitting signals whose wavelengths are far apart from each other, as in cases 1 and 5, is that there is quite a difference in small signal gain between the two wavelengths. While one signal has a gain large enough to compensate for the losses in the link and keep the signal output power at each amplifier relatively constant, the other signal will decrease at each stage, its gain not being sufficiently high to compensate for transmission losses. On the other hand, a system transmitting closely spaced signals will behave almost the same way in both directions. There is thus an advantage in having signals which are closely spaced in wavelength in a bidirectional transmission system. Having signals with higher small signal gains, as in

case 6, also has the advantage of further compressing the ASE peak. We can also note from the output spectra in case 5 that the ASE tends to peak more sharply when under less compression: the combination of signals at 1543 nm and 1551 nm in case 5 induces less ASE compression in the amplifiers than the signals at 1538 nm and 1540 nm do in case 6. We have seen such a behaviour in chapter 2 while looking at ASE and gain compression.

We will now examine the effect of signal wavelength on system performance for the case of three in-line amplifiers by looking at cases 7 and 9. The two contra-propagating signals are closely spaced in wavelength in both cases 7 and 9. From Figure 2.8, we can see that there is a small difference in small signal gain between the three wavelengths involved here: 1538, 1540, 1543 nm. We can see in Figure 2.9 that signals at these three wavelengths have different output saturation powers, which means that they will experience different gain compression for the same input power. The difference between cases 7 and 9 is the forward propagating signal wavelength: 1538 nm in case 7 and 1543 nm in case 9. The small signal gain for these two wavelengths is about 2 dB different and their output saturation power is also different. The 1538 nm signal being more compressed in a saturated amplifier (smaller saturation output power), the gain difference between a 1538 nm and a 1543 nm signal in cases 7 and 9 comes out to be less than 2 dB. This effect is also seen in a single amplifier system: the difference in gain between the two wavelengths decreases with amplifier saturation. On the other hand, in a single amplifier, the difference in output signal to ASE ratio between the two wavelengths is small and relatively constant. The changes in signal to ASE ratio observed are thus due to system effects that would not be observed in a single amplifier, single wavelength system.

We saw in section 2.2.4 that the amount of gain compression varies with the saturating wavelength. The 1540 nm signal experiences less cross-saturation from the 1543 nm signal in case 9 than from the 1538 nm signal in case 7. This explains why the 1540 nm signal has a slightly higher gain in case 9 than in case 7.

4.4.2 Signal power

Another criterion to consider in analyzing a bidirectional transmission system with cascaded EDFAs is the range of signal powers that will yield an acceptable signal to noise ratio.

To assess the effect on system performance of the launched signal powers, we will compare results from experimental cases 1, 3, and 4. The only variable parameter in these

three cases is the launched signal power. As one would expect, the gain is larger for the small input power of case 1 and the output power is larger for large input powers of case 4. In the latter case, we also notice a larger signal to ASE ratio than in the other cases and more ASE compression. Launching a large signal seems advantageous from the point of view of large output power, signal to ASE ratio, and ASE compression over lower input signal powers. The deciding factor is likely to be the SNR, which is higher for large launched signal powers than small signal powers in any given system examined. Systems with lower signal power are likely to be more distance limited their large signal power counterpart.

The launched power is lowest in case 1 and highest in case 4. One would thus expect the saturation to be more important and the gain lower in case 4 than in case 1. This is what we observe in Figures 4.6, 4.16, and 4.21 for cases 1, 3, and 4 respectively.

Larger signal power causes amplifiers to operate deeper into saturation than for small launched power, yielding lower gain but further compressing the output ASE power and improving the signal to ASE ratio. This is what we see in cases 1, 3, and 4 where the launched power is increasing from -20 dBm to -5 dBm.

The gain of the 1551 nm signal is always lower than the gain of the 1543 nm signal as seen in chapter 2.

The pre/post amplifiers are saturated by the launched signal, especially for large powers. The input signal to the in-line amplifier is not as large but the accumulated ASE forces the amplifier to operate further into the saturated regime.

4.4.3 Inter-amplifier link length

To assess the influence of the fibre link lengths on system performance, we will look at results from experimental cases 3 and 5. We have here two pre/post amplifier schemes with a total of either 100 km or 150 km of transmission fibre links.

Obviously, it is not desirable to have a transmission system where the inter-amplifier loss is larger than the amplifier gain. We mentioned this previously for systems with widely

spaced signal wavelengths. The limit of fibre link length one can use is thus dictated by the amplifier gain. Having two signal wavelengths for which there is a large difference in small signal gain complicates the task as the maximum link length must be computed for the smaller gain signal. We will look at ways to equalize the gain and signal output power in a multi-wavelength system in section 4.6. The difference in gain brings a penalty in distance for the larger gain signal. By studying cases 3 and 5, we can see the implications of using a system with inter-amplifier loss greater than the amplifier gain. In case 3, the gain of signal at 1543 nm is close to the inter-amplifier loss and the output power stays relatively constant at each amplifier. On the other hand, the gain of the 1551 nm signal is too small to compensate for the transmission losses. In case 5, the inter-amplifier loss has increased by about 5 dB. The input power to the in-line amplifier is larger in case 3, where the inter-amplifier link is 50 km long, than in case 5, where the inter-amplifier link is 75 km long; the amplifier gain is thus larger in case 5 where the amplifier is less saturated. In case 5, the signal at 1543 nm still manages to stay relatively constant over the cascade, but the signal at 1551 nm now drops by 10 dB at each stage, its signal gain being too small to compensate for transmission losses.

From chapter 2, gain compression is known to be less important for a 1551 nm signal than for a 1543 nm signal. In cases 3 and 5, the small gain compression experienced by the 1551 nm signal enables significant ASE build up to occur. The ASE power at the gain peak (1535 nm) experiences very little compression due to the 1551 nm signal and increases at each stage of the system to become dominant over the propagating 1551 nm signal by the end of the transmission link. The gain experienced by the ASE peak is larger than the gain of the 1551 nm signal.

Due to large inter-amplifier attenuation in case 5, the amplifiers in this case are less saturated than in case 3 and exhibit a larger gain.

The greater saturation of amplifier 3 in case 3, compared to case 5, and the fact that the 1543 nm signal is almost constant along the system allows it to have a larger signal to ASE ratio than in case 5 where the signal has decreased after three amplifiers and the ASE compression is not as important.

In conclusion, in a long distance system, it is desirable to transmit signals closely spaced in wavelength along a link with inter-amplifier loss no greater than the small signal gain of the signals.

4.4.4 Amplifier position

Erbium-doped fibre amplifiers can be used in an optical bidirectional transmission system as both pre/post and as in-line amplifiers. Pre/post amplifiers are mainly used to boost the signal before detection and improve the receiver sensitivity. As in-line amplifiers, the EDFAs' main purpose is to compensate for transmission losses.

To assess the influence of amplifier position on system performance, we will look at results from experimental cases 6 and 7. We have here two different cases, one with two pre/post amplifiers and an in-line amplifier, and the other case with all in-line amplifiers. The transmission distance is comparable in the two cases: 150 km and 170 km. We can notice from the graphs in Figures 4.38 and 4.43 that the signal gain and signal to ASE ratio at each amplifier in case 6 (pre/post amplifiers) are larger than in the case where all EDFAs are used as in-line amplifiers (case 7). ASE peaking in the in-line amplifier case is quite important and does certainly add to the gain compression of each amplifier in the link.

Because of the presence of additional attenuation before amplifier 1 and after amplifier 3, the launched powers are smaller and the amplifiers are less saturated in case 7 than in case 6 even if there is more ASE accumulation at the end of the transmission link in case 7.

There appears to be a contradiction when we look at Figures 4.31 and 4.36. If the amplifiers in case 7 are less saturated than in case 6, why is their gain lower? The only explanation to this comes from the ASE. We can see by comparing Figures 4.28, 4.29, 4.33, and 4.34 that there is quite a bit more ASE accumulation in case 7 and an evident peaking of the ASE around 1535 nm. This ASE peaking effect is due to the Rayleigh backscattering in the fibre added in case 7 to operate all three amplifiers as in-line amplifiers. The ASE peak at 1535 nm acts as a third saturating signal in the system and has a significant effect in the compression of the other signals (section 2.2.4). So, even if the total power at the input of each amplifier in case 7 is less than what it is in case 6, the amplifier gain is lower in case 7 because of the added compression due to the ASE peak. The importance of the ASE peaking in case 7 is due to the extra Rayleigh backscattering in fibre links before and after the first and last amplifiers, links that are absent in case 6.

We saw in chapter 2 that signals at 1538 nm and 1540 nm have almost the same small signal gain, the gain at 1538 nm being a little higher than the gain at 1540 nm, but a

different output saturation power. This means that the 1538 nm signal, with a smaller output saturation power (Figure 2.9), sees its gain decrease faster with input power than the 1540 nm signal. It also means that in the highly saturated regime the signal at 1540 nm will have a gain advantage over the signal at 1538 nm. The gain saturation curves will cross at a certain point from which the 1540 nm gain will be higher than the 1538 nm gain for a given input power. Knowing that amplifier 1 and amplifier 3 are highly saturated in both cases 6 and 7, this explains why we get higher gain at 1540 nm than at 1538 nm. As to why the 1540 nm gain advantage is larger for amplifier 3 than for amplifier 1, it could be explained by the influence of ASE on signal compression which is larger on the 1538 nm signal than on the 1540 nm signal. The fact that amplifier 1 has a smaller pump power and lower population inversion than amplifier 3 may also offer an answer since the difference in gain at the two wavelengths is smaller for a low pump power than for large pump power.

The pre/post amplifier scheme seems advantageous over the in-line amplifier case since it yields larger signal to ASE ratio, received power, and ASE compression.

4.4.5 Rayleigh backscattering

Rayleigh backscattering has been known to have an influence in optical systems [26]-[31]. Preventing the Rayleigh backscattered light from impacting on system performance is one of the reasons why isolators are used in unidirectional transmission systems. In bidirectional transmission systems, we cannot use isolators and these are thus more sensitive to the effects of Rayleigh backscattering and even double Rayleigh backscattering, which we did not considered in our theoretical analysis in chapter 2.

To assess the influence of Rayleigh backscattering in an open bidirectional cascade of EDFAs, we will look at the results from experimental cases 7 and 8. We have here two systems of in-line amplifiers where the fibre spools in case 7 have been replaced by attenuators of same loss in case 8. The Rayleigh backscattering coefficient of the transmission fibre used in these experiments was measured [32] to be -31.5 and -33.2 dB for fibre made by Northern Telecom and Corning, respectively. We can thus study the effect of Rayleigh backscattering on the system performance between case 7 where it is present, and case 8 where it is not.

A main source of saturation in case 7 is the large ASE accumulation and peaking effect (section 4.4.4). We mentioned in the previous section that this can be attributed to Rayleigh backscattering. By looking at the results for case 8 (Figures 4.38 and 4.39), we see that in the absence of Rayleigh backscattering the ASE accumulation is substantially lower and that is does not exhibit a peaking effect. The ASE sharp peaking behaviour is present in the case with Rayleigh backscattering (case 7) and induces more gain compression in the system; the peak around 1535 nm gets as large as the signal after three amplifiers in the case where there is Rayleigh backscattering compared to about 12 dB lower for the case where Rayleigh backscattering is not present (case 8).

The 2 dB increase in gain seen in case 8, compared to case 7, is attributed to the smaller saturation effect of the accumulated ASE power. The Rayleigh backscattered signal in case 7 has a smaller effect in compressing the signal gain than the accumulated ASE, but even then case 8 has the advantage of totally eliminating saturation effects from Rayleigh backscattered light. We will see in section 4.6 some suggestions to reduce the effect of Rayleigh backscattering in a bidirectional transmission system with EDFAs.

In conclusions, Rayleigh backscattering certainly does have an effect on bidirectional transmission systems and brings a penalty without impinging the feasibility of bidirectional transmission systems in the future.

4.5 Comparison between simulated and experimental results

In chapter 3, we studied bidirectional transmission systems with EDFAs through a set of nine simulation cases to learn about the properties of the system before putting the principles to use in a laboratory experiment. Up to this point in chapter 4, we studied bidirectional transmission systems with EDFAs by repeating nine setup cases with actual devices and experimental work. The question is: how well do computer simulated and experimentally obtained data match?

The computer simulation designed in chapter 3 is two fold: the first part uses an EDFA simulation from [25] to compute gain and output power (signal and ASE) of each amplifier as a function of the input power; the second part uses the signal and noise propagation equation to compute the input power to a given amplifier as a function of the output power from every other amplifier in the system, the inter-amplifier link losses, and Rayleigh backscattering coefficients.

We will first look at the EDFA simulation on its own. Figure 4.48 shows the experimental data for the forward ASE spectrum of amplifier #303 with a co-propagating input signal of wavelength 1539 nm and power of -35 dBm (small signal regime) and the simulation of the same case. As mentioned in section 4.2, the emission cross-section provided by NOI were here modified to better fit the small signal regime ASE spectrum of the actual amplifiers.

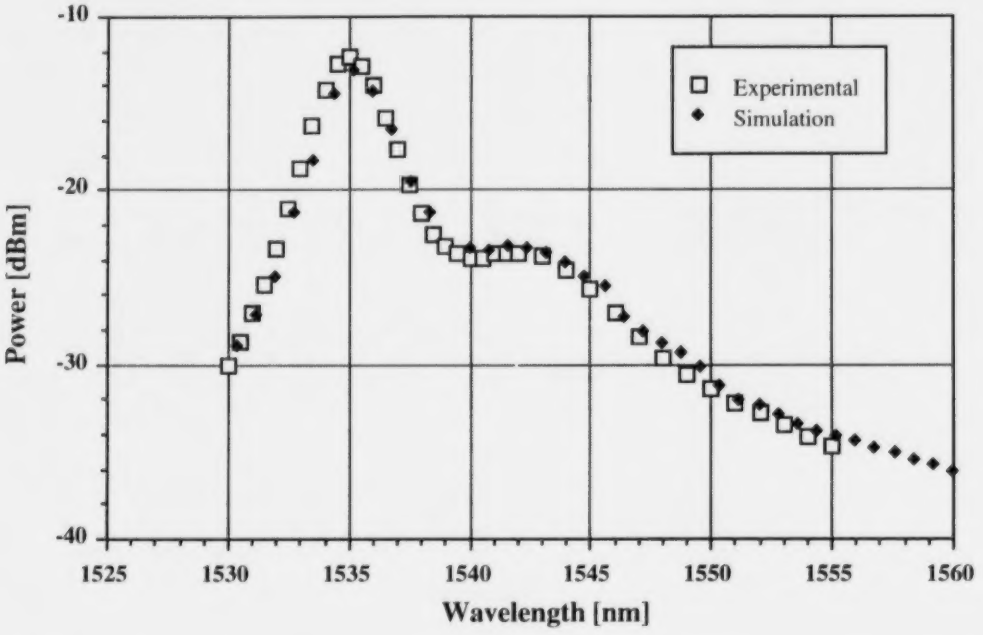

Figure 4.48 - Comparison of simulation and experiment for small signal regime

Now let's look at the performance of the computer simulation in the saturated regime. Figure 4.49 shows a comparison between experimental and simulated ASE spectrum similar to the previous case, but now the input signal power is at -10 dBm (saturated regime). The signal wavelength is still at 1539 nm and the modified cross sections from Figure 4.1 were used in the calculations. We can see that the simulation does not quite handle saturated regime adequately: the simulated compression is about 2 dB less than what the experimental results show.

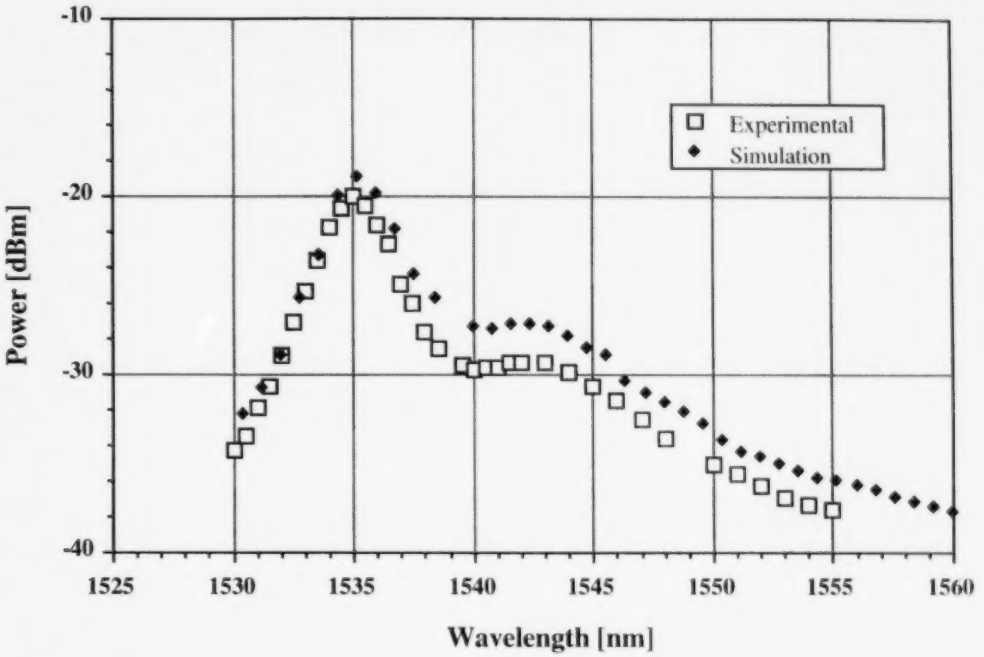

Figure 4.49 - Comparison of simulation and experiment for saturated regime

We will now look at the performance of the overall simulation package to predict the behaviour of bidirectional transmission systems with EDFAs. In the first place, we look at a simple case. We simulated the experimental case 8 where Rayleigh backscattering is not included. Figures 4.50 and 4.51 compare simulated and experimental forward and backward output spectra for case 8 (see Table 4.4). The agreement is reasonable especially considering the limitation of the EDFA simulation in the saturated regime, as discussed above. The discrepancy between simulated and experimental data is largest at the ASE peak around 1535 nm and increases with propagation in the system (larger at third amplifier for forward signal and at first amplifier for backward signal). The simulated compression, as we saw earlier, is less than in reality. As we are simulating a cascade of amplifiers, the simulated gain and output power of the first amplifier in the link are going to be larger than reality and the discrepancy will build up at each amplifier. We must not forget the inherent experimental error that can become significant in a setup where there are about twenty different devices connected to each other. The error in estimating the insertion loss of all of these components can amount to close to 1 dB. In this regard, the simulation is considered to be adequate to give an understanding of a bidirectional transmission system with

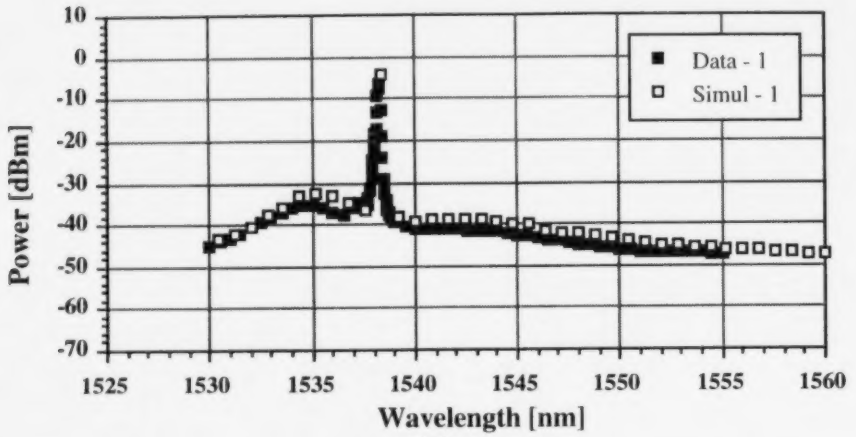

(a)

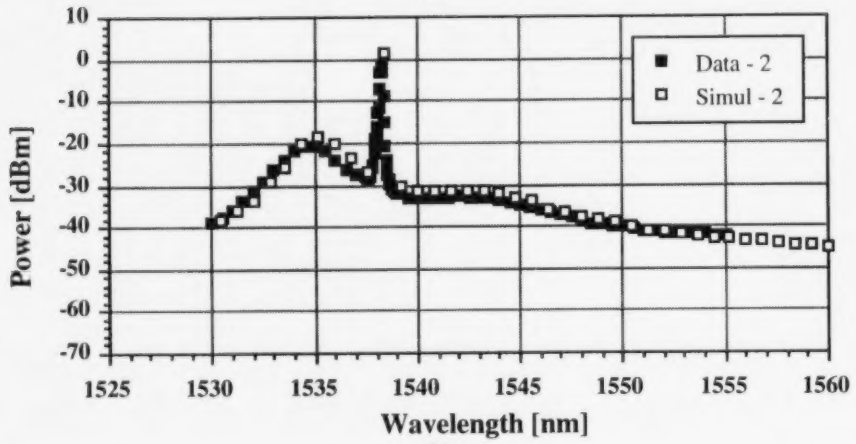

(b)

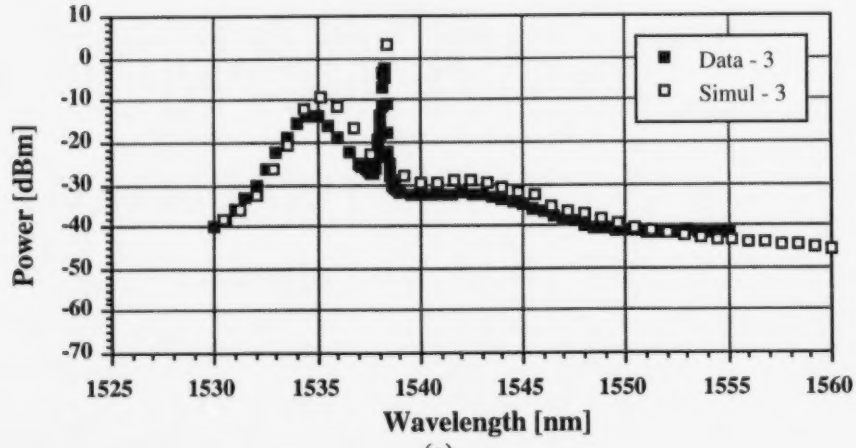

(c)

Figure 4.50 - Comparison of simulation and experiment for forward spectra of case 8. (a) Amplifier 1, (b) amplifier 2, (c) amplifier 3.

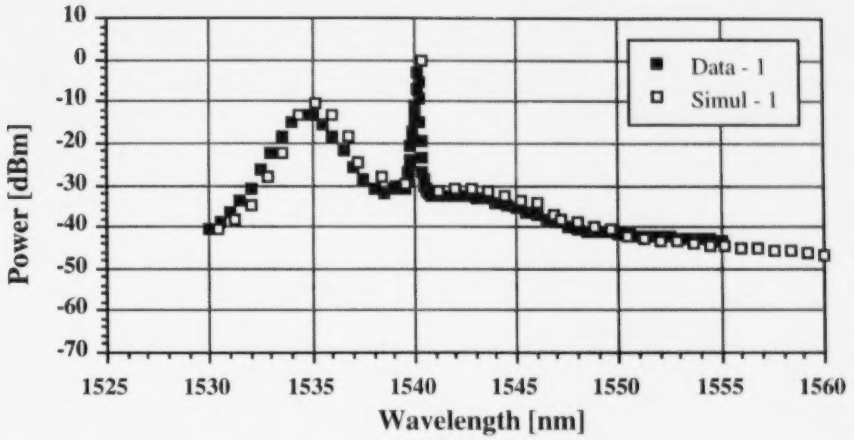

(a)

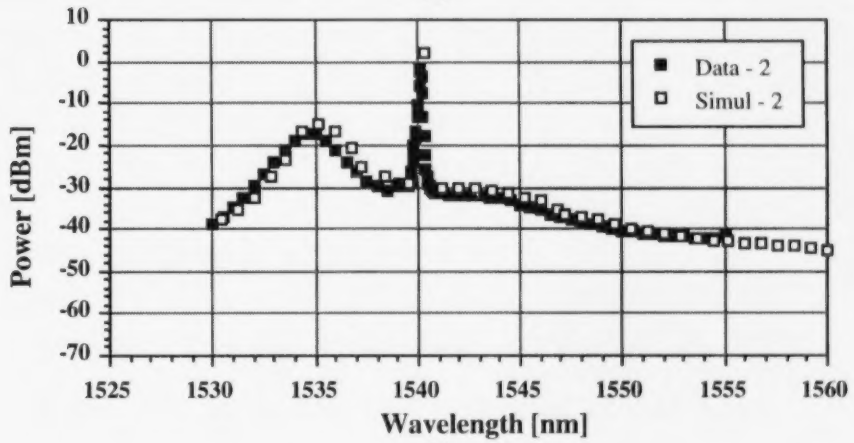

(b)

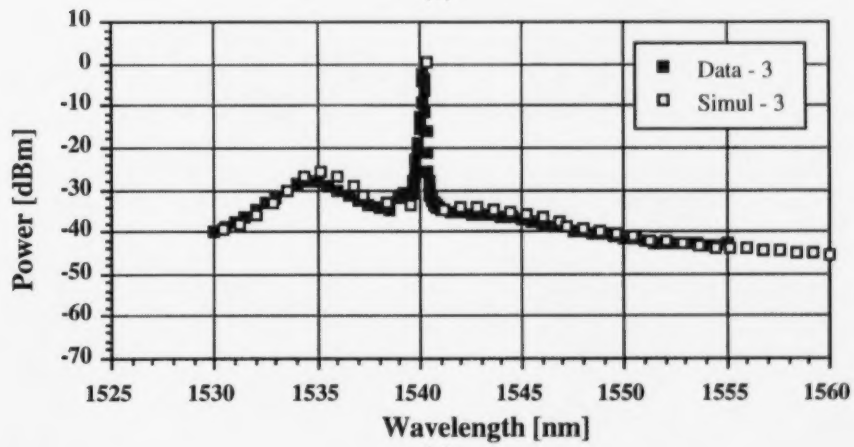

(c)

Figure 4.51 - Comparison of simulation and experiment for backward spectra of case 8. (a) Amplifier 1, (b) amplifier 2, (c) amplifier 3.

EDFAs. More work should probably be done to look into how well the computer simulation handles the saturated regime and make the appropriate modifications. A comparison between simulation and experimental results for a larger cascade of amplifiers would also be interesting.

Lastly, we look at the simulation of experimental case 7, which is the equivalent of case 8 but with Rayleigh backscattering present. Figures 4.52 and 4.53 show both simulated and experimental results for case 7 (see Table 4.4). The discrepancy is still present and increases more rapidly along the cascade. We must understand that the amplifiers in case 7 are driven even more into saturation than in case 8 because of the quicker (and more important) build up of ASE. We can see in Figures 4.52c and 4.53a that after three amplifiers the ASE peak is larger than the propagating signal.

The Rayleigh backscattered signal is larger in the simulation case than the experimental case, and the discrepancy is larger than for the propagating signal. We have to remember here that the simulated output signal of an amplifier is larger than reality to begin with. It is then backscattered and re amplified with a gain that is larger that what the signal in the experimental case experiences. This leads to a bigger discrepancy between simulated and experimental results for the Rayleigh backscattering signal than for the propagating signal.

Finally, uncertainties about the erbium-doped fibre parameters such as absorption and emission cross sections, erbium dopant concentration and confinement are factors that limit the accuracy of the simulation. We had to modify the emission cross section data provided by NOI to reach a reasonable agreement with experimental results; the original emission cross sections gave results that were not satisfying. This illustrates the importance of accurate knowledge of the erbium-doped fibre parameters for the simulation to predict performance more adequately. Unfortunately, very accurate values for the fibre parameters are not easy to obtain.

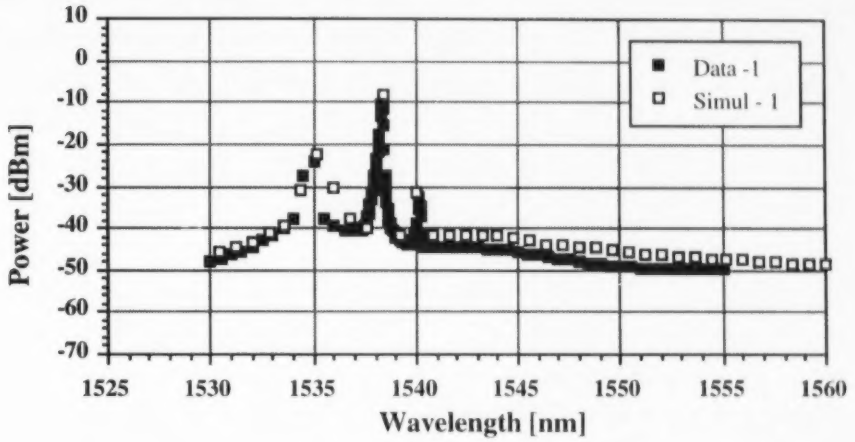

(a)

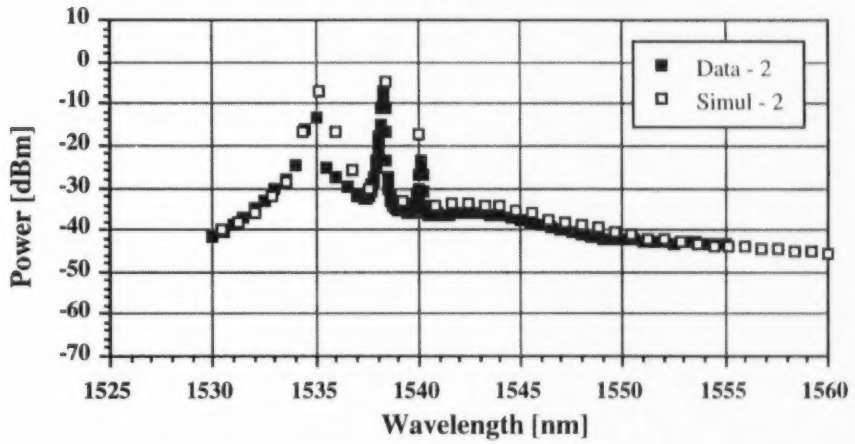

(b)

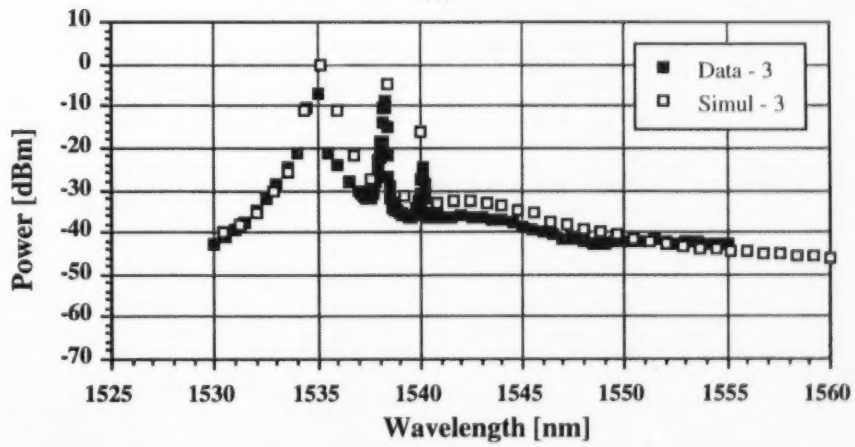

(c)

Figure 4.52 - Comparison of simulation and experiment for forward spectra of case 7. (a) Amplifier 1, (b) amplifier 2, (c) amplifier 3.

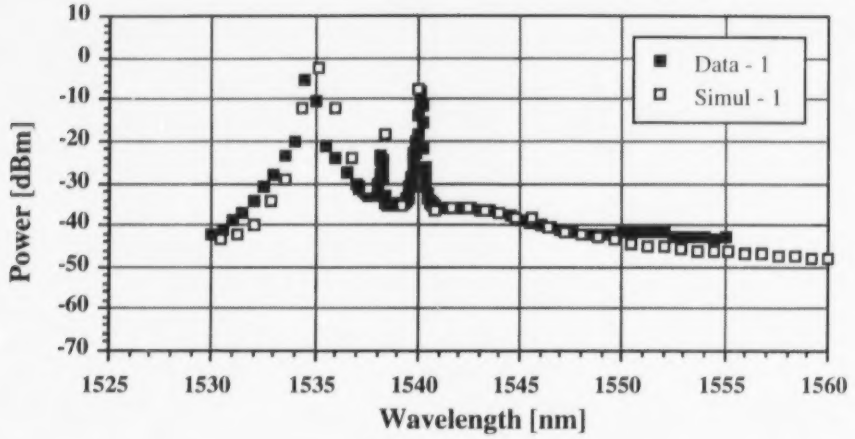

(a)

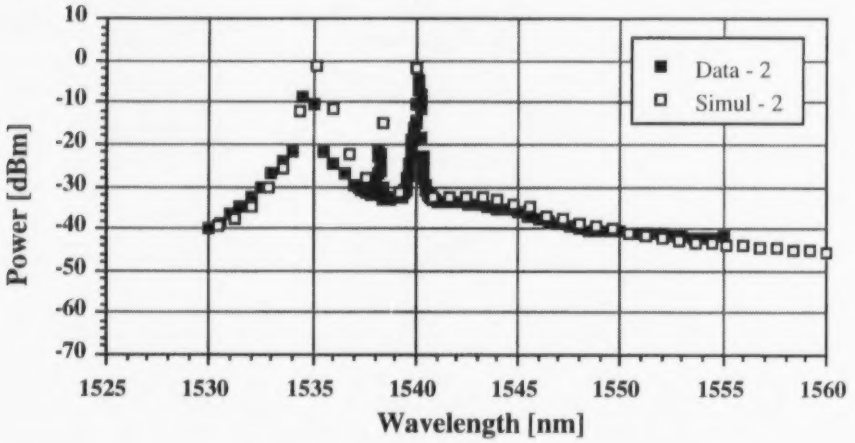

(b)

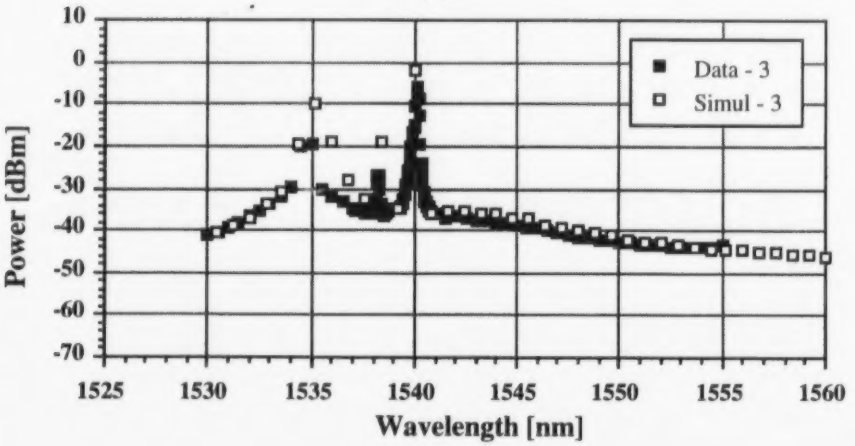

(c)

Figure 4.53 - Comparison of simulation and experiment for backward spectra of case 7. (a) Amplifier 1, (b) amplifier 2, (c) amplifier 3.

4.6 Discussion

In the two previous sections, we have presented, analyzed, interpreted and compared to theory the experimental results obtained from a bidirectional transmission setup with three amplifiers. In this section, we will present our results in the context of the current literature and discuss some suggestions for improvement in the performance of bidirectional transmission system with EDFAs.

In section 4.4.1, we looked at the influence of the signal wavelength on the performance of the system. A Japanese research group studying multi-channel optical communication systems using EDFAs has reached the conclusions in [33] that a flat gain profile cannot be obtained with saturated amplifiers except for closely spaced signals in a small region around 1550 nm. That study was done for a single amplifier used in unidirectional transmission but the conclusions are still valid in our case as we have seen similar gain discrepancies in signal gain over the amplifier gain spectrum. It is certain that operating a multi wavelength system with signals at wavelengths for which there is a large difference in small signal gain and saturation power will bring some limitations in the system design.

Methods to equalize signal power over the amplifier spectrum are presented in [34]-[37]. Equalization using a Mach-Zender optical filter in transmission systems using cascaded EDFAs is presented in [34] for twenty-nine multiplexed channels with wavelengths from 1548 to 1555 nm. Another research group [35] used acousto-optic tunable filters to achieve power equalization of two signals at 1539 and 1568 nm transmitted in a circulating loop to simulate a cascaded amplifier system. Questioning the practicality and cost-effectiveness of the power equalization techniques mentioned above, one group presented in [36] an algorithm to adjust the channel powers at the transmitter to equalize either the output powers or the signal to noise ratio. This technique makes adjustment to the launched signal powers using information provided by system telemetry to get equal signal powers or signal to noise ratio at the output. These techniques are not gain equalization techniques: they modify the power of each channel to obtain equalized output powers or signal to noise ratios taking into account that each channel experiences a different gain. A group showed that inhomogeneously broadened amplifiers can be inserted periodically in a cascade to provide inter channel gain equalization in [37]. An amplifier cooled to 77 K presents inhomogeneous broadening and its gain self regulates on a channel-per-channel basis, avoiding gain competition between channels. By placing an inhomogeneous amplifier at every third stage in the system they were able to reduce the channel power

spread by 11 dB after six amplifiers. In this case, power equalization is obtained by boosting the weak channels rather than attenuating the strong channels. Erbium-doped fibre amplifiers do not have flat gain characteristics and in long amplifier cascades, the gain difference between channels will accumulate at each stage and lead to some channels having unacceptable bit error rates. The papers mentioned above present methods of equalizing signal power or gain to solve the problem of differential gain in multi-wavelength systems with cascaded EDFAs. Of all the equalization methods looked at, the one in [37] is the only one that is actually modifying the amplifier behaviour to achieve gain equalization while the others will modify the power of the channels, according to their gain, to achieve power equalization. Concepts presented in [34],[35], and [37] were tested in a laboratory experiment while the concept presented in [36] was simulated only. More work has to be done to come up with an efficient, practical, reliable, and cost-effective way to equalize channel powers in multi-wavelength systems with long amplifier cascades.

In section 4.4.3, we studied the influence of the inter-amplifier link length on system performance. We looked at two setups with a total of 100 km and 150 km of transmission fibre. Bidirectional transmission up to 195 km [38] and 218 km [13] in two-amplifier systems have been presented. The latter uses dispersion shifted fibre. We present in section 4.7 bidirectional transmission of digital signals in a system equivalent to up to 218 km of fibre. To date, the study of bidirectional transmission systems with EDFAs does not show a possible use in long-haul systems which span over thousands of kilometers. Bidirectional systems with optical amplifiers would probably be best suited for applications in network subscriber loops.

In section 4.4.5, we focused on the influence of Rayleigh backscattering in an open cascade of EDFAs. We noticed that Rayleigh backscattering adds a significant amount of gain compression in the system and that it would be desirable to reduce its effects on the system performance. Although we did not use any isolators or bandpass filters in the transmission system for our experiments, ways of using isolators and filters to reduce effects of Rayleigh backscattering and accumulating ASE in bidirectional transmission systems are presented in [39],[12]. In those cases, the transmission fibre is used in a bidirectional fashion while the optical amplifiers are used in a unidirectional manner. Figure 4.54 illustrates the concept of a "bidirectional fibre amplifier" presented in [39],[12].

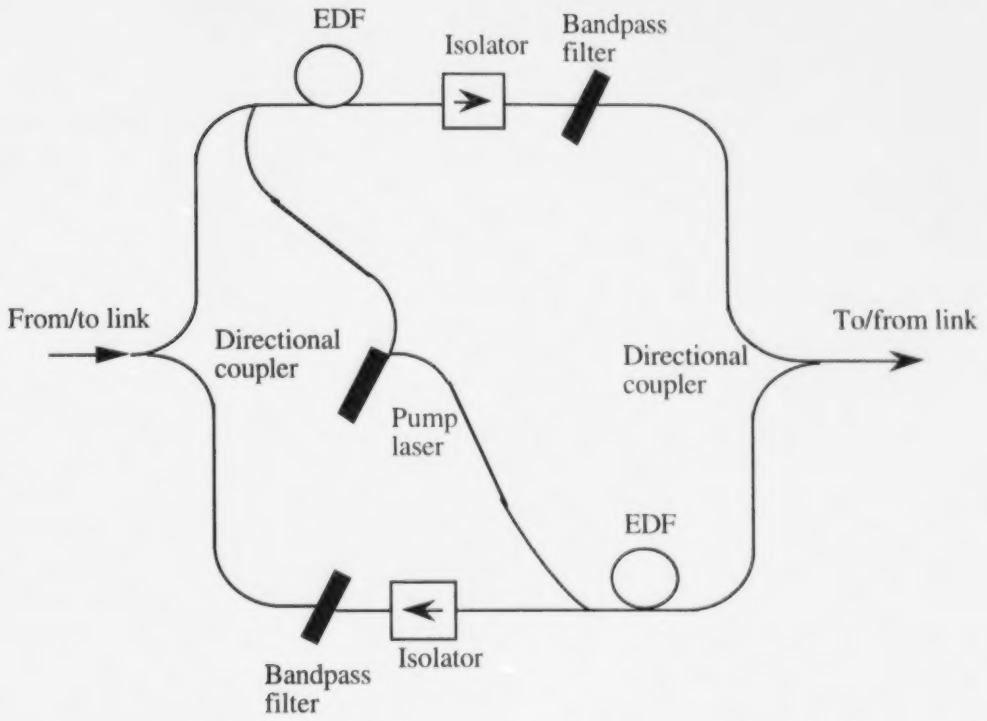

Figure 4.54 - Bidirectional fibre amplifier [39],[12]

It should be noted that twice as many amplifiers are needed when using such a configuration thus increasing cost. On the other hand, the system performance should be improved by the reduction of ASE and Rayleigh backscattered light propagating in the system.

An other solution called a "bidirectional isolator" is illustrated in Figure 4.55 [40].

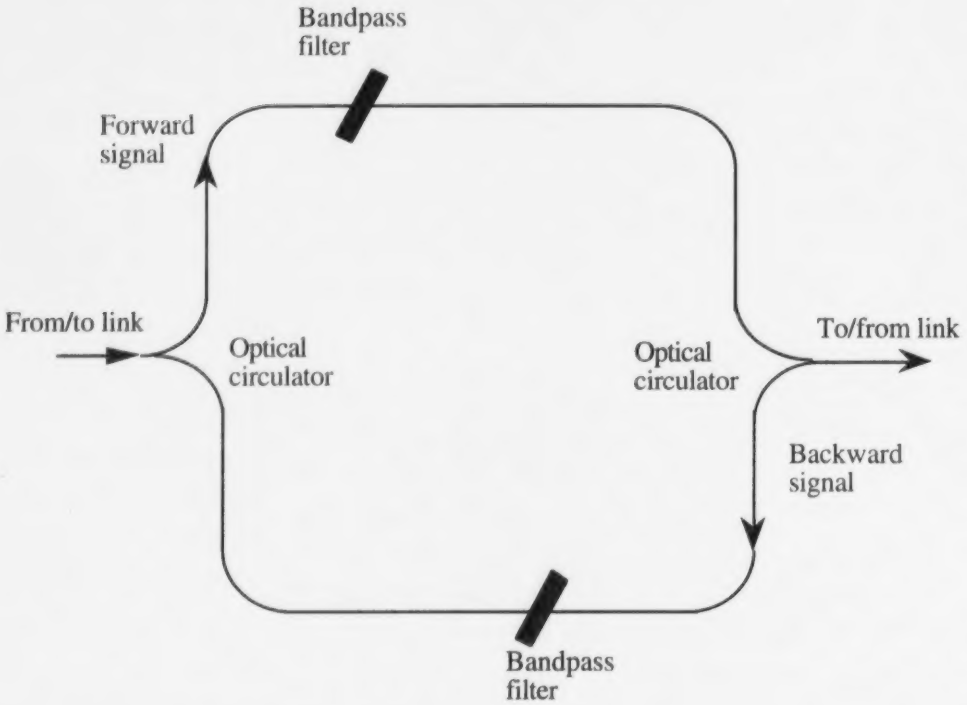

Figure 4.55 - Bidirectional isolator

Such a configuration presents the possibility of using bandpass filters to limit ASE propagation and accumulation while using the same number of amplifiers as in the open cascade as we used experimentally. The concept of the "bidirectional isolator" has not been tested in laboratory. We thus did not verify how much improvement such a design would bring to bidirectional transmission systems with EDFAs. We expect some improvement would be noticed since with the design shown in Figure 4.55, backreflections, Rayleigh backscattering, backward ASE propagation, and ASE accumulation are limited. We have seen in this chapter that all those are limiting factors of the performance of a bidirectional system.

4.7 Bit error rate measurements

This far in the thesis, we have been looking at transmission of continuous wave (CW) light in a bidirectional system. The study of propagation of CW light in the system enables us to learn about the properties of transmission systems with EDFAs and the properties of the amplifiers themselves. At this point, it is interesting to look at digital transmission in

bidirectional transmission system to assess the possibilities of such systems for real life applications.

The first thing we looked at is how well we can transmit digital information in system configurations we studied earlier. We looked at the bit error rate obtained for transmission of digital signals in a setup identical to experimental cases 7 and 8, the difference between those two cases being the presence or absence of Rayleigh backscattering. We modulated the two laser sources at 622.08 Mb/s (OC-12). An HP70841A pattern generator produced pseudo-random sequence of pattern length 2^7-1. The Northern Telecom OC-12 receiver used has limited low frequency response thus the use of a short word length. Results showed error free transmission for both signals in both configurations. The same experiment was repeated with signal sources at 1538 nm and 1543 nm instead of 1538 nm and 1540 nm and again error free transmission was achieved.

The second bit error rate experiment was done to see what impact total link length in a bidirectional system of three amplifiers with two pre/post amplifiers and one in-line amplifier has on the system bit error rate. The experimental setup used for this measurement is illustrated in Figure 4.56. Two laser sources at 1538 nm and 1540 nm are modulated at 622.08 Mb/s. The inter-amplifier losses, L_1 and L_2, are kept equal (symmetric system) and are either composed of a variable attenuator or a spool of 50 km of transmission fibre and a variable attenuator. The variable attenuator is always adjacent to the in-line amplifier. Bit error rate measurements are taken while varying the total system link loss and the results are shown in Figure 4.57. As predicted by the results obtained in the previous section, the setup without Rayleigh backscattering yields better signal to noise ratio and thus better performance than the case with transmission fibre. For a target bit error rate of 10^{-9}, we can tolerate a total link loss of about 47 dB with Rayleigh backscattering present and 54.5 dB with Rayleigh backscattering absent, which is equivalent to a transmission distance of 235 km and 272.5 km assuming 0.20 dB/km transmission fibre. The presence of Rayleigh backscattering is thus always a concern and a limiting factor in open bidirectional cascades of EDFAs where no isolators or bandpass filters are used to limit the influence of backscattering and ASE.

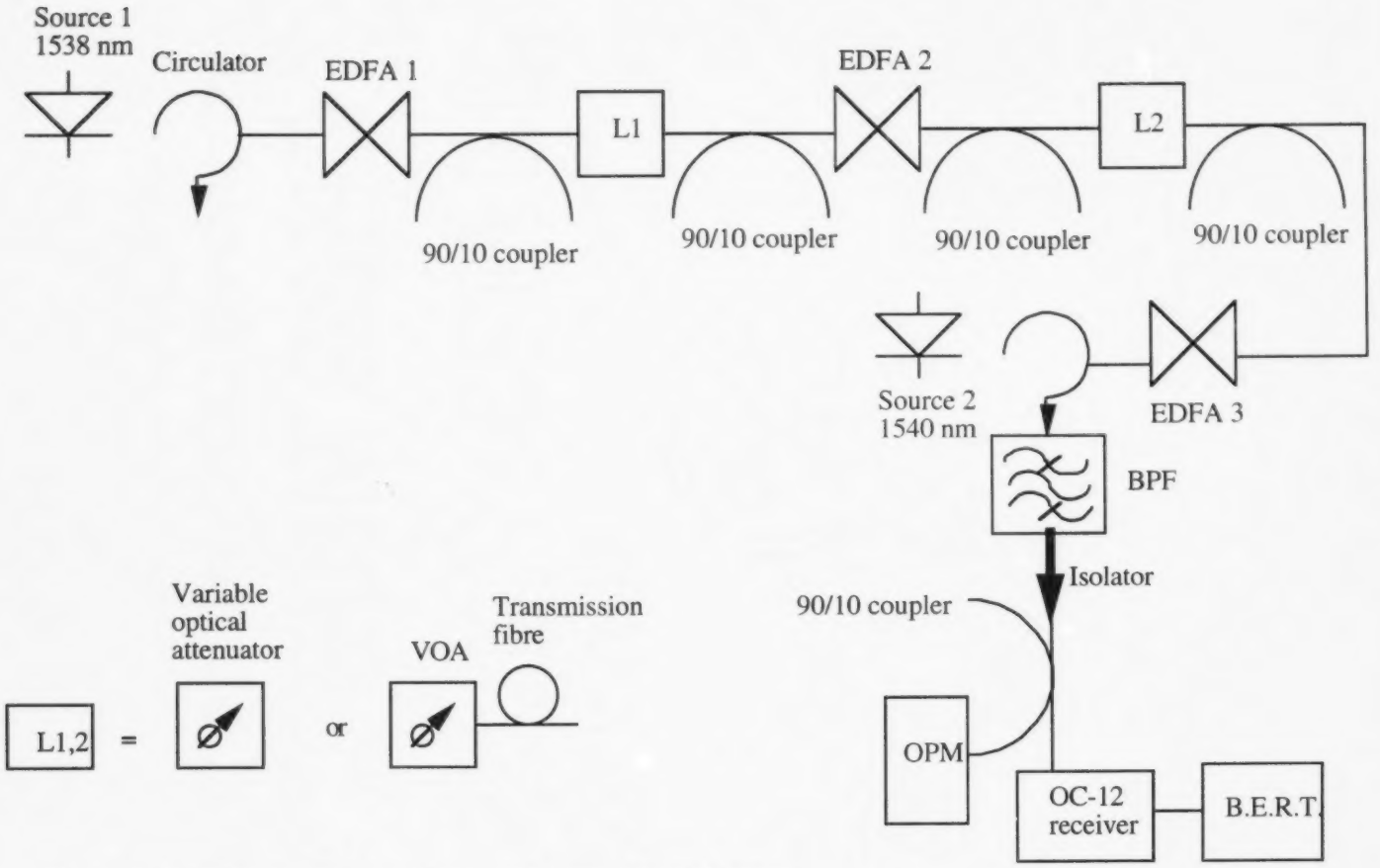

Figure 4.56 - Bit error rate measurements experimental setup

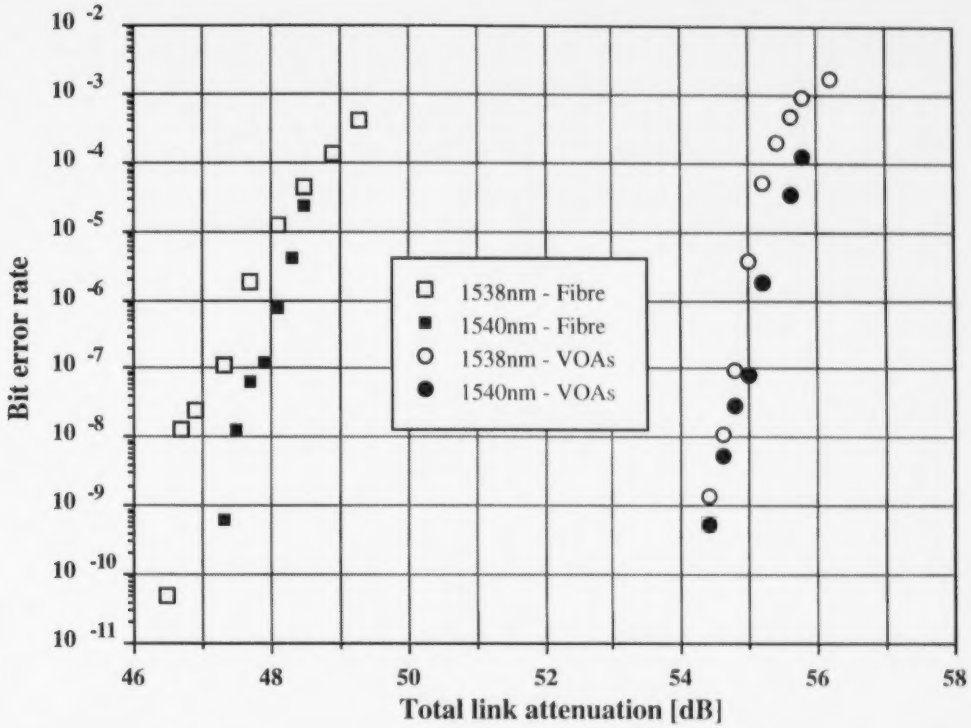

Figure 4.57 - Bit error rate measurements in pre/post configuration

Another way to present bit error rate results is to present the degradation in receiver sensitivity due to the presence of EDFAs in the system. Figure 4.58 presents the setup used to measure the nominal receiver sensitivity for both sources in a back-to-back configuration.

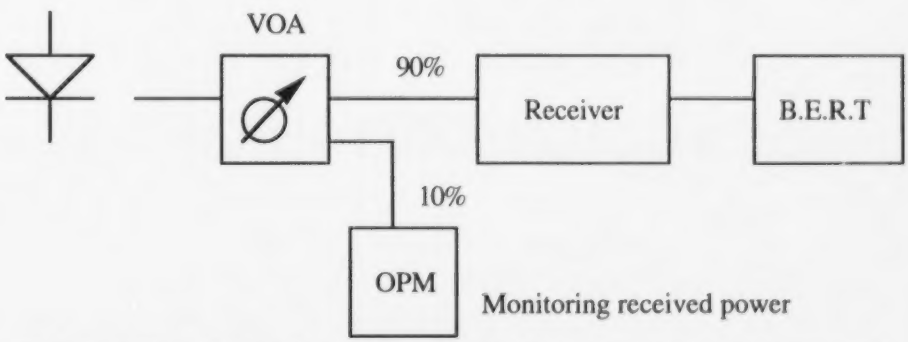

Figure 4.58 - Setup for back-to-back bit error rate measurements

Figure 4.59 presents the receiver nominal sensitivity for both sources as well as the receiver sensitivities for the bidirectional transmission system in Figure 4.56. The received power is the input power to the OC-12 receiver as monitored with a 90/10 coupler and is the sum of signal and ASE when ASE is present.

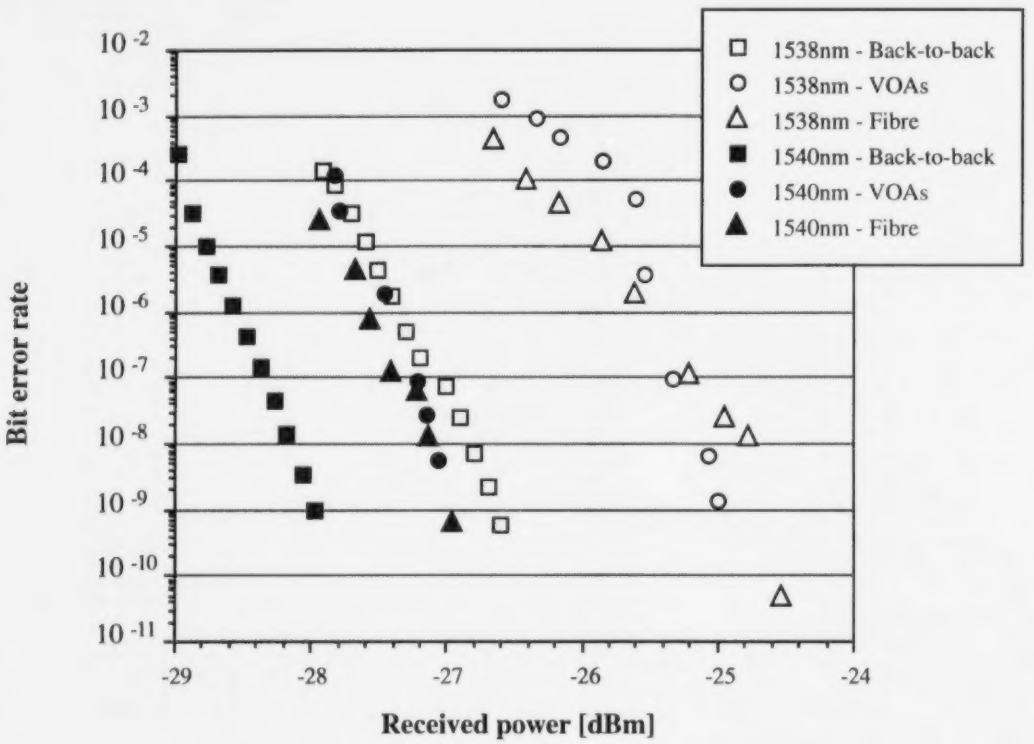

Figure 4.59 - Bit error rate vs. received power

The results presented in Figure 4.59 are the same as those presented in Figure 4.57 but plotted as a function of the received power instead of the total link loss. The difference in receiver sensitivities for both sources comes from the fact that the lasers have different extinction ratios.

We can see that the presence of the three amplifiers in the cascade brings a power penalty to the receiver sensitivity. This penalty is about 1 dB for the 1540 nm signal and 2 dB for the 1538 nm signal. The received inband ASE around 1538 nm is higher than around 1540 nm; the added penalty in receiver sensitivity is around 1 dB. The penalty due to Rayleigh backscattering seems to be negligible compared to the penalty due to the accumulation of ASE, as the sensitivities for the cases with or without Rayleigh backscattering are almost

the same. From [27] we know that the relative intensity noise (RIN) penalty from Rayleigh backscattering is given by

$$\text{Penalty} = -5\log[1 - 72G^2R_{bs}^2] \qquad (4.1)$$

The fact that we observed a rather small receiver sensitivity penalty due to Rayleigh backscattering (less than 0.5 dB) is due to the fact that we are using relatively low gain amplifiers. We can see from equation 4.1 that the penalty is related to the amplifier gain and the Rayleigh backscattering coefficient. This equation was derived for the case of a system with a single amplifier used as a pre amplifier, but the notion that high gain amplifiers will bring a greater penalty to the system due to increased RIN from Rayleigh backscattering is still valid in a multi-amplifier system. Thus the ASE accumulation is here the most important factor in bringing a receiver sensitivity power penalty. Repeating this experiment with narrower filters would eliminate even more of the ASE power at the receiver.

Let's finally compare bit error rate measurements to theoretical calculations. The BER calculations are done following the theory presented in chapter 3 in equations 3.30 to 3.35 derived from [4]. The equations in chapter 3 assume an extinction ratio of zero while in our experiments we have finite extinction ratios. When considering non-zero extinction ratios, equations 3.30 to 3.33 become:

$$\begin{aligned}\sigma_{shot_1}^2 &= 2eB_e\eta(I_{s1} + I_n)\\ \sigma_{shot_0}^2 &= 2eB_e\eta(I_{s0} + I_n)\end{aligned} \qquad (4.2)$$

$$\sigma_{th}^2 = \frac{4kTB_e}{R} \qquad (4.3)$$

$$\begin{aligned}\sigma_{s\_sp_1}^2 &= 4\eta^2 I_{s1} I_n \frac{B_e}{B_o} B_e\\ \sigma_{s\_sp_0}^2 &= 4\eta^2 I_{s0} I_n \frac{B_e}{B_o} B_e\end{aligned} \qquad (4.4)$$

$$\sigma_{sp\_sp}^2 = 2\eta^2 I_n^2 \frac{(2B_o - B_e)}{B_o^2} B_e \qquad (4.5)$$

Where I_{s0} and I_{s1} are the received intensities for a digital zero or one, respectively. Since we are dealing with non-zero extinction ratios,

$$r = \frac{I_{s0}}{I_{s1}} \qquad (4.6)$$

where r is the extinction ratio. The received intensities for a zero and a one can then be expressed as:

$$\begin{aligned} I_{s1} &= \frac{2}{r+1} I_s \\ I_{s0} &= \frac{2r}{r+1} I_s \\ I_s &= \frac{I_{s0} + I_{s1}}{2} \end{aligned} \qquad (4.7)$$

where I_S is the average received optical intensity.

Using equations 4.2 to 4.5 we can express the total noise as:

$$\begin{aligned} \sigma_1^2 &= \sigma_{th}^2 + \sigma_{shot_1}^2 + \sigma_{s\_sp_1}^2 + \sigma_{sp\_sp}^2 \\ \sigma_0^2 &= \sigma_{th}^2 + \sigma_{shot_0}^2 + \sigma_{s\_sp_0}^2 + \sigma_{sp\_sp}^2 \end{aligned} \qquad (4.8)$$

The Q factor is the given by:

$$Q = \frac{\eta(I_{s1} - I_{s0})}{\sigma_1 + \sigma_2} = \frac{2\eta \frac{1-r}{1+r} I_s}{\sigma_1 + \sigma_2} \qquad (4.9)$$

In the back-to-back case, thermal noise is dominant and we thus neglect other sources of noise to get:

$$Q = \frac{\eta \frac{1-r}{1+r} I_s}{\sigma_{thermal}} \qquad (4.10)$$

The bit error rate is then given by:

$$BER = \frac{1}{2}\text{erfc}\left(\frac{Q}{\sqrt{2}}\right) \quad \textbf{(4.11)}$$

Knowing that a bit error rate of 10^{-9} is achieved for Q=6, we compute the thermal noise of our receiver using equation 4.10 and measured the received intensity for a bit error rate of 10^{-9} in the back-to-back case. The thermal noise does not vary with the received power so the same value of thermal noise is used to compute a bit error rate curve over the range of received powers.

Figures 4.60 and 4.61 compare measured and calculated bit error rates vs. received power for both signals.

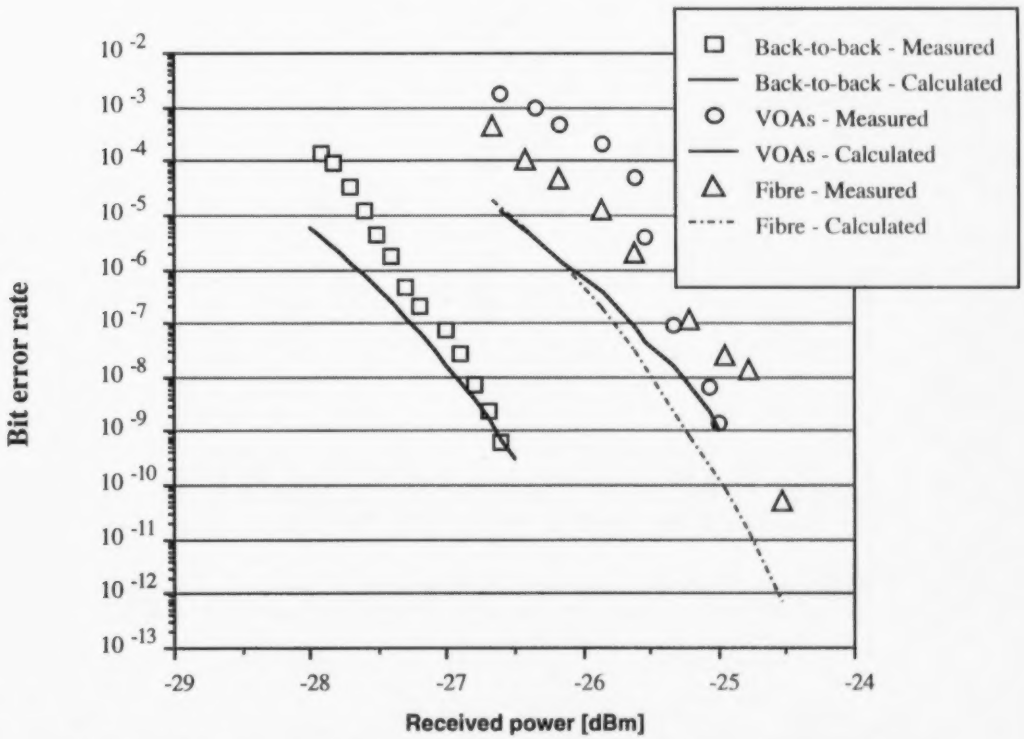

Figure 4.60 - Comparison between measured and calculated receiver sensitivities at 1538 nm

The discrepancy between experimental and calculated values in the back-to-back cases can be attributed to an electronic problem in the receiver. Other work, previously done at TRLabs, shows the same behaviour of the receiver for back-to-back operation. The difference between experimental and calculated values for the system of bidirectional amplifiers is between 0 and 0.5 dB; the difference being smaller in the case where the link attenuation is provided by the attenuators only. The 0.5 dB difference between experimental and calculated values in a bidirectional transmission system can be attributed to RIN due to single and double Rayleigh backscattering and experimental uncertainties in the measurements.

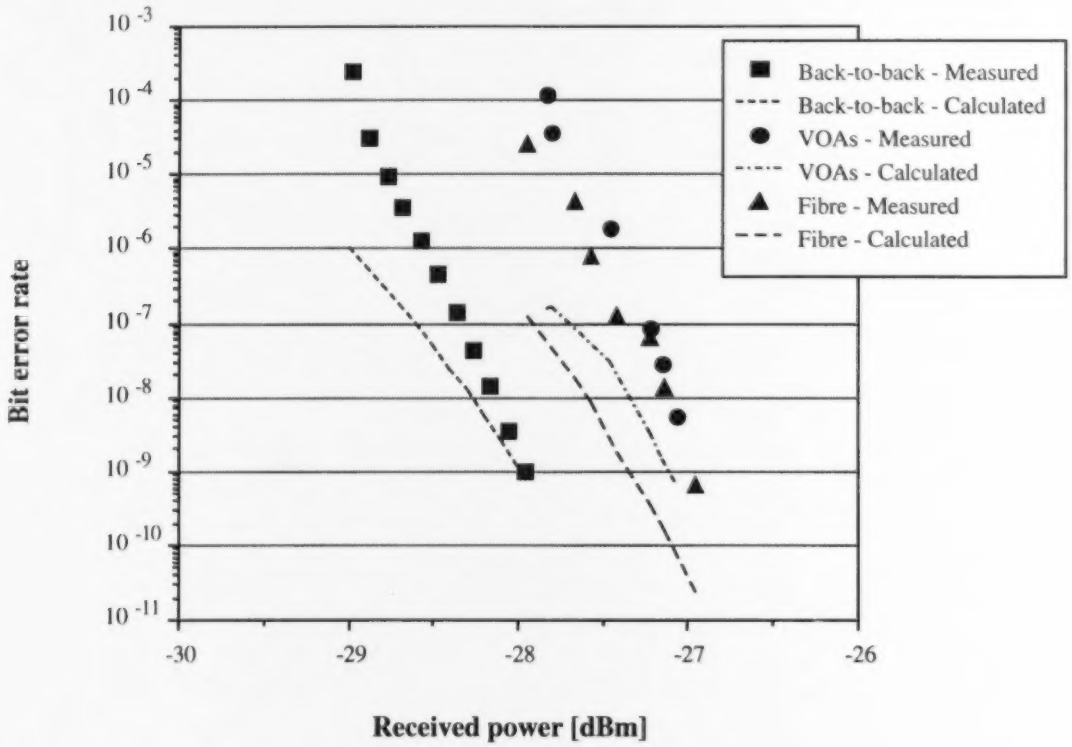

Figure 4.61 - Comparison between measured and calculated receiver sensitivities at 1540 nm.

5. Conclusion

This thesis has studied characteristics of signal and noise propagation in an optical bidirectional transmission system with cascaded erbium-doped fibre amplifiers. Chapter 2 described, theoretically and experimentally, the behaviour of an EDFA. This knowledge is critical to an understanding of the behaviour of optical amplifiers in a cascaded system.

Chapter 3 looked at a mathematical model for signal and noise propagation in a bidirectional transmission system of cascaded EDFAs. The model looks at the propagation of two contra-propagating signals in a bidirectional transmission link along with forward and backward propagating ASE and Rayleigh backscattered light. Double Rayleigh backscattering was neglected. A computer simulation package was developed based on the model equations. The simulation enables us to study the performance of a bidirectional transmission system with EDFAs while varying parameters such as launched signal wavelength and power, inter amplifier link length, amplifier position, and presence of Rayleigh backscattering.

Chapter 4 looked at experimental results obtained with a bidirectional transmission setup with three EDFAs. Characteristics of bidirectional transmission in cascaded EDFAs have been studied through the measurement of the forward and backward output spectra of each amplifier in nine different setups. Bidirectional transmission of two digital signal at 622.08 Mb/s over the equivalent of 235 km for a bit error rate of 10^{-9} was also achieved with two amplifiers used as pre/post amplifiers and one used as an in-line amplifier.

In analyzing the experimental results in chapter 4, we learned that the accumulation of ASE and the Rayleigh backscattered light in the system have an important effect in compressing the gain of the amplifiers. A large accumulated ASE power peak at 1535 nm can in fact be considered as an additional saturating signal with non negligible effect on gain compression. We saw in section 4.4.4 that a large ASE peak could induce enough gain compression in the amplifier to yield a lower gain than in a more saturated amplifier with less accumulated ASE.

We have seen that it is desirable to use signal wavelengths with similar small signal gains in a bidirectional transmission system with inter-amplifier link loss no greater than the smallest small signal gain in the system. This allows each signal to maintain a relatively constant power level along the system.

We also saw that Rayleigh backscattering in an open bidirectional cascade of amplifiers introduces a penalty by lowering the gain of the amplifiers in the system. We presented in section 4.6 some ideas for reducing the effect of Rayleigh backscattering without eliminating the possibility of bidirectional transmission of signals.

Comparison between the simulation and experimental data showed a reasonable agreement. The discrepancies can be explained by:

a) The somewhat limited capacity of the EDFA simulation to handle highly saturated regime.
b) Experimental measurement errors and estimation of insertion loss of each component in the set-up.
c) Uncertainties about the erbium-doped fibre (EDF) parameters such as absorption and emission cross sections, erbium dopant concentration and confinement, and others. We, in fact, had to modify the emission cross section data provided by NOI, the manufacturer of the EDF, to reach a reasonable agreement with experimental data, the original emission cross sections giving unsatisfying results.
d) Discrepancies between simulated and experimental results increasing at each stage in the cascaded system.

As far as future work is concerned, it would be interesting to look in more depth at the capacity of the EDFA simulation to handle highly saturated regime.

Double Rayleigh backscattering could also be included in the model for signal and noise propagation.

Using narrower bandpass filters in the bidirectional transmission setup would allow better filtering of the ASE and Rayleigh backscattered signal, and may permit transmission of more closely spaced signals.

Bidirectional transmission with more amplifiers in the system would also be of interest in order to see how additional stages would change the performance of the transmission system and if the discrepancies between simulated and experimental results would continue to increase. A recirculating loop experiment could alleviate the burden of having to deal with a great number of amplifiers.

Finally, bidirectional transmission in open cascades of EDFAs is a rather new field of research and more work needs to be done before such a system becomes common in field applications.

References

[1] E.Desurvire, C.R.Giles,J.R.Simpson, "Gain Saturation Effects in High-Speed, Multichannel Erbium-Doped Fiber Amplifiers at $\lambda = 1.55$ m," Journal of Lightwave Technology, vol. 7, no. 12, Dec. 1989, pp.2095-2104.

[2] L.Eskildsen, E.Goldstein, "High-Performance Amplified Optical Links Without Isolators or Bandpass Filers," IEEE Photonics Technology Letters, vol. 4, no. 1, Jan. 1992, pp. 55-58.

[3] K.Inoue, H.Toba, K.Nosu, "Multichannel Amplification Utilizing an Er^{3+}-Doped Fiber Amplifier," Journal of Lightwave Technology, vol. 9, no. 3, March 1991, pp. 368-374.

[4] N.A.Olsson, "Lightwave Systems with Optical Amplifiers," Journal of Lightwave Technology, vol. 7, no. 7, July 1989, pp. 1071-1082.

[5] P.M.Gabla, J.L.Pamart, R.Uhel, E.Leclerc, J.O.Frorud, F.X.Ollivier, S.Borderieux, "401 km, 622 Mb/s and 357 km, 2.4888 Gb/s IM/DD Repeaterless Transmission Experiments Using Erbium-Doped Fibre Amplifiers and Error Correcting Code," IEEE Photonics Technology Letters, vol. 4, no. 10, Oct. 1992, pp.1148-1151.

[6] P.M.Gabla, J.O.Frorud, E.Leclerc, S.Gauchard, H.Havard, "1111 km, Two-Channel IM-DD Transmission Experiment at 2.5 Gb/s Through 21 In-line Erbium-Doped Fibre Amplifier," IEEE Photonics Technology Letters, vol. 4, no. 7, July 1992, pp. 717-720.

[7] J.Aspell, N.S.Bergano, "Erbium Doped Fiber Amplifiers for Future Undersea Tranmission Systems," IEEE LCS, Nov. 1990, pp. 63-66.

[8] J.A.Chiddix, J.A.Vaughan, R.W.Wolfe, "The Use of Fibre Optics in Cable Communications Network," Journal of Lightwave Technology, vol. 11, no. 1, Jan. 1993, pp. 154-166.

[9] E.Desurvire, "Erbium-doped fiber amplifiers for new generations of optical communication systems," Optics and Photonics News, Jan. 1991, pp. 6-11.

[10] S.Shamada, "Impact of Erbium-Doped amplifiers on optical communication systems," Optics and Photonics News, Jan. 1990, pp. 6-12.

[11] M.Suyama, S.Watanabe, I.Yokota, H.Kuwahara, "Bidirectional Transmission Scheme Using Intensity Modulation of 1.48 um Pump Laser Diode for Erbium-Doped Fibre Amplifiers," Electronics Letters, vol. 27, no. 1, 3 rd Jan. 1991, pp. 89-91.

[12] Y.H.Cheng, N.Kagi, A.Oyobe, K.Nakamura, "622 Mb/s, 144 km Transmission Using a Bidirectional Fibre Amplifier Repeater," IEEE Photonics Technology Letters, vol. 5, no. 3, March 1993, pp. 356-358.

[13] R.J.Orazi, M.N.McLandrich, "Bidirectional Transmission at 1.55 Microns Using Fused Fiber Narrow Channel Wavelength Division Multiplexers and Erbium-Doped Fiber Amplifiers," IEEE Photonics Technology Letters, vol. 6, no. 4, April 1994, pp.571-574.

[14] J.Haugen, J.Freeman, J.Conradi, "Bidirectional Transmission at 622 Mb/s Utilizing Erbium-Doped Fiber Amplifiers," IEEE Photonics Technology Letters, vol. 4, no. 8, Aug. 1992, pp. 913-916.

[15] C.R.Giles, E.Desurvire, "Modeling Erbium-Doped Fiber Amplifiers". Journal of Lightwave Technology, vol. 9, no. 2, Feb. 1991, pp. 271-283.

[16] C.R.Giles, E.Desurvire, "Propagation of Signal and Noise in Concatenated Erbium-Doped Fiber Optical Amplifiers", Journal of Lightwave Technology, vol. 9, no. 2, Feb. 1991, pp. 147-154.

[17] J.R.Armitage, "Three-level laser amplifier: a theoretical model", Applied Optics, vol. 27, no. 23, Dec. 1988, pp. 4831-4836.

[18] M.Artiglia, P.DiVita, M.Potenza, "Numerical Analysis of Erbium-Doped Optical Fiber Amplifiers", Journal of Optical Comunications., vol. 13, no. 3, 1992, pp. 104-113.

[19] M.J.F.Digonnet, C.J.Gaeta, "Theoretical analysis of optical fiber laser amplifiers and oscillators," Applied Optics, vol. 24, no. 3, Feb. 1985, pp. 333-342.

[20] T.Georges, E.Delevaque, "Analytic modeling of high-gain erbium-doped fiber amplifiers", Optics Letters, vol. 17, no. 16, August 15, 1992, pp. 1113-1115.

[21] B.Pedersen, A.Bjarklev, J.H.Polvsen, K.Dybdal, C.C.Larsen, "The Design of Erbium-Doped Fiber Amplifiers", Journal of Lightwave Technology, vol. 9, no. 9, Sept. 1991, pp. 1105-1112.

[22] A.A.M.Saleh, R.M.Jopson, J.D.Evankow, J.Aspell, "Modeling of Gain in Erbium-Doped Fiber Amplifiers," IEEE Photonics Technology Letters, vol. 2, no. 10, Oct. 1990, pp.714-717.

[23] E.Desurvire, *Erbium-doped fibre amplifiers: principles and applications*, John Wiley and Sons, New York, 1994, chapters 1 and 2.

[24] E.Desurvire, J.R.Simpson, "Amplification of Spontaneous Emission in Erbium-Doped Single-Mode Fibers," Journal of Lightwave Technology, vol. 7, no. 5, May 1989, pp. 835-845.

[25] J.Freeman, Theory, Design, and Characterization of EDFAs, M.Sc. thesis, University of Alberta, Fall 1991.

[26] J.Conradi, R.Maciejko, "Digital Optical Receiver Sensitivity Degradation Caused by Crosstalk in Bidirectional Fiber Optic Systems," IEEE Transactions on Communications, vol. COM-29, no. 7, July 1981, pp.1012-1016.

[27] J.L.Gimlett, M.Z.Iqbal, N.K.Cheung, A.Righetti, F.Fontana, G.Grasso, "Observation of Equivalent Rayleigh Scattering Mirrors in Lightwave Systems with Optical Amplifiers," IEEE Photonics Technology Letters, vol. 2, no. 3, March 1990, pp. 211-213.

[28] P.Gysel, R.K.Staubli, "Spectral Properties of Rayleigh Backscattered Light from Single-Mode Fibers Caused by a Modulated Probe Signal," Journal of Lightwave Technology, vol. 8, no. 12, Dec. 1990, pp. 1792-1798.

[29] S.L.Hansen, K.Dybdal, C.C.Larsen, "Gain Limit in Erbium-Doped Fiber Amplifiers Due to Internal Rayleigh Backscattering," IEEE Photonics Technology Letters, vol. 4, no. 6, June 1992, pp. 559-561.

[30] N.Henmi, Y.Aoki, S.Fujita, Y.Sunuhara, M.Shikada, "Rayleigh Scattering Influence on Performance of 10 Gb/s Optical Receiver with Er-Doped Optical Fiber Preamplifier," IEEE Photonics Technology Letters, vol. 2, no. 4, April 1990, pp. 277-278.

[31] R.K.Staubli, P.Gysel, "Crosstalk Penalties Due to Coherent Rayleigh Noise in Bidirectional Optical Communication Systems," Journal of Lightwave Technology, vol. 9, no. 3, March 1991, pp. 375-380.

[32] T.Cherniwchan, "Frequency Response of Rayleigh Backscattering in Single Mode Fiber at 1550 nm," EE 595 Research Project Report, April 1993.

[33] Y.H.Cheng, N.Kagi, A.Oyobe, K.Nakamura, "Gain competition in Multichannel Optical Communication Systems Using Erbium-Doped Fiber Amplifiers," Fiber and Integrated Optics, vol. 11, 1992, pp. 105-110.

[34] K.Inoue, T.Kominato, H.Toba, "Tunable Gain Equalization Using a Mach-Zehnder Optical Filter in Multistage Fiber Amplifiers," IEEE Photonics Technology Letters, vol. 3, no. 8, Aug. 1991, pp. 719-720.

[35] S.F.Su, R.Olshansky, G.Joyce, D.A.Smith, J.E.Baran, "Gain Equalization in Multiwavelength Lightwave Systems Using Acoustooptic Tunable Filters," IEEE Photonics Technology Letters, vol. 4, no. 3, March 1992, pp. 269-271.

[36] A.R.Chraplyvy, J.A.Nagel, R.W.Tkach, "Equalization in Amplified WDM Lightwave Transmission Systems," IEEE Photonics Technology Letters, vol. 4, no. 8, Aug. 1992, pp. 920-922.

[37] L.Eskildsen, E.Goldstein, V.da Silva, M.Andrejco, Y.Silberberg, "Optical Power Equalization for Multiwavelength Fiber-Amplifier Cascades Using Periodic Inhomogeneous Broadening," IEEE Photonics Technology Letters, vol. 5, no. 10, Oct. 1993, pp. 1188-1190.

[38] J.Haugen, J.Freeman, J.Conradi, "Full Duplex Bidirectional Transmission @ 622 Mb/s with two Erbium-Doped Fiber Amplifiers," at OFC/IOOC 93, 1993 OSA Technical Digest Series, vol. 4, Optical Society of America, Wachington, D.C., paper TuI6.

[39] C.W.Barnard, J.Chrostowski, M.Kavehrad "Bidirectional Fiber Amplifiers," IEEE Photonics Technolofy Letters, vol. 4, no. 8, August 1992., pp. 911-913.

[40] J.Conradi. Private communication, 1994.

[41] G.Keiser. *Optical Fiber Communications*. McGraw-Hill, 2nd edition, 1991, 461 p.

[42] J.M.Senior. *Optical Fiber Communications - Principles and Practice*, Prentice Hall, International Series in Optoelectronics, 2nd edition, 1992, 922 p.

Appendix A : Rayleigh scattering

Optical fibres are made of glass and in that glass there are some discontinuities and little imperfections that simply cannot be avoided during manufacturing. Hence, scattering losses arise from microscopic variations and structural inhomogeneities or defects in the fibre [41]. Refractive index variations occur within the glass over small distances compared to the wavelength. These variations cause Rayleigh scattering of the light. The percentage of scattered photon varies with the wavelength of the launched signal as

$$\gamma_R \propto \frac{1}{\lambda^4} \qquad (A.1)$$

The loss of power caused by Rayleigh scattering can be expressed as [42]

$$\mathcal{L} = \exp(-\gamma_R L) \qquad (A.2)$$

where L : length of fibre

γ_R : Rayleigh scattering coefficient

The Rayleigh scattered light is scattered in almost all directions and part of it is recaptures and guided by the fibre in the forward and backward directions. Of interest here is the amount of scattered light coupled into the fibre and travelling in the opposite direction from the original signal, which gives rise to the Rayleigh backscattering phenomenon.

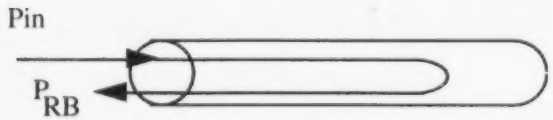

Figure A.1 - Rayleigh backscattering in an optical fibre

The Rayleigh backscattering coefficient is a measure of the amount of power coming back at the entrance of a fibre for a given input power, as illustrated in figure A.1, so that

$$P_{RB} = \alpha_{RB} P_{in} \qquad (A.3)$$

The Rayleigh backscattering coefficient is in general around -30 to -33 dB for silica transmission fibre. We used two types of transmission fibre in our experiments with Rayleigh backscattering coefficient measured to be as follows [32]:

Fibre type	Rayleigh backscattering coefficient [dB]
Northern Telecom	-31.5
Corning	-33.2

Table A.1 - Rayleigh backscattering coefficient of different transmission fibres used

Appendix B : Bidirectional cascaded EDFAs simulation code

We here present the code that was specifically written from the signal and noise propagation model developed in chapter 3 of this thesis. The simulation uses Freeman's EDFA and PDATA programs which we do not print here for economy of space but rather refer the reader to reference [25] for more information.

The user only has to enter the desired parameters in the text files "param_file_1" and "launched_params" to simulate bidirectional transmission in a cascade of EDFAs.

Listing of bi-di-tx.c:

```
/*
  C-coded simulation of bidirectional transmission system with cascaded EDFAs.  Uses
Jim Freeman's EDFA and PDATA programs.  User definable parameters are in text files
"param_file_1" and "launched_params".
*/


#include <stdio.h>
#include "const.h"
#include "fcns.h"
#include <math.h>
#include "param_gbls.h"

double
                pout[50],
                *GBL_link_loss,
                *GBL_alpha_R_fwd,
                *GBL_alpha_R_bwd,
                *GBL_fwd_pump,
                *GBL_bwd_pump,
                alphac1,
                alphac2,
                *GBL_fwd_psd,
                *GBL_bwd_psd;
int
                GBL_n_amps,
                GBL_ite_max,
                selection;
```

```
main()
{
int i, j, ite, amp_num;
double          pfin[10][50], pbin[10][50],
        pbout[10][50], pfout[10][50],
        pumpf[10],pumpb[10],
        pf[50], pb[50],
        alpha[50],alphaRfwd[50],alphaRbwd[50],
        dummy;
FILE    *f_ptr,*f_ptr2;
static char     filename[15];
extern double   pout[50];


read_params();
read_launched_params();

for (j=0;j<GBL_n_channels;++j)
{
        pf[j]=0; pb[j]=0;
        for (i=0;i<GBL_n_amps;++i)
        {
                pfin[i][j]=0; pfout[i][j]=0;
                pbin[i][j]=0; pbout[i][j]=0;
        }
}

for (i=0;i<=GBL_n_amps;++i)
{
        dummy=*(GBL_link_loss+i);
        alpha[i]=dummy;
}

for (i=0;i<=GBL_n_amps;++i)
{
        dummy=*(GBL_alpha_R_fwd+i);
        alphaRfwd[i]=dummy;
}

for (i=0;i<=GBL_n_amps;++i)
{
        dummy=*(GBL_alpha_R_bwd+i);
        alphaRbwd[i]=dummy;
}

for (i=0;i<GBL_n_amps;++i)
{
        dummy=*(GBL_fwd_pump+i);
        pumpf[i]=dummy;

        dummy=*(GBL_bwd_pump+i);
        pumpb[i]=dummy;
}
```

```
for (i=0;i<GBL_n_channels;++i)
{
        dummy=*(GBL_fwd_psd+i);
        pf[i]=dummy;

        dummy=*(GBL_bwd_psd+i);
        pb[i]=dummy;
}

for (ite=0; ite<GBL_ite_max; ++ite)
{
/* Propagating fwd signal from amp 1 to amp N       */


        f_ptr=fopen("param_file_2","w");
        sprintf(filename,"pfin1-ite%d",ite);
        f_ptr2=fopen(filename,"w");
        for (i=0;i<GBL_n_channels;++i)
        {
                pfin[0][i]=pf[i]*alphac1*alpha[0] + pbout[0][i]*alphaRbwd[0];
                fprintf (f_ptr,"%g\n",pfin[0][i]);
                fprintf (f_ptr2,"%g\n",pfin[0][i]);

        }
        fclose(f_ptr2);
        sprintf(filename,"pbin1-ite%d",ite);
        f_ptr2=fopen(filename,"w");
        for (i=0;i<GBL_n_channels;++i)
        {
                pbin[0][i]=pfout[0][i]*alphaRfwd[1] + pbout[1][i]*alpha[1];
                fprintf(f_ptr,"%g\n",pbin[0][i]);
                fprintf (f_ptr2,"%g\n",pbin[0][i]);

        }
        fclose(f_ptr2);

        fprintf(f_ptr,"%g\n%g\n",pumpf[0],pumpb[0]);
        fclose(f_ptr);

edfa();
sprintf(filename,"pfout1-ite%d",ite);
f_ptr=fopen(filename,"w");
selection=1;
pdata();
for (i=0;i<GBL_n_channels;++i)
{
        pfout[0][i]=pout[i];
        fprintf(f_ptr,"%g\n",pfout[0][i]);
}
fclose(f_ptr);

sprintf(filename,"pbout1-ite%d",ite);
f_ptr=fopen(filename,"w");
```

```
selection=2;
pdata();
for (i=0;i<GBL_n_channels;++i)
{
        pbout[0][i]=pout[i];
                fprintf(f_ptr,"%g\n",pbout[0][i]);
}
fclose(f_ptr);

if (GBL_n_amps>2)
        for (amp_num=1; amp_num<(GBL_n_amps-1); ++amp_num)
        {
                f_ptr=fopen("param_file_2","w");
                sprintf(filename,"pfin%d-ite%d",amp_num+1,ite);
                f_ptr2=fopen(filename,"w");
                for (i=0;i<GBL_n_channels;++i)
                {
                        pfin[amp_num][i]=pfout[amp_num-1][i]*alpha[amp_num] +
pbout[amp_num][i]*alphaRbwd[amp_num];
                        fprintf(f_ptr,"%g\n",pfin[amp_num][i]);
                        fprintf(f_ptr2,"%g\n",pfin[amp_num][i]);

                }
                fclose(f_ptr2);
                sprintf(filename,"pbin%d-ite%d",amp_num+1,ite);
                f_ptr2=fopen(filename,"w");
                for (i=0;i<GBL_n_channels;++i)
                {
                        pbin[amp_num][i]=pfout[amp_num][i]*alphaRfwd[amp_num+1] +
pbout[amp_num+1][i]*alpha[amp_num+1];
                        fprintf(f_ptr,"%g\n",pbin[amp_num][i]);
                        fprintf(f_ptr2,"%g\n",pbin[amp_num][i]);
                }
                fclose(f_ptr2);

                fprintf(f_ptr,"%g\n%g\n",pumpf[amp_num],pumpb[amp_num]);
                fclose(f_ptr);

                edfa();
                sprintf(filename,"%s%d%s%d","pfout",amp_num+1,"-ite",ite);
                f_ptr=fopen(filename,"w");
                selection=1;
                pdata();
                for (i=0;i<GBL_n_channels;++i)
                {
                        pfout[amp_num][i]=pout[i];
                        fprintf(f_ptr,"%g\n",pfout[amp_num][i]);
                }
                fclose(f_ptr);

                sprintf(filename,"%s%d%s%d","pbout",amp_num+1,"-ite",ite);
                f_ptr=fopen(filename,"w");
                selection=2;
                pdata();
```

```
                for (i=0;i<GBL_n_channels;++i)
                {
                        pbout[amp_num][i]=pout[i];
                        fprintf(f_ptr,"%g\n",pbout[amp_num][i]);
                }
                fclose(f_ptr);
        }

f_ptr=fopen("param_file_2","w");
sprintf(filename,"pfin%d-ite%d",GBL_n_amps,ite);
f_ptr2=fopen(filename,"w");
for (i=0;i<GBL_n_channels;++i)
{
        pfin[GBL_n_amps-1][i]=pfout[GBL_n_amps-2][i]*alpha[GBL_n_amps-1] +
pbout[GBL_n_amps-1][i]*alphaRbwd[GBL_n_amps];
        fprintf(f_ptr,"%g\n",pfin[GBL_n_amps-1][i]);
        fprintf(f_ptr2,"%g\n",pfin[GBL_n_amps-1][i]);
}
fclose(f_ptr2);
sprintf(filename,"pbin%d-ite%d",GBL_n_amps,ite);
f_ptr2=fopen(filename,"w");
for (i=0;i<GBL_n_channels;++i)
{
        pbin[GBL_n_amps-1][i]=pb[i]*alphac2*alpha[GBL_n_amps] +
pfout[GBL_n_amps-1][i]*alphaRfwd[GBL_n_amps-1];
        fprintf(f_ptr,"%g\n",pbin[GBL_n_amps-1][i]);
        fprintf(f_ptr2,"%g\n",pbin[GBL_n_amps-1][i]);
}
fclose(f_ptr2);

fprintf(f_ptr,"%g\n%g\n",pumpf[GBL_n_amps-1],pumpb[GBL_n_amps-1]);
fclose(f_ptr);

edfa();
sprintf(filename,"pfout%d-ite%d",GBL_n_amps,ite);
f_ptr=fopen(filename,"w");
selection=1;
pdata();
for (i=0;i<GBL_n_channels;++i)
{
        pfout[GBL_n_amps-1][i]=pout[i];
        fprintf(f_ptr,"%g\n",pfout[GBL_n_amps-1][i]);
}
fclose(f_ptr);

sprintf(filename,"pbout%d-ite%d",GBL_n_amps,ite);
f_ptr=fopen(filename,"w");
selection=2;
pdata();
for (i=0;i<GBL_n_channels;++i)
{
        pbout[GBL_n_amps-1][i]=pout[i];
        fprintf(f_ptr,"%g\n",pbout[GBL_n_amps-1][i]);
}
```

```
fclose(f_ptr);


/* Propagating bwd signals from amplifier N-1 to amplifier 2          */

if (GBL_n_amps>2)
        for (amp_num=(GBL_n_amps-2); amp_num>=1; --amp_num)
        {
                f_ptr=fopen("param_file_2","w");
                sprintf(filename,"pfin%d-ite%d",amp_num+1,ite);
                f_ptr2=fopen(filename,"w");
                for (i=0;i<GBL_n_channels;++i)
                {
                        pfin[amp_num][i]=pfout[amp_num-1][i]*alpha[amp_num] +
pbout[amp_num][i]*alphaRbwd[amp_num];
                        fprintf(f_ptr,"%g\n",pfin[amp_num][i]);
                        fprintf(f_ptr2,"%g\n",pfin[amp_num][i]);

                }
                fclose(f_ptr2);
                sprintf(filename,"pbin%d-ite%d",amp_num+1,ite);
                f_ptr2=fopen(filename,"w");
                for (i=0;i<GBL_n_channels;++i)
                {
                        pbin[amp_num][i]=pfout[amp_num][i]*alphaRfwd[amp_num+1] +
pbout[amp_num+1][i]*alpha[amp_num+1];
                        fprintf(f_ptr,"%g\n",pbin[amp_num][i]);
                        fprintf(f_ptr2,"%g\n",pbin[amp_num][i]);
                }
                fclose(f_ptr2);

                fprintf(f_ptr,"%g\n%g\n",pumpf[amp_num],pumpb[amp_num]);
                fclose(f_ptr);

                edfa();
                sprintf(filename,"%s%d%s%d","pfout",amp_num+1,"-ite",ite);
                f_ptr=fopen(filename,"w");
                selection=1;
                pdata();
                for (i=0;i<GBL_n_channels;++i)
                {
                        pfout[amp_num][i]=pout[i];
                        fprintf(f_ptr,"%g\n",pfout[amp_num][i]);
                }
                fclose(f_ptr);

                sprintf(filename,"%s%d%s%d","pbout",amp_num+1,"-ite",ite);
                f_ptr=fopen(filename,"w");
                selection=2;
                pdata();
                for (i=0;i<GBL_n_channels;++i)
                {
                        pbout[amp_num][i]=pout[i];
```

```
                fprintf(f_ptr,"%g\n",pbout[amp_num][i]);
            }
            fclose(f_ptr);
        }


}

exit(0);

}


/****
 *   FUNCTION:      read_launched_params
 *
 ****/

read_launched_params()
{
int     i,num;
FILE    *f_ptr;
float   float_in;
int     short_in;
char    *malloc();

f_ptr=fopen("launched_params","r");
if (f_ptr==NULL)
{
        printf ("\nERROR: UNABLE TO OPEN 'launched_params' file.\n");
        exit(1);
}

num=fscanf(f_ptr,"%d %*[^\n]\n",&short_in);
GBL_n_amps=short_in;
if (num!=1) {printf("\nERROR: in 'launched_params' file: amps number.\n"); exit(1);}

GBL_fwd_pump=(double*) malloc(sizeof(double)*(GBL_n_amps));
for (i=0;i<GBL_n_amps;++i)
{
        num=fscanf(f_ptr,"%g %*[^\n]\n",&float_in);
        *(GBL_fwd_pump+i)=(double) float_in;
        if (num!=1) {printf("\nERROR: in 'launched_params' file: fwd pump power.\n");
exit(1);}
}

GBL_bwd_pump=(double*) malloc(sizeof(double)*(GBL_n_amps));
for (i=0;i<GBL_n_amps;++i)
{
        num=fscanf(f_ptr,"%g %*[^\n]\n",&float_in);
        *(GBL_bwd_pump+i)=(double) float_in;
        if (num!=1) {printf("\nERROR: in 'launched_params' file: bwd pump power.\n");
exit(1);}
}
```

```
GBL_link_loss=(double*) malloc(sizeof(double)*(GBL_n_amps+1));
for (i=0;i<=GBL_n_amps;++i)
{
        num=fscanf(f_ptr,"%g %*[^\n]\n",&float_in);
        *(GBL_link_loss+i)=(double) float_in;
        if (num!=1) {printf("\nERROR: in 'launched_params' file: link loss.\n"); exit(1);}
}

GBL_alpha_R_fwd=(double*) malloc(sizeof(double)*(GBL_n_amps+1));
for (i=0;i<=GBL_n_amps;++i)
{
        num=fscanf(f_ptr,"%g %*[^\n]\n",&float_in);
        *(GBL_alpha_R_fwd+i)=(double) float_in;
        if (num!=1) {printf("\nERROR: in 'launched_params' file: alphaR\n"); exit(1);}
}

GBL_alpha_R_bwd=(double*) malloc(sizeof(double)*(GBL_n_amps+1));
for (i=0;i<=GBL_n_amps;++i)
{
        num=fscanf(f_ptr,"%g %*[^\n]\n",&float_in);
        *(GBL_alpha_R_bwd+i)=(double) float_in;
        if (num!=1) {printf("\nERROR: in 'launched_params' file: alphaR\n"); exit(1);}
}

num=fscanf(f_ptr,"%g %*[^\n]\n",&float_in);
alphac1=(double) float_in;
if (num!=1) {printf("\nERROR: in 'launched_params' file: alphac1.\n"); exit(1);}

num=fscanf(f_ptr,"%g %*[^\n]\n",&float_in);
alphac2=(double) float_in;
if (num!=1) {printf("\nERROR: in 'launched_params' file: alphac2.\n"); exit(1);}

num=fscanf(f_ptr,"%d %*[^\n]\n",&short_in);
GBL_n_channels=short_in;
if (num!=1) {printf("\nERROR: in 'launched_params' file: channel number.\n"); exit(1);}

GBL_fwd_psd=(double*) malloc(sizeof(double)*GBL_n_channels);
GBL_bwd_psd=(double*) malloc(sizeof(double)*GBL_n_channels);

for (i=0;i<GBL_n_channels;++i)
{
        num=fscanf(f_ptr,"%g %*[^\n]\n",&float_in);
        *(GBL_fwd_psd+i)=(double) float_in;
        if (num!=1) {printf("\nERROR: in 'launched_params' file: fwd psd.\n"); exit(1);}
}

for (i=0;i<GBL_n_channels;++i)
{
        num=fscanf(f_ptr,"%g %*[^\n]\n",&float_in);
        *(GBL_bwd_psd+i)=(double) float_in;
        if (num!=1) {printf("\nERROR: in 'launched_params' file: bwd psd.\n"); exit(1);}
}
```

```
num=fscanf(f_ptr,"%d %*[^\n]\n",&short_in);
GBL_ite_max=short_in;
if (num!=1) {printf("\nERROR: in 'launched_params' file: iteration number.\n"); exit(1);}

close(f_ptr);

return;

}
```

Listing of launched_params:

```
3.0     /* Number of amplifiers in the cascade */
22      /* Forward pump power for amplifier 1      */
50      /* Forward pump power for amplifier 2      */
50      /* Forward pump power for amplifier 3      */
0       /* Backward pump power for amplifier 1     */
0       /* Backward pump power for amplifier 2     */
0       /* Backward pump power for amplifier 3     */
1       /* Loss of link 0 */
8.7096e-3       /* Loss of link 1 */
6.0954e-3       /* Loss of link 2 */
1       /* Loss of link 4 */
0       /* Forward Rayleigh backscattering coefficient of link 1*/
5.1286e-4       /* Forward Rayleigh backscattering coefficient of link 2*/
5.1286e-4       /* Forward Rayleigh backscattering coefficient of link 3*/
0       /* Forward Rayleigh backscattering coefficient of link 4*/
0       /* Backward Rayleigh backscattering coefficient of link 1*/
3.4674e-4       /* Backward Rayleigh backscattering coefficient of link 2*/
3.4674e-4       /* Backward Rayleigh backscattering coefficient of link 3*/
0       /* Backward Rayleigh backscattering coefficient of link 4*/
1.0     /* Entrance coupling ratio */
1.0     /* Exit coupling ratio */
38.0    /* Number of channels */
0e-17   /* PSD of fwd channel 0 */
0e-17   /* PSD of fwd channel 1 */
```

0e-17 /* PSD of fwd channel 2 */
0e-17 /* PSD of fwd channel 3 */
0e-17 /* PSD of fwd channel 4 */
0e-17 /* PSD of fwd channel 5 */
0e-17 /* PSD of fwd channel 6 */
0e-17 /* PSD of fwd channel 7 */
0e-17 /* PSD of fwd channel 8 */
0e-17 /* PSD of fwd channel 9 */
0e-17 /* PSD of fwd channel 10 */
0e-17 /* PSD of fwd channel 11 */
0e-17 /* PSD of fwd channel 12 */
0e-17 /* PSD of fwd channel 13 */
0e-17 /* PSD of fwd channel 14 */
3.4046e-12 /* PSD of fwd channel 15 */
0e-17 /* PSD of fwd channel 16 */
0e-17 /* PSD of fwd channel 17 */
0e-17 /* PSD of fwd channel 18 */
0e-17 /* PSD of fwd channel 19 */
0e-17 /* PSD of fwd channel 20 */
0e-17 /* PSD of fwd channel 21 */
0e-17 /* PSD of fwd channel 22 */
0e-17 /* PSD of fwd channel 23 */
0e-17 /* PSD of fwd channel 24 */
0e-17 /* PSD of fwd channel 25 */
0e-17 /* PSD of fwd channel 26 */
0e-17 /* PSD of fwd channel 27 */
0e-17 /* PSD of fwd channel 28 */
0e-17 /* PSD of fwd channel 29 */
0e-17 /* PSD of fwd channel 30 */
0e-17 /* PSD of fwd channel 31 */
0e-17 /* PSD of fwd channel 32 */
0e-17 /* PSD of fwd channel 33 */
0e-17 /* PSD of fwd channel 34 */
0e-17 /* PSD of fwd channel 35 */
0e-17 /* PSD of fwd channel 36 */
0e-17 /* PSD of fwd channel 37 */

```
0e-17   /* PSD of bwd channel 0 */
0e-17   /* PSD of bwd channel 1 */
0e-17   /* PSD of bwd channel 2 */
0e-17   /* PSD of bwd channel 3 */
0e-17   /* PSD of bwd channel 4 */
0e-17   /* PSD of bwd channel 5 */
0e-17   /* PSD of bwd channel 6 */
0e-17   /* PSD of bwd channel 7 */
0e-17   /* PSD of bwd channel 8 */
0e-17   /* PSD of bwd channel 9 */
0e-17   /* PSD of bwd channel 10 */
0e-17   /* PSD of bwd channel 11 */
0e-17   /* PSD of bwd channel 12 */
0e-17   /* PSD of bwd channel 13 */
0e-17   /* PSD of bwd channel 14 */
0e-17   /* PSD of bwd channel 15 */
0e-17   /* PSD of bwd channel 16 */
0e-17   /* PSD of bwd channel 17 */
0e-17   /* PSD of bwd channel 18 */
0e-17   /* PSD of bwd channel 19 */
0e-17   /* PSD of bwd channel 20 */
0e-17   /* PSD of bwd channel 21 */
0e-17   /* PSD of bwd channel 22 */
0e-17   /* PSD of bwd channel 23 */
0e-17   /* PSD of bwd channel 24 */
0e-17   /* PSD of fwd channel 25 */
3.4046e-12      /* PSD of fwd channel 26 */
0e-17   /* PSD of fwd channel 27 */
0e-17   /* PSD of fwd channel 28 */
0e-17   /* PSD of fwd channel 29 */
0e-17   /* PSD of fwd channel 30 */
0e-17   /* PSD of fwd channel 31 */
0e-17   /* PSD of fwd channel 32 */
0e-17   /* PSD of fwd channel 33 */
0e-17   /* PSD of fwd channel 34 */
0e-17   /* PSD of fwd channel 35 */
```

```
0e-17  /* PSD of fwd channel 36 */
0e-17  /* PSD of fwd channel 37 */
6      /*Maximum number of iterations */
```

Listing of param_file_1 :

```
2.38     /* core radius, a (um)                                    */
1.4637    /* value of n_core                                       */
1.457    /* value of n_clad                                        */
3.59e18   /* value of N_0 (cm^-3)                                  */
1.54e-21   /* absorption cross section at pump w-l, sig_A_p (cm^2)  */
2.0     /* value of 'w_factor' n(r) = e^-(w_factor*(r/a)^2)        */
1.0      /* value to divide P0 by (usually 1000 or 1)             */
0.0000  /* eta                                                    */
11e-3    /* tau (s)                                               */
30.0e2   /* value of max_length (max. fibre length in cm)         */
0.980    /** pump wavelength, lambda_p (um)                       */
10.      /** min. forward pump input power in mW (for gain calcs) */
40.      /** max. forward pump input power in mW (for gain calcs) */
10.      /** min. backward pump input power in mW (for gain calcs)*/
40.      /** max. backward pump input power in mW (for gain calcs)*/
38       /** number of signal channels                            */
1.5304     /** CH.0 signal wavelength, lambda_s (um)              */
1.025e11    /** CH.0 delta_nu_s, the linewidth of signal source (Hz) */
1.5312     /** CH.1 signal wavelength, lambda_s (um)              */
1.025e11    /** CH.1 delta_nu_s, the linewidth of signal source (Hz) */
1.532     /** CH.2 signal wavelength, lambda_s (um)               */
1.025e11    /** CH.2 delta_nu_s, the linewidth of signal source (Hz) */
1.5328     /** CH.3 signal wavelength, lambda_s (um)              */
1.025e11    /** CH.3 delta_nu_s, the linewidth of signal source (Hz) */
1.5336     /** CH.4 signal wavelength, lambda_s (um)              */
1.025e11    /** CH.4 delta_nu_s, the linewidth of signal source (Hz) */
1.5344     /** CH.5 signal wavelength, lambda_s (um)              */
```

```
1.025e11    /** CH.5 delta_nu_s, the linewidth of signal source (Hz)    */
1.5352      /** CH.6 signal wavelength, lambda_s (um)                   */
1.025e11    /** CH.6 delta_nu_s, the linewidth of signal source (Hz)    */
1.536       /** CH.7 signal wavelength, lambda_s (um)                   */
1.025e11    /** CH.7 delta_nu_s, the linewidth of signal source (Hz)    */
1.5368      /** CH.8 signal wavelength, lambda_s (um)                   */
1.025e11    /** CH.8 delta_nu_s, the linewidth of signal source (Hz)    */
1.5376      /** CH.9 signal wavelength, lambda_s (um)                   */
1.025e11    /** CH.9 delta_nu_s, the linewidth of signal source (Hz)    */
1.5384      /** CH.10 signal wavelength, lambda_s (um)                  */
1.025e11    /** CH.10 delta_nu_s, the linewidth of signal source (Hz)   */
1.5392      /** CH.11 signal wavelength, lambda_s (um)                  */
1.025e11    /** CH.11 delta_nu_s, the linewidth of signal source (Hz)   */
1.54        /** CH.12 signal wavelength, lambda_s (um)                  */
1.025e11    /** CH.12 delta_nu_s, the linewidth of signal source (Hz)   */
1.5408      /** CH.13 signal wavelength, lambda_s (um)                  */
1.025e11    /** CH.13 delta_nu_s, the linewidth of signal source (Hz)   */
1.5416      /** CH.14 signal wavelength, lambda_s (um)                  */
1.025e11    /** CH.14 delta_nu_s, the linewidth of signal source (Hz)   */
1.5424      /** CH.15 signal wavelength, lambda_s (um)                  */
2.5e10      /** CH.15 delta_nu_s, the linewidth of signal source (Hz)   */
1.5432      /** CH.16 signal wavelength, lambda_s (um)                  */
1.025e11    /** CH.16 delta_nu_s, the linewidth of signal source (Hz)   */
1.544       /** CH.17 signal wavelength, lambda_s (um)                  */
1.025e11    /** CH.17 delta_nu_s, the linewidth of signal source (Hz)   */
1.5448      /** CH.18 signal wavelength, lambda_s (um)                  */
1.025e11    /** CH.18 delta_nu_s, the linewidth of signal source (Hz)   */
1.5456      /** CH.19 signal wavelength, lambda_s (um)                  */
1.025e11    /** CH.19 delta_nu_s, the linewidth of signal source (Hz)   */
1.5464      /** CH.20 signal wavelength, lambda_s (um)                  */
1.025e11    /** CH.20 delta_nu_s, the linewidth of signal source (Hz)   */
1.5472      /** CH.21 signal wavelength, lambda_s (um)                  */
1.025e11    /** CH.21 delta_nu_s, the linewidth of signal source (Hz)   */
1.548       /** CH.22 signal wavelength, lambda_s (um)                  */
1.025e11    /** CH.22 delta_nu_s, the linewidth of signal source (Hz)   */
1.5488      /** CH.23 signal wavelength, lambda_s (um)                  */
```

```
1.025e11     /** CH.23 delta_nu_s, the linewidth of signal source (Hz)      */
1.5496      /** CH.24 signal wavelength, lambda_s (um)                      */
1.025e11     /** CH.24 delta_nu_s, the linewidth of signal source (Hz)      */
1.5504      /** CH.25 signal wavelength, lambda_s (um)                      */
1.025e11     /** CH.25 delta_nu_s, the linewidth of signal source (Hz)      */
1.5512      /** CH.26 signal wavelength, lambda_s (um)                      */
2.5e10      /** CH.26 delta_nu_s, the linewidth of signal source (Hz)       */
1.552       /** CH.27 signal wavelength, lambda_s (um)                      */
1.025e11     /** CH.27 delta_nu_s, the linewidth of signal source (Hz)      */
1.5528      /** CH.28 signal wavelength, lambda_s (um)                      */
1.025e11     /** CH.28 delta_nu_s, the linewidth of signal source (Hz)      */
1.5536      /** CH.29 signal wavelength, lambda_s (um)                      */
1.025e11     /** CH.29 delta_nu_s, the linewidth of signal source (Hz)      */
1.5544      /** CH.30 signal wavelength, lambda_s (um)                      */
1.025e11     /** CH.30 delta_nu_s, the linewidth of signal source (Hz)      */
1.5552      /** CH.31 signal wavelength, lambda_s (um)                      */
1.025e11     /** CH.31 delta_nu_s, the linewidth of signal source (Hz)      */
1.556       /** CH.32 signal wavelength, lambda_s (um)                      */
1.025e11     /** CH.32 delta_nu_s, the linewidth of signal source (Hz)      */
1.5568      /** CH.33 signal wavelength, lambda_s (um)                      */
1.025e11     /** CH.33 delta_nu_s, the linewidth of signal source (Hz)      */
1.5576      /** CH.34 signal wavelength, lambda_s (um)                      */
1.025e11     /** CH.34 delta_nu_s, the linewidth of signal source (Hz)      */
1.5584      /** CH.35 signal wavelength, lambda_s (um)                      */
1.025e11     /** CH.35 delta_nu_s, the linewidth of signal source (Hz)      */
1.5592      /** CH.36 signal wavelength, lambda_s (um)                      */
1.025e11     /** CH.36 delta_nu_s, the linewidth of signal source (Hz)      */
1.56        /** CH.37 signal wavelength, lambda_s (um)                      */
1.025e11     /** CH.37 delta_nu_s, the linewidth of signal source (Hz)      */
1e-12       /** CH.0 min. signal input power in mW (for gain calcs)         */
1e-8        /** CH.0 max. signal input power in mW (for gain calcs)         */
1e-12       /** CH.1 min. signal input power in mW (for gain calcs)         */
1e-8        /** CH.1 max. signal input power in mW (for gain calcs)         */
1e-12       /** CH.2 min. signal input power in mW (for gain calcs)         */
1e-8        /** CH.2 max. signal input power in mW (for gain calcs)         */
1e-12       /** CH.3 min. signal input power in mW (for gain calcs)         */
```

```
1e-8    /** CH.3 max. signal input power in mW (for gain calcs)     */
1e-12   /** CH.4 min. signal input power in mW (for gain calcs)     */
1e-8    /** CH.4 max. signal input power in mW (for gain calcs)  */
1e-12   /** CH.5 min. signal input power in mW (for gain calcs)     */
1e-8    /** CH.5 max. signal input power in mW (for gain calcs)  */
1e-12   /** CH.6 min. signal input power in mW (for gain calcs)     */
1e-8    /** CH.6 max. signal input power in mW (for gain calcs)     */
1e-12   /** CH.7 min. signal input power in mW (for gain calcs)     */
1e-8    /** CH.7 max. signal input power in mW (for gain calcs)  */
1e-12   /** CH.8 min. signal input power in mW (for gain calcs)     */
1e-8    /** CH.8 max. signal input power in mW (for gain calcs)  */
1e-12   /** CH.9 min. signal input power in mW (for gain calcs)     */
1e-8    /** CH.9 max. signal input power in mW (for gain calcs)     */
1e-12   /** CH.10 min. signal input power in mW (for gain calcs)     */
1e-8    /** CH.10 max. signal input power in mW (for gain calcs)      */
1e-12   /** CH.11 min. signal input power in mW (for gain calcs)     */
1e-8    /** CH.11 max. signal input power in mW (for gain calcs)      */
1e-12   /** CH.12 min. signal input power in mW (for gain calcs)     */
1e-8    /** CH.12 max. signal input power in mW (for gain calcs)     */
1e-12   /** CH.13 min. signal input power in mW (for gain calcs)     */
1e-8    /** CH.13 max. signal input power in mW (for gain calcs)      */
1e-12   /** CH.14 min. signal input power in mW (for gain calcs)     */
1e-8    /** CH.14 max. signal input power in mW (for gain calcs)      */
1e-12   /** CH.15 min. signal input power in mW (for gain calcs)     */
1e-8    /** CH.15 max. signal input power in mW (for gain calcs)     */
1e-12   /** CH.16 min. signal input power in mW (for gain calcs)     */
1e-8    /** CH.16 max. signal input power in mW (for gain calcs)      */
1e-12   /** CH.17 min. signal input power in mW (for gain calcs)     */
1e-8    /** CH.17 max. signal input power in mW (for gain calcs)      */
1e-12   /** CH.18 min. signal input power in mW (for gain calcs)     */
1e-8    /** CH.18 max. signal input power in mW (for gain calcs)     */
1e-12   /** CH.19 min. signal input power in mW (for gain calcs)     */
1e-8    /** CH.19 max. signal input power in mW (for gain calcs)      */
1e-12   /** CH.20 min. signal input power in mW (for gain calcs)     */
1e-8    /** CH.20 max. signal input power in mW (for gain calcs)      */
1e-12   /** CH.21 min. signal input power in mW (for gain calcs)     */
```

```
1e-8      /** CH.21 max. signal input power in mW (for gain calcs)      */
1e-12     /** CH.22 min. signal input power in mW (for gain calcs)      */
1e-8      /** CH.22 max. signal input power in mW (for gain calcs)      */
1e-12     /** CH.23 min. signal input power in mW (for gain calcs)      */
1e-8      /** CH.23 max. signal input power in mW (for gain calcs)      */
1e-12     /** CH.24 min. signal input power in mW (for gain calcs)      */
1e-8      /** CH.24 max. signal input power in mW (for gain calcs)      */
1e-12     /** CH.25 min. signal input power in mW (for gain calcs)      */
1e-8      /** CH.25 max. signal input power in mW (for gain calcs)      */
1e-12     /** CH.26 min. signal input power in mW (for gain calcs)      */
1e-8      /** CH.26 max. signal input power in mW (for gain calcs)      */
1e-12     /** CH.27 min. signal input power in mW (for gain calcs)      */
1e-8      /** CH.27 max. signal input power in mW (for gain calcs)      */
1e-12     /** CH.28 min. signal input power in mW (for gain calcs)      */
1e-8      /** CH.28 max. signal input power in mW (for gain calcs)      */
1e-12     /** CH.29 min. signal input power in mW (for gain calcs)      */
1e-8      /** CH.29 max. signal input power in mW (for gain calcs)      */
1e-12     /** CH.30 min. signal input power in mW (for gain calcs)      */
1e-8      /** CH.30 max. signal input power in mW (for gain calcs)      */
1e-12     /** CH.31 min. signal input power in mW (for gain calcs)      */
1e-8      /** CH.31 max. signal input power in mW (for gain calcs)      */
1e-12     /** CH.32 min. signal input power in mW (for gain calcs)      */
1e-8      /** CH.32 max. signal input power in mW (for gain calcs)      */
1e-12     /** CH.33 min. signal input power in mW (for gain calcs)      */
1e-8      /** CH.33 max. signal input power in mW (for gain calcs)      */
1e-12     /** CH.34 min. signal input power in mW (for gain calcs)      */
1e-8      /** CH.34 max. signal input power in mW (for gain calcs)      */
1e-12     /** CH.35 min. signal input power in mW (for gain calcs)      */
1e-8      /** CH.35 max. signal input power in mW (for gain calcs)      */
1e-12     /** CH.36 min. signal input power in mW (for gain calcs)      */
1e-8      /** CH.36 max. signal input power in mW (for gain calcs)      */
1e-12     /** CH.37 min. signal input power in mW (for gain calcs)      */
1e-8      /** CH.37 max. signal input power in mW (for gain calcs)      */
38        /** number of reflected channels                              */
1.5304      /** CH.0 signal wavelength, lambda_s (um)                   */
1.025e11    /** CH.0 delta_nu_s, the linewidth of signal source (Hz)    */
```

```
1.5312      /** CH.1 signal wavelength, lambda_s (um)                *
1.025e11     /** CH.1 delta_nu_s, the linewidth of signal source (Hz)      */
1.532      /** CH.2 signal wavelength, lambda_s (um)                *
1.025e11     /** CH.2 delta_nu_s, the linewidth of signal source (Hz)      */
1.5328      /** CH.3 signal wavelength, lambda_s (um)                */
1.025e11     /** CH.3 delta_nu_s, the linewidth of signal source (Hz)      */
1.5336      /** CH.4 signal wavelength, lambda_s (um)                *
1.025e11     /** CH.4 delta_nu_s, the linewidth of signal source (Hz)      */
1.5344      /** CH.5 signal wavelength, lambda_s (um)                *
1.025e11     /** CH.5 delta_nu_s, the linewidth of signal source (Hz)      */
1.5352      /** CH.6 signal wavelength, lambda_s (um)                */
1.025e11     /** CH.6 delta_nu_s, the linewidth of signal source (Hz)      */
1.5360      /** CH.7 signal wavelength, lambda_s (um)                */
1.025e11     /** CH.7 delta_nu_s, the linewidth of signal source (Hz)      */
1.5368      /** CH.8 signal wavelength, lambda_s (um)                */
1.025e11     /** CH.8 delta_nu_s, the linewidth of signal source (Hz)      */
1.5376      /** CH.9 signal wavelength, lambda_s (um)                */
1.025e11     /** CH.9 delta_nu_s, the linewidth of signal source (Hz)      */
1.5384      /** CH.10 signal wavelength, lambda_s (um)               */
1.025e11     /** CH.10 delta_nu_s, the linewidth of signal source (Hz)     */
1.5392      /** CH.11 signal wavelength, lambda_s (um)               */
1.025e11     /** CH.11 delta_nu_s, the linewidth of signal source (Hz)     */
1.54      /** CH.12 signal wavelength, lambda_s (um)               */
1.025e11     /** CH.12 delta_nu_s, the linewidth of signal source (Hz)     */
1.5408      /** CH.13 signal wavelength, lambda_s (um)               */
1.025e11     /** CH.13 delta_nu_s, the linewidth of signal source (Hz)     */
1.5416      /** CH.14 signal wavelength, lambda_s (um)               */
1.025e11     /** CH.14 delta_nu_s, the linewidth of signal source (Hz)     */
1.5424      /** CH.15 signal wavelength, lambda_s (um)               */
2.5e10      /** CH.15 delta_nu_s, the linewidth of signal source (Hz)     */
1.5432      /** CH.16 signal wavelength, lambda_s (um)               */
1.025e11     /** CH.16 delta_nu_s, the linewidth of signal source (Hz)     */
1.544      /** CH.17 signal wavelength, lambda_s (um)               */
1.025e11     /** CH.17 delta_nu_s, the linewidth of signal source (Hz)     */
1.5448      /** CH.18 signal wavelength, lambda_s (um)               */
1.025e11     /** CH.18 delta_nu_s, the linewidth of signal source (Hz)     */
```

```
1.5456      /** CH.19 signal wavelength, lambda_s (um)                 */
1.025e11      /** CH.19 delta_nu_s, the linewidth of signal source (Hz)      */
1.5464      /** CH.20 signal wavelength, lambda_s (um)                 */
1.025e11      /** CH.20 delta_nu_s, the linewidth of signal source (Hz)      */
1.5472      /** CH.21 signal wavelength, lambda_s (um)                 */
1.025e11     /** CH.21 delta_nu_s, the linewidth of signal source (Hz)      */
1.548     /** CH.22 signal wavelength, lambda_s (um)                 */
1.025e11      /** CH.22 delta_nu_s, the linewidth of signal source (Hz)      */
1.5488      /** CH.23 signal wavelength, lambda_s (um)                 */
1.025e11      /** CH.23 delta_nu_s, the linewidth of signal source (Hz)      */
1.5496      /** CH.24 signal wavelength, lambda_s (um)                 */
1.025e11      /** CH.24 delta_nu_s, the linewidth of signal source (Hz)      */
1.5504      /** CH.25 signal wavelength, lambda_s (um)                 */
1.025e11      /** CH.25 delta_nu_s, the linewidth of signal source (Hz)      */
1.5512      /** CH.26 signal wavelength, lambda_s (um)                 */
2.5e10     /** CH.26 delta_nu_s, the linewidth of signal source (Hz)      */
1.5520      /** CH.27 signal wavelength, lambda_s (um)                 */
1.025e11      /** CH.27 delta_nu_s, the linewidth of signal source (Hz)      */
1.5528      /** CH.28 signal wavelength, lambda_s (um)                 */
1.025e11      /** CH.28 delta_nu_s, the linewidth of signal source (Hz)      */
1.5536      /** CH.29 signal wavelength, lambda_s (um)                 */
1.025e11      /** CH.29 delta_nu_s, the linewidth of signal source (Hz)      */
1.5544      /** CH.30 signal wavelength, lambda_s (um)                 */
1.025e11      /** CH.30 delta_nu_s, the linewidth of signal source (Hz)      */
1.5552      /** CH.31 signal wavelength, lambda_s (um)                 */
1.025e11      /** CH.31 delta_nu_s, the linewidth of signal source (Hz)      */
1.5560     /** CH.32 signal wavelength, lambda_s (um)                 */
1.025e11      /** CH.32 delta_nu_s, the linewidth of signal source (Hz)      */
1.5568      /** CH.33 signal wavelength, lambda_s (um)                 */
1.025e11      /** CH.33 delta_nu_s, the linewidth of signal source (Hz)      */
1.5576      /** CH.34 signal wavelength, lambda_s (um)                 */
1.025e11      /** CH.34 delta_nu_s, the linewidth of signal source (Hz)      */
1.5584      /** CH.35 signal wavelength, lambda_s (um)                 */
1.025e11      /** CH.35 delta_nu_s, the linewidth of signal source (Hz)      */
1.5592      /** CH.36 signal wavelength, lambda_s (um)                 */
1.025e11      /** CH.36 delta_nu_s, the linewidth of signal source (Hz)      */
```

```
1.5600      /** CH.37 signal wavelength, lambda_s (um)                  */
1.025e11    /** CH.37 delta_nu_s, the linewidth of signal source (Hz)   */
1.5304      /* start wavelength of simulation, lambda_start(um)        */
1.5600      /* end wavelength of simulation, lambda_end(um)            */
0.0008      /* wavelength step of simulation, delta_lambda(um)         */
38          /* # of sigma values in the file 'sigma_a/e_dat'           */
.0008       /* w-l spacing (um) of sigma values for file 'sigma_a/e_dat' */
1.5424              /* gain_lambda - calculate gaun and noise parameters (um) */
50          /* # of runge_kutta invervals                              */
5           /* # of iterations to go thru                              */
15          /* # of signal steps (for gain calcs)                      */
3           /* # of pump steps (for gain calcs)                        */
3           /* pgm_options 1=Pdistrib; 2=Pp/Ps vs. Z; 4=gain; 8=pump thresh */
0           /* print tables to screen? (1=yes, 0=no)                   */
1                       /* write plus, minus, and sum.dat
                           */
0                       /* run program 2
                           */
param_file2             /* param_file2 -- second program parameter file
                           */
```